Identification and Characterization of Expanded RNA Binding Abilities and Cellular Roles for Nuclear RNase P

by

Michael Charles Marvin

A dissertation submitted in partial fulfillment
of the requirements for the degree of
Doctor of Philosophy
(Biological Chemistry)
in The University of Michigan
2011

Doctoral Committee:

Professor David R. Engelke, Chair
Professor Carol A. Fierke
Professor Robert S. Fuller
Professor Michael D. Uhler
Professor Nils G. Walter

To Family

ACKNOWLEDGEMENTS

I would like to first thank my advisor Dave Engelke. I met him when I was an undergraduate while attending a conference at the University of Michigan. Attending that conference and meeting Dave was a fundamental part of why I decided to go to graduate school. His dedication to science and mentoring has been fundamental to my development as a critical thinker, problem solver, and scientist. I have appreciated your helpful and frank advice throughout my graduate career.

The members of the Engelke lab have made lab feel like a family. Paul Good has been the glue of the lab, connecting me to previous generations of Engelke lab members through fly fishing trips and providing much help with lab technical questions. I would also like to thank Scott Walker for always being available for discussions about a crazy idea or technical issue and providing critical help near the end of graduate school that resulted in successfully finishing a project. I could not have been successful without him. I would also like to thank Dan Coughlin for all of his help in the early and mid stages of graduate school. Next I would like to thank the other previous graduate students in the lab during my time here: Shaohua, Becky, and Matt. They provided very valuable lab discussions and also lightened the lab atmosphere. Dave Pai, thanks for the helpful scientific discussion and futile political conversations. Ann Kendall, thanks for the help with lab technical questions and further interesting but futile political conversations. Finally, I would like to thank Mai Tsoi who has been such a constant source of support in the lab and for your genuine kindness.

I would like to thank my committee members: Carol Fierke, Robert Fuller, Nils Walter, and Michael Uhler. Your support has been very valuable over the years in overcoming technical hurdles. I am also grateful for the support that Robert Fuller and Carol Fierke have provided in my search for postdoctoral positions by writing letters of recommendation. I would also like to thank the Department of Biological Chemistry staff, especially Beth Goodwin for all the assistance and support. In addition, I would like to thank Lars Steinmetz and the members of his lab, Sandra Clauder and Zhenyu Xu that collaborated with me for our microarray analysis. Also, for the UMMS Proteomics and Mass Spectrometry Facility, with facility director Scott Shaffer and lab manager Karin Green, at the University of Massachusetts Medical School for high quality and expedited protein identification.

In addition, I am indebted to Carol Fierke and her lab. They have been very supportive and provided many valuable RNase P discussions at our monthly RNase P group meetings. Carol has specifically provided fundamental guidance on many aspects of my projects. I am very grateful for her help and advice throughout graduate school as she has always been a great resource and supportive at every stage of my graduate school career.

The Cellular Biotechnology Training Grant (CBTP) was also extremely fundamental in my success and future career direction. I am grateful for the 2.5 years of funding and the extra training that I received. I am grateful for all the support that Margaret Allen and program director Joel Swanson provided in my search for and successful completion of an industry internship, which has greatly benefited my graduate career. Also I want to thank Sheryl Smith from the Department of Microbiology and

Immunology for dealing with the very difficult process of the reimbursement for my internship. In addition, I would like to thank Rackham Graduate School for funding a Graduate Student Research Grant and for many travel grants for conferences.

Finally, I would like to thank my family and friends for the essential support throughout the years. Without my parent's love and constant support I could never have done all of this. I am grateful for all that you have done and the confidence you have in me. I would also like to thank my sister Michelle who always seems to keep such a positive outlook on life. It was great having a little sister to pester too. I would also like to thank my friends for their support and for the necessary breaks from lab. Finally, I would like to thank Stacie. She is my best friend and loving companion. Her support has meant a great deal to me. I cannot wait to see what comes next.

Publication note: Chapter 1 was adapted from an originally published work in *The Journal of Cellular Biochemistry*. Marvin MC, Engelke DR (2009) Broadening the Mission of an RNA Enzyme. *J Cell Biochem.* **108** (6), 1244-1251. Epub. *doi:10.1002/jcb.22367*.

TABLE OF CONTENTS

LIST OF FIGURES

LIST OF TABLES

ABSTRACT

Ribonuclease P (RNase P) is an essential endoribonuclease that catalyzes the cleavage of the 5′ leader of pre-tRNAs. In addition, a growing number of non-tRNA substrates have been identified in various organisms. RNase P varies in composition as bacterial RNase P contains a catalytic RNA core and one protein subunit while eukaryotic RNase P has multiple protein subunits with a catalytic RNA core. The more complex composition of eukaryotic RNase P provides unique RNA binding abilities not present in bacterial RNase P. A series of *in vitro* and *in vivo* investigations was used to characterize RNA binding with eukaryotic RNase P and how it can translate into cleavage of a diverse set of RNA substrates.

In vitro studies established that single stranded RNA binds and strongly inhibits RNase P catalyzed pre-tRNA cleavage. This inhibition was not sequence dependent as multiple mixed sequence RNAs inhibited RNase P similarly to homopolymer RNA, although only mixed sequence RNA was cleaved. Investigation of RNA binding using crosslinking methods indicated that a diverse set of RNA (pre-tRNA^{Tyr}, polyU_{50} RNA, and mixed sequence RNA) contacts RNase P near the RNA active site of the enzyme. In addition, 2-3 of the 9 proteins in yeast RNase P crosslink to homopolymer RNA.

In vivo studies were used to determine if strong *in vitro* binding and cleavage translated into new RNase P substrates *in vivo*. Using cells containing a temperature sensitive RNase P mutation, pre-mRNA and noncoding RNA were shown to accumulate

strongly using a strand specific microarray. RNase P's role appears to be indirect with pre-mRNA accumulation occurring due to a spliceosome assembly defect that exists in the RNase P mutation strain. Also, a variety of noncoding RNAs were shown to accumulate with a subset indicating inverse changes with overlapping coding regions. It was shown that multiple larger antisense RNA accumulate in the cells with the RNase P mutation, consistent with a previously unknown role of RNase P in degrading some of these antisense RNA *in vivo*.

CHAPTER 1
RNASE P: BROADENING THE MISSION OF AN RNA ENZYME

Introduction

Over 25 years ago the central dogma of biology was expanded with the discovery that, in addition to proteins, RNA can also have enzymatic activity, supporting the "RNA World" hypothesis in which RNA-like macromolecules were thought to encode and catalyze their own duplication. Today these early discoveries have been extended and many more ribozymes have been found to play essential roles in cells, including the ribosome and RNase P. In modern organisms these ribozymes are virtually always ribonuclear protein complexes with catalytic RNA cores, but the proteins act in various vital ways to ensure that the desired reaction is carried out in the correct location. These ribozyme-catalyzed reactions carried out by RNase P and the ribosomes are multiple turnover *in vivo,* defining them as true enzymes (Guerrier-Takada *et al*. 1983; Guerrier-Takada and Altman 1984; Ban *et al*. 2000; Muth *et al*. 2000; Nissen *et al*. 2000). It is worthwhile to note that in our drive to understand RNA catalysis the role of the protein subunits has usually been of secondary interest. Given the large protein content of these important ribonuclear protein complexes in eukaryotes and some archaea, it is important to consider how the protein has played a role in enabling correct processing and possibly has enabled an expansion of processing functions.

One of the best-studied examples of a ribonuclear protein complex has been RNase P. It was one of the first ribozymes discovered and is conserved in almost all

organisms (Guerrier-Takada *et al*. 1983; Guerrier-Takada and Altman 1984; Frank and Pace 1998; Walker and Engelke 2006). RNase P has an RNA core that has adapted to complex cellular environments with the addition of protein subunits. RNase P is an essential ribonuclear protein (RNP) that is best known for catalyzing the 5′-endonucleolytic cleavage of pre-tRNA and this essential processing reaction is conserved throughout all forms of RNase P regardless of composition. The protein composition of the complex differs dramatically, from bacterial RNase P with one protein subunit, to archaeal with 4-5 proteins, to eukaryotes with 9-10 proteins (Fig. 1.1, Table 1.1). In addition to pre-tRNA cleavage, RNase P has been shown to cleave other RNA substrates both *in vitro* and *in vivo* (Table 1.2). Understanding the functions of this dramatic increase in protein content of RNase P can provide insight into the molecular evolution of RNP complexes.

Bacterial RNase P

Structure

Bacterial RNase P contains a single protein subunit that combines *in vivo* with a catalytic RNA subunit. The catalyzed hydrolysis of a phosphodiester bond in the RNA substrate takes place within a conserved active site in the RNA subunit. At high salt *in vitro* the RNA can cleave substrate without protein, but the protein is required for activity *in vivo* (Gössringer *et al*. 2006; Smith *et al*. 2007). There are two major groups of bacterial RNase P based on RNA secondary structure, ancestral type (A-type) and

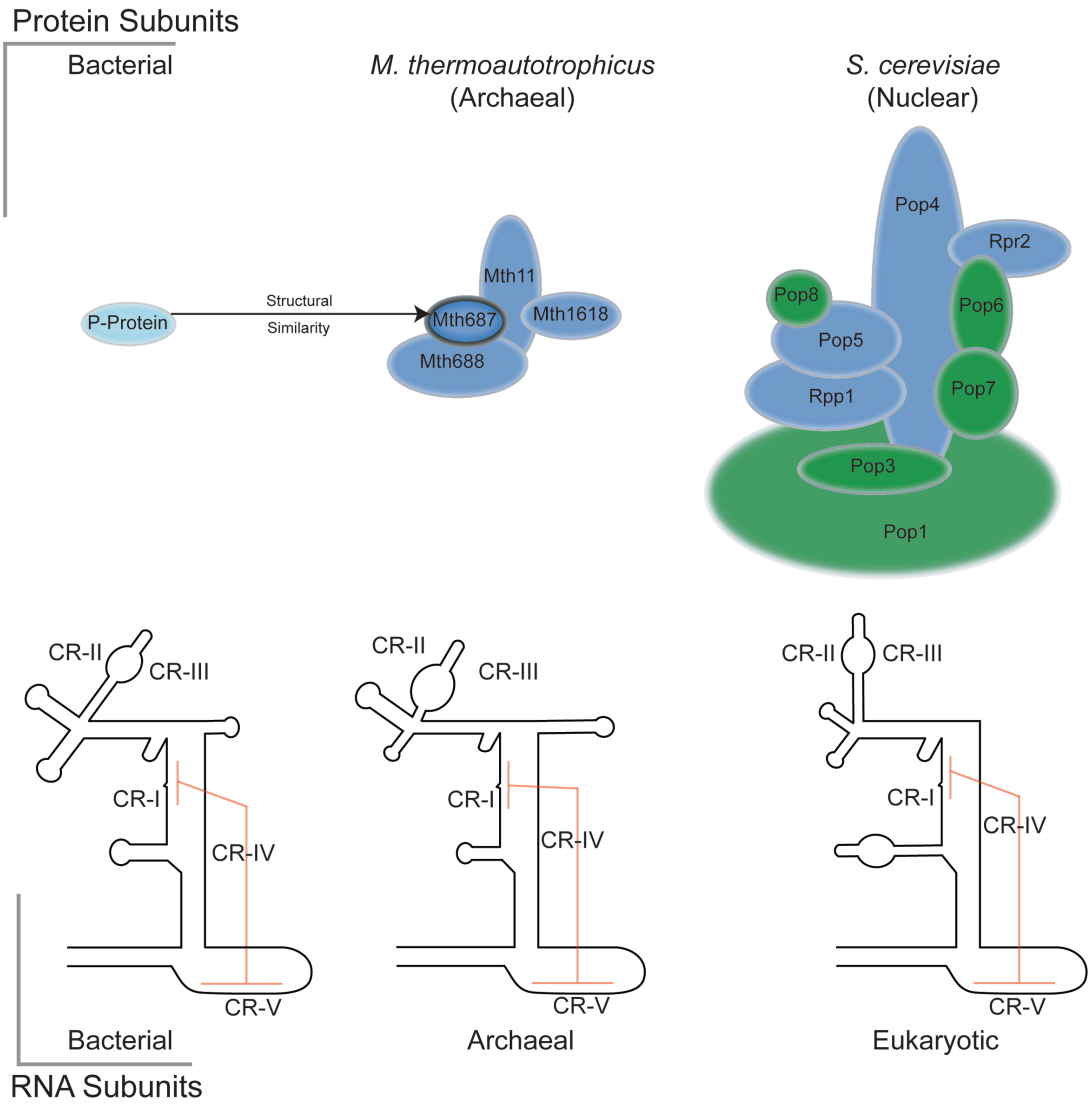

Figure 1.1. The evolution of RNase P from bacteria to eukaryotes.
Archaeal proteins indicated for *M. thermoautotrophicus* (Mth). Color coding indicates protein homology between eukaryotic and archaeal RNase P. Bacterial protein shown with structural homology to Mth687 in archaeal RNase P. Protein subunit interactions are shown from yeast two-hybrid data (Houser-Scott *et al*. 2002; Hall and Brown 2004). The RNA structures illustrate conserved regions (CR), with red lines indicating tertiary interactions, and estimate general structural characteristics of the indicated consensus structures. Refer to RNase P database for more details: http://www.mbio.ncsu.edu/RNaseP/home.html.

Table 1.1. Subunit composition of RNase P: Bacterial, Archaeal, Eukaryal.

Bacteria[a]		Archaea[b]		Eukarya				
	RNase P		RNase P			Yeast Nuclear RNase P[c]	Yeast RNase MRP[c]	Human Nuclear RNase P
Name	Mass (kDa)	Name	Mass (kDa)	Yeast Name	Human Name	Mass (kDa)	Mass (kDa)	Mass (kDa)
PROTEIN								
P-Protein	~14	MTH687p	14.6	POP5	hPOP5	19.6	19.6	19
		MTH11p	10.7	POP4	RPP29	32.9	32.9	29
		MTH688p	27.7	RPP1	RPP30	32.2	32.2	30
		MTH1618p	17	RPR2	RPP21	16.3		21
				POP1	hPOP1	100.5	100.5	115
				POP7	RPP20	15.8	15.8	20
				POP3	RPP38	22.6	22.6	38
				POP6		18.2	18.2	
				POP8		15.5	15.5	
					RPP40			40
					RPP25			25
					RPP14			14
				SNM1			22.5	
				RMP1			23.6	
RNA								
P-RNA	~95-150	*RNPB*	95	*RPR1*		120		
				NME1			112	
					H1			109

[a] Masses are shown with an approximate range of sizes for type A and type B RNase P.
[b] Representative of type A RNase P from *M. thermoautotrophicus* is shown.
[c] *S. cerevisiae*
Solid box indicates sequence homology.
Dashed box represents structural similarity.

Table 1.2. RNase P and RNase MRP *in vitro* and *in vivo* substrates/inhibitors.
Not all substrates or inhibitors have been shown to be functional *in vivo*, illustrating the promiscuity of RNase P *in vitro*.

Bacteria	Eukarya	
RNase P	**Nuclear RNase P**	**RNase MRP**
pre-tRNA	**pre-tRNA**	**pre-rRNA (A3 site)**
mitochondrial RNA primers for DNA replication	HRA1 antisense RNA	mitochondrial RNA primers for DNA replication
pre-4.5S RNA	Box C/D intron encoded snoRNA	CLB2 mRNA
C4 RNA	long non-coding RNA (lncRNA)	
tmRNA (10Sa RNA & *Cyanelle*)	pre-rRNA (multiple sites)	
TYMV Virus RNA		
ColE1 RNA	**Inhibitors:**	
polycistronic mRNA	poly-nucleotides (G>U>A>>C)	
Riboswitches (transient structures)	ssRNA (mixed sequences)	
Small RNA (>5nt)		
Φ-80 induces RNA		
long non-coding RNA (lncRNA)		

Bacillus type (B-type). These RNAs are very similar and were shown to be interchangeable *in vivo* (Wegscheid *et al*. 2006). A universal consensus RNA secondary structure for type A and type B is represented in Figure 1.1. In contrast to the RNA subunit, the bacterial protein in RNase P is ~14 kDa and is small compared to the RNA subunit, which differs in size based on the bacteria (~95-150 kDa) (Fig. 1.1,Table 1.1) (Brown 1999; Evans *et al*. 2006). The protein adopts an α-β sandwich fold and is structurally related to other RNA binding proteins (Stams *et al*. 1998). The primary sequence of the bacterial protein is not tightly conserved, but the crystal structure shows relative conservation of tertiary structure (Smith *et al*. 2007). Even though the bacterial RNA is catalytic *in vitro* at high salt, the protein makes vital contacts with both substrate and the catalytic RNA subunit (Westhof *et al*. 1996; Loria *et al*. 1998; Kurz and Fierke 2002; Sun and Harris 2007). These protein contacts with the RNA subunit help fold and stabilize RNA tertiary structure enabling more efficient cleavage. In addition, the protein subunit appears to normalize the rates of pre-tRNA cleavage between different tRNAs by expanding the active site, thus enabling efficient processing of all pre-tRNAs (Sun *et al*. 2006). The example of RNase P in bacteria serves as a model system and provides fundamental information to understanding other examples of RNase P that contain more protein subunits.

Substrate Recognition

RNase P's best-studied substrate, pre-tRNA, has varied primary sequence but common structural features that are important for cleavage. One of the techniques used to investigate how RNase P recognizes tRNA is to make deletions of regions in the

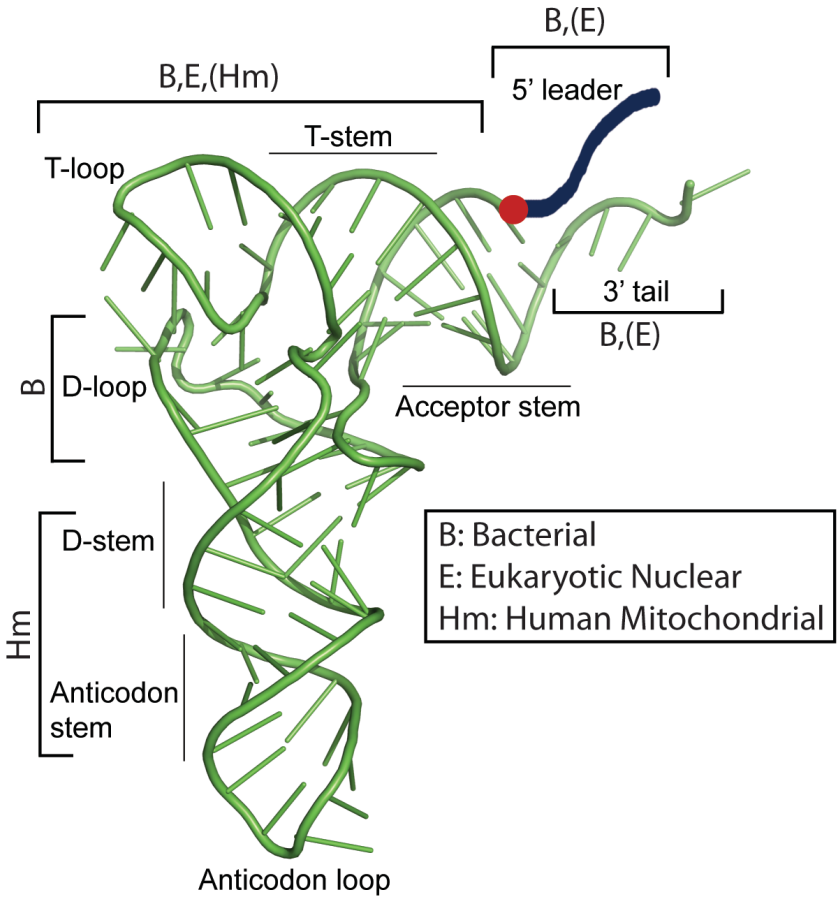

Figure 1.2. Important structural regions for RNase P recognition have variations between types of RNase P.
Crystal structure of yeast $tRNA^{Phe}$ (PDB code: 1EHZ) (Shi and Moore 2000). Cleavage site is indicated by a red dot. Parenthesis around type of RNase P indicate probable interactions but lack of supporting data. Figure created with MacPyMol; http:// www.pymol.org.

substrate to determine the minimal structure needed for successful cleavage. Bacterial RNase P can cleave a minimal substrate that contains just the T-arm and acceptor-stems of the tRNA (Fig. 1.2). These stems stack to form a coaxial helix that is recognized and cleaved by RNase P in bacteria (Shi and Moore 2000; Hansen *et al*. 2001).

In addition to minimal substrate data, biochemical data have indicated that *in vitro* at high salt, the RNA alone makes multiple contacts with the pre-tRNA substrate: near the cleavage site, D-loop, T-stem, T-loop, acceptor stem, and CCA tail (Fig. 1.2) (Thurlow *et al*. 1991; Kirsebom and Svärd 1994; Pan and Jakacka 1996). The DNA-encoded CCA 5′-tail found in most bacterial pre-tRNAs has been shown to make specific contacts with the cognate RNA subunits in the P15 loop (Kirsebom and Svärd 1994; Kirsebom 2007). Where this interaction is missing, for example in *Chlamydia*, the protein subunit appears to be able to compensate for the loss of the 5′ interaction with the RNA subunit (Herrmann *et al*. 2000). It appears that the importance of the P15 RNA subunit interaction with substrate seems to be overshadowed when protein is present.

Further characterization has shown that there are important contacts between the protein subunit and substrate (Niranjanakumari *et al*. 1998a; Niranjanakumari *et al*. 1998b; Smith *et al*. 2007). In pre-tRNAs, this interaction is clearly with the substrate leader sequences immediately upstream of the cleavage site. Residues in the central cleft region of the protein structure have been shown to directly contact the pre-tRNA 5′ leader approximately 4-7 nucleotides 5′ to the cleavage site (Niranjanakumari *et al*. 1998b). This interaction serves to normalize recognition of varied substrates and compensates for inefficient cleavage by the RNA subunit alone (Loria *et al*. 1998; Kirsebom 2007; Smith *et al*. 2007). It is worth reiterating that all of these effects on pre-

tRNA cleavage are being produced by binding of a relatively small (~14kDa) protein that is about one-tenth the mass of the RNA subunit and about half the mass of the pre-tRNA substrate.

The broadening of substrate recognition by the protein subunit has also had the effect of expanding the use of the ribozyme's catalytic domain beyond specifically cleaving pre-tRNA (Table 1.2). One set of non-tRNA substrates in bacteria appears to form structures that are similar to tRNA. These RNAs include the following: tmRNA precursors from *E. coli* (10Sa) and Cyanelle, TYMV viral RNA, ColE1 RNA, and long nuclear retained RNA (lncRNA) (Giegé *et al*. 1993; Komine *et al*. 1994; Jung and Lee 1995; Gimple and Schön 2001; Wilusz *et al*. 2008). RNase P cleavage of these substrates further illustrates that the shape of the substrate is what is most important for recognition and cleavage and not the primary sequence.

The 4.5S RNA substrate represents a different sort of substrate cleaved by bacterial RNase P. The structure of 4.5S RNA is thought to be a long hairpin that is distinct from tRNA (Peck-Miller and Altman 1991). RNase P RNA can cleave pre-4.5S RNA weakly without protein *in vitro*, but the protein subunit lowers the K_m 85-fold (Peck-Miller and Altman 1991). Another substrate, bacteriophage ϕ80-induced RNA, is also cleaved by RNase P. It is thought to form a structure very similar to 4.5S RNA (Bothwell *et al*. 1976). This versatility of substrate recognition by RNase P was further investigated by *in vitro* selection of RNA that can be cleaved with or without the protein subunit. When the RNA enzyme was present without protein, most cleaved substrates resembled tRNA in structure, but when the protein was added to the RNA subunit, non-tRNA substrates were more readily cleaved (Liu and Altman 1994). This is consistent

with the observed effect of protein on substrate recognition, expanding the active site to accommodate many different substrates.

The trend of increased substrate recognition was extended further when it was found that the holoenzyme, but not the RNA alone, could cleave single stranded RNA as small as 5 nt (Hansen *et al*. 2001). The products of these cleavages were chemically consistent with a normal RNase P mechanism. Cleavage was relatively fast with single turnover rates of 0.1 to 0.7 min^{-1} depending on identity. In addition, transient structures in riboswitches were indicated to be cleaved by RNase P (Altman *et al*. 2005).

In addition, RNase P has been shown to cleave intergenic RNA, mRNAs, and antisense transcripts of coding regions. For example, bacterial RNase P has been shown to work in concert with RNase E to process polycistronic mRNA (Alifano *et al*. 1994). This RNA is very unstable in precursor form, however, after cleavage by RNase P its half-life increases almost 10-fold (Alifano *et al*. 1994). A larger role for various intergenic regions in polycistronic mRNA in *E. coli* was also indicated by microarray analysis (Li and Altman 2003). In addition, antisense RNA precursor C4 from bacteriophages P1 and P7 is cleaved by RNase P, which results in inhibition of anti-repressor (Ant) synthesis (Hartmann *et al*. 1995). RNase P cleaved C4 RNA is required for this inhibition to occur. Combined, these results clearly illustrate that adding protein can increase the capacity for substrate recognition and suggests that the more complex eukaryotic RNase P could have significantly more substrates than the bacterial version.

Archaeal RNase P: Increased Protein Complexity

Structure and Homologous Proteins

Archaeal RNase P serves as an evolutionary intermediate that contains an RNA subunit and 4-5 protein subunits (Fig. 1.1 & Table 1.1). Two main branches of archaeal RNase P are delineated by RNA subunit structure as ancestral, type A, and type M, which is mainly from *Methanococci* (Harris *et al*. 2001). The main difference is that most type A RNase P RNAs have been shown to have activity without protein subunits while none of the type M RNase P RNAs have activity without protein. The *in vitro* catalytic activity of the archaeal RNA is more dependent on salt then the bacterial RNA, suggesting more dependence on protein subunits for folding or substrate binding (Pannucci *et al*. 1999). The protein subunits in archaeal RNase P are related to eukaryotic proteins and most were identified via sequence homology to yeast protein subunits (Fig. 1.1) (Hall and Brown 2002). For *M. thermoautotrophicus* these proteins are, with names of the corresponding yeast proteins in parentheses, Mth11p (Pop4), Mth687p (Pop5), Mth688p (Rpp1), and Mth1618p (Rpr2) (Table 1.1). Yeast two-hybrid analysis has indicated protein-protein interactions for these RNase P subunits (Fig. 1.1) (Hall and Brown 2004). In addition, one of the protein subunits, *Pyrococcus furiosus* Pop5, appears to adopt a fold similar to that of the bacterial protein subunit (Fig. 1.1) (Wilson *et al*. 2006). This suggests that this eukaryotic protein might carry out some of the same functions as the bacterial RNase P protein, namely, protein contacts with either pre-tRNA substrate and/or RNA subunit. The structures of the other protein subunits in archaeal RNase P have been determined also (Evans *et al*. 2006). *Archaeoglobus fulgidus* Pop4 was shown to adopt an oligonucleotide fold, which is present in many other RNA-binding proteins indicating

probable RNA binding roles (Sidote *et al*. 2004). *Pyrococcus horikoshii* Rpp1 folds into an αβ barrel similar to the metallo-dependent hydrolase superfamily of proteins, while *P. horikoshii* Rpr2 folds into two α-helices with interactions at hydrophobic amino acids at the N-terminus along with a central domain comprised of an unstructured loop and a C-terminal zinc ribbon (Takagi *et al*. 2004; Kakuta *et al*. 2005). These structures are useful since the high degree of sequence homology between archaea and eukarya proteins is expected to extend to homology of tertiary, and possibly quaternary structures.

The effect of the protein on archaeal RNase P has been studied with the aid of bacterial precedence and eukaryotic homology. Fundamental roles of protein in the simple bacterial RNase P system have been preserved in the archaeal system, partially supported by the effect of adding protein to the archaeal RNase P RNA in reconstitution experiments. These experiments showed the addition of one to four protein subunits lowered the *in vitro* salt requirement for cleavage significantly while k_{cat} increased 25-fold and K_m decreased 170-fold (Tsai *et al*. 2006). It is not clear to what extent these changes are due to structural stabilization of the RNA subunit versus direct substrate interactions as both are probably occurring.

Eukaryotic RNase P: Diverse Functions From Related Origins

Like many other biosynthetic processes in eukaryotes, eukaryotic RNase P has been partitioned and localized into specific sub-cellular locations to allow for additional functions and more complex regulation (Walker and Engelke 2006). This partitioning has been accompanied by a split into multiple distinct enzymes, composed of varying levels of protein and RNA, and in some cases no RNA at all (see below). The simpler bacterial and archaeal RNase P holoenzymes have been replaced by nuclear RNase P, RNase

MRP, mitochondrial RNase P, and chloroplast RNase P. The archaeal trend of increased protein content compared to bacteria is further extended in these complexes, presumably to keep pace with an increase in the complexity of the RNA biosynthetic pathways in these systems.

RNase MRP

In eukaryotes another enzyme is added into the RNase P milieu, RNase MRP, which is closely related to nuclear RNase P but with different substrates (Chang and Clayton 1987; Schmitt and Clayton 1993; Gill *et al*. 2004). RNase MRP has only been found in eukaryotes thus far and shares many of the protein subunits with RNase P. Except for the RNase P-specific protein, Rpr2, RNase MRP in yeast has all the RNase P proteins and two additional RNase MRP-specific proteins, Snm1 and Rmp1 (Table 1.1) (Schmitt and Clayton 1994; Chamberlain *et al*. 1998; Salinas *et al*. 2005). RNase MRP also has its own RNA subunit, encoded by the *NME1* gene in yeast, which appears to be evolutionarily and structurally related to RNase P RNA (Forster and Altman 1990; Walker and Engelke 2006). In humans, RNase MRP also has a unique RNA subunit (7-2 RNA) which likely combines with seven of the ten human RNase P proteins: Rpp20, 25, 29, 30, 38, hPop5, and hPop1 (Table 1.1) (Forster and Altman 1990; Stolc and Altman 1997; Pluk *et al*. 1999; van Eenennaam *et al*. 1999; van Eenennaam *et al*. 2001; Welting *et al*. 2004; Walker and Engelke 2006). Many of these proteins show homology with yeast proteins and the RNA subunit is also similar (Table 1.1). The overlap in protein identity with RNase P points towards similar evolutionary origins for the complexes.

RNase MRP was originally shown to cleave mitochondrial RNA primers for DNA replication *in vitro*, leading to the enzyme's name (RNase Mitochondrial RNA

Processing) (Chang and Clayton 1987). Interestingly, bacterial RNase P has also been shown to have this capability (Table 1.2) (Potuschak *et al*. 1993). This RNase MRP cleavage result was controversial, as most RNase MRP was shown to localize to the nucleolus (Jacobson *et al*. 1995). RNase MRP has since been shown to process pre-rRNA by being required for cleavage at the A3 site within the ITS1 spacer, generating mature 5.8S rRNA *in vivo* (Schmitt and Clayton 1993). Recent localization of RNase MRP has shown that a minor fraction of the enzyme is also present in cytoplasmic processing bodies (P-bodies) in yeast, where it is proposed to be involved in processing Clb2 mRNA and possibly other mRNAs (Gill *et al*. 2004; Gill *et al*. 2006). This localization is relatively transient and dependent on the cell cycle. Thus, the main population of RNase MRP seems to be in the nucleolus but significant micro-populations can appear where its involvement in other RNA processing pathways is needed.

Mitochondrial RNase P

Mitochondrial RNase P activities are relatively diverse. Two of the best-studied examples are from yeast and human. In *S. cerevisiae* the holoenzyme is composed of an essential RNA subunit, Rpm1 (490 nt but varied by strain), that is encoded in the mitochondrial genome, and a nuclear encoded protein, Rpm2 (105 kDa) (Miller and Martin 1983; Dang and Martin 1993). Rpm1 has lost structural complexity compared to nuclear RNase P RNA Rpr1 but does still share a few conserved regions (Seif *et al*. 2003). Given the relatively large size of the Rpm2 protein, the loss in complexity of the RNA could be compensated for by the protein subunit. Rpm2 can localize to the nucleus, as well as the mitochondrion, and act as a transcriptional activator of mitochondrial

mRNAs used for mitochondrial chaperones and import (Stribinskis and Ramos 2007). In addition it appears that it plays a role in coordination of transcription and mRNA decay and storage in cytoplasmic P-bodies (Stribinskis and Ramos 2007).

Despite the widespread presence of RNA subunits in yeast mitochondrial RNase P, it is increasingly accepted that organelles in other organisms may have developed alternative RNase P activities through convergent evolution to solve the same problem without RNA. Recent evidence shows that at least human mitochondrial RNase P does not contain an RNA subunit, as only three protein subunits were required to reconstitute pre-tRNA cleavage activity (Holzmann *et al*. 2008). These proteins are as follows: a tRNA methyltransferase (MRPP1), a short-chain dehydrogenase/reductase family member (MRPP2), and a previously unidentified metallonuclease (MRPP3) (Holzmann and Rossmanith 2009). This collection of protein components, none of which are homologous to known RNase P proteins, combines to provide specific pre-tRNA recognition and cleavage products that are indistinguishable from other examples of RNase P.

Not surprisingly, differences in substrate recognition are observed between human mitochondrial RNase P and other examples of RNase P. Due to the lack of RNA in the complex, key determinants for recognition appear to be drastically different from "traditional" RNase P. Mutations in the D-domain and anticodon stem were shown to specifically affect processing by mitochondrial RNase P but not nuclear RNase P (Fig. 1.2) (Rossmanith and Karwan 1998). There are presumably contacts near the active site as cleavage is the same as canonical RNase P processing, though this has not yet been investigated in detail.

Chloroplast RNase P

The nature of chloroplast RNase P appears to mirror mitochondrial RNase P in its varied RNA content. Cyanelle of primitive alga *Cyanophora paradoxa* have been shown to have both RNA and protein subunits that are required for activity (Cordier and Schön 1999). This is in contrast to spinach chloroplasts where there has not been an RNA subunit identified (Thomas *et al*. 2000). Recently, in chloroplasts and mitochondria of *Arabidopsis thaliana* it was shown that an ortholog of the human mitochondrial RNase P protein *MRPP3*, termed *PRORP1*, had RNase P activity (Gobert *et al*. 2010). It is interesting that the cleavage of pre-tRNA can be carried out with either an RNA active site or a protein only active site.

Nuclear RNase P

One example of nuclear RNase P is in *S. cerevisiae* where the complex is composed of an RNA subunit with nine essential proteins (Lee and Engelke 1989; Chamberlain *et al*. 1998). The RNA subunit has conserved features of the bacterial RNA, however, certain regions are added or deleted in the structure (Fig. 1.1) (Frank *et al*. 2000; Evans *et al*. 2006). The RNA subunit and all of the protein subunits are required for RNase P activity, which is essential for life in yeast (Lee *et al*. 1991; Lygerou *et al*. 1994; Chu *et al*. 1997; Dichtl and Tollervey 1997; Stolc and Altman 1997; Chamberlain *et al*. 1998). Also, yeast are estimated to have only ~200 molecules of unstable enzyme per cell. The instability of RNase P and low amount of material combined with the insolubility of most of the protein components has limited the types of experiments that can be carried out with this complex.

The RNA component of RNase P in *S. cerevisiae* is Rpr1 and is 369 nt long in mature form (Lee *et al*. 1991). It is transcribed by RNA polymerase III as a 487 nt precursor that is processed at some point during its assembly with the protein subunits (Fig. 1.1) (Lee *et al*. 1991; Srisawat *et al*. 2002). The protein subunits interact with both the RNA subunit and each other to form the RNase P complex. In yeast these subunits are Pop1, Pop3, Pop4, Pop5, Pop6, Pop7, Pop8, Rpp1, and Rpr2 (Fig. 1.1, Table 1.1) (Chamberlain *et al*. 1998). It appears that Pop1 and Pop4 make contacts with the RNA subunit, with Pop1 interacting with the eukaryote-specific P3 loop (Houser-Scott *et al*. 2002). In addition, bacterially expressed yeast Pop6/Pop7 were shown to form a heterodimer and bind specifically to the P3 loop of the RNA subunit (Perederina *et al*. 2007). Thus, the P3 loop in the RNA subunit appears to accommodate many protein contacts. The other proteins have not been shown to bind directly to the RNA subunit in yeast but have been shown to bind to other protein subunits in the complex (Fig. 1.1) (Houser-Scott *et al*. 2002). There are, however, two proteins that appear to be added after an active precursor complex has been formed: Pop3 and Rpr2 (Srisawat *et al*. 2002). The roles of Pop3 and Rpr2 can be inferred as not essential for pre-tRNA binding and cleavage *in vitro*, but the fact that they are present in the majority of RNase P in the cell and that Rpr2 is a unique protein subunit of RNase P, points towards important roles in the complex (Srisawat *et al*. 2002).

Nuclear RNase P from humans has also been extensively studied. Human RNase P has a single RNA subunit, H1, and at least ten proteins, seven of which are homologous to yeast RNase P proteins (Table 1.1) (Bartkiewicz *et al*. 1989; Baer *et al*. 1990; Lygerou *et al*. 1996; Jarrous *et al*. 1999; van Eenennaam *et al*. 1999; Ame *et al*. 2001; Jarrous and

Altman 2001; van Eenennaam *et al*. 2001; Jarrous 2002). In human RNase P it has been shown that Rpp14, Rpp29 and Rpp21 can bind the tRNA substrate *in vitro* (Jarrous *et al*. 2001). One difficulty with these types of experiments is that most RNase P proteins have large patches of mostly basic amino acids (KKD/E) that have a high potential for binding single stranded RNA (Xiao *et al*. 2002). Further, seven of the yeast proteins have calculated pI values higher than 9 except for Pop8 and Pop5, which have pIs of 4.6 and 7.8. These motifs could combine to serve as specific RNA binding sites for either substrates or the RNA subunit when correctly assembled *in vivo* but when over expressed *in vitro* these binding sites could be relatively non-specific.

Like its evolutionarily related cousin RNase MRP, RNase P is found primarily in the nucleolus in yeast (Bertrand *et al*. 1998; Srisawat *et al*. 2002). In humans the localization is less constant, with proteins and/or the RNA subunit found in the nucleoplasm, cytoplasm, cajal bodies, and the perinucleolar compartment (Jarrous 2002). Multiple localizations of RNase P would be consistent with the behavior of the highly related RNase MRP, which in turn is consistent with the discovery of multiple types of substrate (Table 1.2) (Gill *et al*. 2006).

Substrate Recognition

Despite the high protein content in nuclear RNase P it appears that the mechanism of pre-tRNA cleavage remains the same as bacterial RNase P and is housed in the RNA subunit. Early phosphorothioate substitution experiments with substrates showed that yeast RNase P has the same type of Mg^{2+} dependence and chemical products that bacterial RNase P does (Pfeiffer *et al*. 2000). Also it was recently shown that the human RNase P RNA can cleave tRNA without protein, albeit with extremely low activity and at

high salt (Kikovska *et al*. 2007). It is interesting to note that with all the increased complexity of eukaryotic RNase P compared to bacterial RNase P, the overall mechanism of pre-tRNA cleavage appears to be roughly the same with an initial burst of tRNA formation followed by a rate-limiting step after pre-tRNA cleavage, which is most likely product release (Hsieh *et al*. 2008). In addition, the same study suggested that there appears to be a kinetically important conformational change during catalysis akin to the bacterial RNase P.

In eukaryotes the nature of pre-tRNA transcripts is somewhat different from those in bacteria. Pre-tRNAs are synthesized by RNA polymerase III and are terminated by a 5′-polyuridine (U_{4-6}) sequence soon after the end of the aminoacyl stem (Geiduschek and Tocchini-Valentini 1988). This tail sequence is usually present when RNase P cleaves the 5′-leader, and usually has the capacity to form a short Watson-Crick stem with the 5′-leader sequence. However, if this 5′ leader/3′ trailer pairing forms a continuous extension of the acceptor stem, RNase P is unable to cleave, suggesting that the 5′ leader and 3′ trailer might need to be separated for cleavage to occur (Lee *et al*. 1997). Another change in recognition by nuclear RNase P is that there does not appear to be any interaction between 3′ trailers of pre-tRNAs and internal RNase P sequences, as sometimes found with the bacterial RNase P RNA P15 region (Kirsebom and Svärd 1994). It is not yet clear what portion of the RNase P holoenzyme interacts with the pre-tRNA leader and trailer, since removal of these sequences has relatively minor effects on substrate K_m (Ziehler *et al*. 2000). My work shown in CHAPTER 2 will indicate that pre-tRNA makes only limited contacts with the RNA subunit of RNase P. However, protein contacts could only be obtained with single stranded RNA and not pre-tRNA.

In addition to the substrate differences, minimal substrate requirements are also altered in eukaryotic RNase P. The same major contacts that are important in bacterial RNase P are required with pre-tRNAs in eukaryotes, namely the T stem plus acceptor stem coaxial structure, but there is an extra requirement of a bulge between the two stems for eukaryotic RNase P (Fig. 1.2) (Yuan and Altman 1995). This bulge can be as small as one nucleotide but more flexibility appears to improve cleavage rates.

Accompanying the loss of some of the bacterial pre-tRNA contacts, nuclear RNase P has acquired new eukaryotic-specific single-stranded RNA contacts. Eukaryotic RNase P binds more strongly to single-stranded RNA than bacterial RNase P, inhibiting pre-tRNA cleavage only in yeast RNase P (Ziehler *et al*. 2000). Proteins seem probable sites for these interactions, as most of the nine protein subunits are very basic. This binding showed strong sequence dependence with RNA homopolymers (polyG>U>>A>>>C) (Table 1.2) (Ziehler *et al*. 2000). In contrast to single stranded RNAs, a highly structured RNA, 5S rRNA, showed little or no competition with tRNA (Ziehler *et al*. 2000). It seems likely that the tight binding resulting in inhibition is a collaboration between more than one individual RNA binding site, since short homopolymers (U_7 and U_{11}) had no effect, and the 3′ oligoU trailer on pre-tRNAs does not strongly affect the K_m of the yeast nuclear RNase P (Ziehler *et al*. 2000). CHAPTER 2 of this work will show how single stranded RNA interacts with RNase P, indicating that it makes contacts with the RNase P proteins Pop4, Rpr2, and Pop1 in addition to interacting with the RNA subunit Rpr1 in a similar position to the pre-tRNA substrate.

In eukaryotes there have also been non-tRNA substrates discovered and a much larger number of possible substrates suggested, though this has not yet been explored

extensively (Table 1.2). One example is a noncoding, antisense RNA, Hra1, which is cleaved by RNase P in *S. cerevisiae* (Yang and Altman 2007). Recently, RNase P in yeast has been shown to be involved in one of the pathways for the maturation of box C/D intron-encoded small nucleolar RNAs (snoRNAs) (Coughlin *et al*. 2008). Although highly selective cleavage could not be reproduced *in vitro* using deproteinated intron substrates, the pre-snoRNAs co-immunoprecipitated with RNase P and *in vivo* analysis of RNase P conditional mutants confirmed accumulation of precursor snoRNAs in RNase P-deficient strains.

A broad range of additional RNA has been identified as potential RNase P substrates in addition to the ones outlined in Table 1.2. These RNAs were identified as ones that co-purified with RNase P and whose abundance or size is affected by defects in RNase P RNA (Rpr1), the RNase P-specific protein subunit (Rpr2), and/or the largest protein subunit (Pop1). These studies found that several groups of RNA were affected by and associated physically with RNase P (Coughlin *et al*. 2008). The RNA included mRNAs that encode protein subunits of the ribosome, mRNAs from subunits of RNA polymerases I, II, III, translation initiation factor mRNA, intron encoded box C/D snoRNA, and transcripts from six intergenic regions. The methodology employed for the original binding studies did not detect non-coding region (inter-ORF) RNAs and did not differentiate between "sense" and "antisense" strands in each region, leaving open the possibility that RNase P might be interacting with either strand, or even possible sense/antisense hybrids. Thus, additional studies are needed to further parse the potential substrate dataset based on strand specificity.

Other potential yeast RNase P substrates were identified in a separate study with the depletion of Rpp1, a protein that is a subunit of both RNase P and RNase MRP (Samanta *et al*. 2006). These data had relatively little overlap with the Coughlin *et al.* study, possibly indicating RNase MRP substrates. However, one interesting set of potential substrates identified were several novel non-coding RNAs that were either adjacent or antisense to protein coding genes (Samanta *et al*. 2006). This dataset was limited by probe design and because the protein that was mutated was shared by RNase P and RNase MRP. A strand specific, high-density microarray analysis of the RNA that accumulates with RNase P depletion is presented in CHAPTER 3.

Conclusion

The evolutionary pressure to retain the RNA subunit of RNase P appears to be very strong. Regardless of what additional substrates RNase P might have been co-opted to cleave, the need for pre-tRNA cleavage is fundamental. This was recently shown with *Nanoarchaeum equitans* in which the lack of pre-tRNA 5′ leader sequences in primary transcripts from this very compact and relatively simplified genome seems to have resulted in the loss of RNase P activity (Randau *et al*. 2008). Contrasted with this leaderless tRNA genome, most organisms have retained the catalytic RNA core of the enzyme, while adding protein content to allow it to selectively recognize the increasing number of possible RNA substrates in more complex organisms and still maintaining pre-tRNA cleavage. It appears that the RNA processing ability of the RNA subunit has needed "shoring up" by more and more proteins to cope with further cellular complexity (Fig. 1.1). Although the current discussion has focused on the likelihood that the extra proteins have increased potential for substrate recognition, protein complexity might also

be required for correct cellular localization, RNA subunit stabilization, and cooperation with other RNA processing components. The end result is that all of these factors have provided increased functionality to the RNA core.

Objectives of This Work

Many laboratories have worked to understand how RNase P recognizes and cleaves various substrates. Detailed kinetic and structural studies have been carried out with bacterial RNase P and archaeal RNase P using reconstituted complexes. In the more complex eukaryotic RNase P large-scale purifications of active RNase P must be carried out before any experiment can be done. Thus limited types of experiments are feasible with eukaryotic RNase P.

In this work I used rapid purification of RNase P from *S. cerevisiae* to determine how RNA interacts with RNase P *in vitro* (CHAPTER 2). In order to understand how RNase P interacts with non-tRNA substrates and inhibitors I strove to understand how single stranded RNA interacts with purified RNase P (CHAPTER 2). I used inhibitor studies and *in vitro* cleavage analysis combined with UV crosslinking studies to characterize how RNA interacts with the purified complex. In CHAPTER 3 I expand upon the *in vitro* findings in CHAPTER 2 to *in vivo* roles of RNase P. Using a high-density, strand specific microarray I identified RNA that accumulates with RNase P temperature sensitive mutation. This study points towards potential non-tRNA substrates for RNase P and possible broad indirect effects on RNA accumulation due to depleting RNase P from nuclei. CHAPTER 4 discusses the implications of this work and indicates further experiments that would expand upon my findings in the future.

Acknowledgments

I would like to thank Dr. Scott Walker for discussion of RNase P background information. He was a great resource for background information and experimental details. In addition, the RNase P group meeting held jointly with the Carol Fierke Lab was vital for a full exposure to RNase P research with their work using bacterial RNase P. This work was supported by grants from the Cellular Biotechnology Training Grant NIH T32-GM08353, and GM034869 and GM082875-01A1 (both to D.R.E) from NIH. Further funding was provided by the Horace H. Rackham School of graduate studies at the University of Michigan.

References

Alifano P, Rivellini F, Piscitelli C, Arraiano C, Bruni C, Carlomagno M. 1994. Ribonuclease E provides substrates for ribonuclease P-dependent processing of a polycistronic mRNA. *Genes Dev* **8**(24): 3021-3031.

Altman S, Wesolowski D, Guerrier-Takada C, Li Y. 2005. RNase P cleaves transient structures in some riboswitches. *Proc Natl Acad Sci USA* **102**(32): 11284-11289.

Ame JC, Schreiber V, Fraulob V, Dolle P, de Murcia G, Niedergang CP. 2001. A bidirectional promoter connects the poly(ADP-ribose) polymerase 2 (PARP-2) gene to the gene for RNase P RNA. structure and expression of the mouse PARP-2 gene. *J Biol Chem* **276**(14): 11092-11099.

Baer M, Nilsen TW, Costigan C, Altman S. 1990. Structure and transcription of a human gene for H1 RNA, the RNA component of human RNase P. *Nucleic Acids Res* **18**(1): 97-103.

Ban N, Nissen P, Hansen J, Moore PB, Steitz TA. 2000. The complete atomic structure of the large ribosomal subunit at 2.4 A resolution. *Science* **289**(5481): 905-920.

Bartkiewicz M, Gold H, Altman S. 1989. Identification and characterization of an RNA molecule that copurifies with RNase P activity from HeLa cells. *Genes & Development* **3**(4): 488-499.

Bertrand E, Houser-Scott F, Kendall A, Singer RH, Engelke DR. 1998. Nucleolar localization of early tRNA processing. *Genes Dev* **12**(16): 2463-2468.

Bothwell AL, Stark BC, Altman S. 1976. Ribonuclease P substrate specificity: cleavage of a bacteriophage phi80-induced RNA. *Proc Natl Acad Sci USA* **73**(6): 1912-1916.

Brown JW. 1999. The Ribonuclease P Database. *Nucleic Acids Res* **27**(1): 314.

Chamberlain JR, Lee Y, Lane WS, Engelke DR. 1998. Purification and characterization of the nuclear RNase P holoenzyme complex reveals extensive subunit overlap with RNase MRP. *Genes Dev* **12**(11): 1678-1690.

Chang DD, Clayton DA. 1987. A novel endoribonuclease cleaves at a priming site of mouse mitochondrial DNA replication. *EMBO J* **6**(2): 409-417.

Chu S, Zengel JM, Lindahl L. 1997. A novel protein shared by RNase MRP and RNase P. *RNA (New York, NY)* **3**(4): 382-391.

Cordier A, Schön A. 1999. Cyanelle RNase P: RNA structure analysis and holoenzyme properties of an organellar ribonucleoprotein enzyme. *J Mol Biol* **289**(1): 9-20.

Coughlin DJ, Pleiss JA, Walker SC, Whitworth GB, Engelke DR. 2008. Genome-wide search for yeast RNase P substrates reveals role in maturation of intron-encoded box C/D small nucleolar RNAs. *Proc Natl Acad Sci USA* **105**(34): 12218-12223.

Dang YL, Martin NC. 1993. Yeast mitochondrial RNase P. Sequence of the RPM2 gene and demonstration that its product is a protein subunit of the enzyme. *J Biol Chem* **268**(26): 19791-19796.

Dichtl B, Tollervey D. 1997. Pop3p is essential for the activity of the RNase MRP and RNase P ribonucleoproteins *in vivo*. *The EMBO Journal* **16**(2): 417-429.

Evans D, Marquez SM, Pace NR. 2006. RNase P: interface of the RNA and protein worlds. *Trends Biochem Sci* **31**(6): 333-341.

Forster AC, Altman S. 1990. Similar cage-shaped structures for the RNA components of all ribonuclease P and ribonuclease MRP enzymes. *Cell* **62**(3): 407-409.

Frank DN, Adamidi C, Ehringer MA, Pitulle C, Pace NR. 2000. Phylogenetic-comparative analysis of the eukaryal ribonuclease P RNA. *RNA* **6**(12): 1895-1904.

Frank DN, Pace NR. 1998. Ribonuclease P: unity and diversity in a tRNA processing ribozyme. *Annu Rev Biochem* **67**: 153-180.

Geiduschek EP, Tocchini-Valentini GP. 1988. Transcription by RNA polymerase III. *Annu Rev Biochem* **57**: 873-914.

Giegé R, Florentz C, Dreher TW. 1993. The TYMV tRNA-like structure. *Biochimie* **75**(7): 569-582.

Gill T, Aulds J, Schmitt ME. 2006. A specialized processing body that is temporally and asymmetrically regulated during the cell cycle in *Saccharomyces cerevisiae*. *The Journal of Cell Biology* **173**(1): 35-45.

Gill T, Cai T, Aulds J, Wierzbicki S, Schmitt ME. 2004. RNase MRP cleaves the CLB2 mRNA to promote cell cycle progression: novel method of mRNA degradation. *Mol Cell Biol* **24**(3): 945-953.

Gimple O, Schön A. 2001. *In vitro* and *in vivo* processing of cyanelle tmRNA by RNase P. *Biol Chem* **382**(10): 1421-1429.

Gobert A, Gutmann B, Taschner A, Gößringer M, Holzmann J, Hartmann RK, Rossmanith W, Giegé P. 2010. A single Arabidopsis organellar protein has RNase P activity. *Nat Struct Mol Biol* **17**(6): 740-744.

Gössringer M, Kretschmer-Kazemi Far R, Hartmann RK. 2006. Analysis of RNase P protein (rnpA) expression in *Bacillus subtilis* utilizing strains with suppressible rnpA expression. *J Bacteriol* **188**(19): 6816-6823.

Guerrier-Takada C, Altman S. 1984. Catalytic activity of an RNA molecule prepared by transcription *in vitro*. *Science* **223**(4633): 285-286.

Guerrier-Takada C, Gardiner K, Marsh T, Pace N, Altman S. 1983. The RNA moiety of ribonuclease P is the catalytic subunit of the enzyme. *Cell* **35**(3 Pt 2): 849-857.

Hall TA, Brown JW. 2002. Archaeal RNase P has multiple protein subunits homologous to eukaryotic nuclear RNase P proteins. *RNA* **8**(3): 296-306.

Hall TA, Brown JW. 2004. Interactions between RNase P protein subunits in archaea. *Archaea* **1**(4): 247-254.

Hansen A, Pfeiffer T, Zuleeg T, Limmer S, Ciesiolka J, Feltens R, Hartmann RK. 2001. Exploring the minimal substrate requirements for trans-cleavage by RNase P holoenzymes from *Escherichia coli* and *Bacillus subtilis*. *Mol Microbiol* **41**(1): 131-143.

Harris JK, Haas ES, Williams D, Frank DN, Brown JW. 2001. New insight into RNase P RNA structure from comparative analysis of the archaeal RNA. *RNA* **7**(2): 220-232.

Hartmann RK, Heinrich J, Schlegl J, Schuster H. 1995. Precursor of C4 antisense RNA of bacteriophages P1 and P7 is a substrate for RNase P of *Escherichia coli*. *Proc Natl Acad Sci USA* **92**(13): 5822-5826.

Herrmann B, Pettersson B, Everett KD, Mikkelsen NE, Kirsebom LA. 2000. Characterization of the rnpB gene and RNase P RNA in the order Chlamydiales. *Int J Syst Evol Microbiol* **50 Pt 1**: 149-158.

Holzmann J, Frank P, Löffler E, Bennett KL, Gerner C, Rossmanith W. 2008. RNase P without RNA: identification and functional reconstitution of the human mitochondrial tRNA processing enzyme. *Cell* **135**(3): 462-474.

Holzmann J, Rossmanith W. 2009. tRNA recognition, processing, and disease: hypotheses around an unorthodox type of RNase P in human mitochondria. *Mitochondrion* **9**(4): 284-288.

Houser-Scott F, Xiao S, Millikin CE, Zengel JM, Lindahl L, Engelke DR. 2002. Interactions among the protein and RNA subunits of *Saccharomyces cerevisiae* nuclear RNase P. *Proc Natl Acad Sci USA* **99**(5): 2684-2689.

Hsieh J, Walker SW, Fierke CA, Engelke DR. 2008. Pre-tRNA turnover catalyzed by the yeast nuclear RNase P holoenzyme is limited by product release. *RNA,* **15**(2): 1565-1577 .

Jacobson MR, Cao LG, Wang YL, Pederson T. 1995. Dynamic localization of RNase MRP RNA in the nucleolus observed by fluorescent RNA cytochemistry in living cells. *The Journal of Cell Biology* **131**(6 Pt 2): 1649-1658.

Jarrous N. 2002. Human ribonuclease P: subunits, function, and intranuclear localization. *RNA* **8**(1): 1-7.

Jarrous N, Altman S. 2001. Human ribonuclease P. *Meth Enzymol* **342**: 93-100.

Jarrous N, Eder PS, Wesolowski D, Altman S. 1999. Rpp14 and Rpp29, two protein subunits of human ribonuclease P. *RNA (New York, NY)* **5**(2): 153-157.

Jarrous N, Reiner R, Wesolowski D, Mann H, Guerrier-Takada C, Altman S. 2001. Function and subnuclear distribution of Rpp21, a protein subunit of the human ribonucleoprotein ribonuclease P. *RNA* **7**(8): 1153-1164.

Jung YH, Lee Y. 1995. RNases in ColE1 DNA metabolism. *Mol Biol Rep* **22**(2-3): 195-200.

Kakuta Y, Ishimatsu I, Numata T, Kimura K, Yao M, Tanaka I, Kimura M. 2005. Crystal structure of a ribonuclease P protein Ph1601p from *Pyrococcus horikoshii* OT3:

an archaeal homologue of human nuclear ribonuclease P protein Rpp21. *Biochemistry* **44**(36): 12086-12093.

Kikovska E, Svärd SG, Kirsebom LA. 2007. Eukaryotic RNase P RNA mediates cleavage in the absence of protein. *Proc Natl Acad Sci USA* **104**(7): 2062-2067.

Kirsebom LA. 2007. RNase P RNA mediated cleavage: substrate recognition and catalysis. *Biochimie* **89**(10): 1183-1194.

Kirsebom LA, Svärd SG. 1994. Base pairing between *Escherichia coli* RNase P RNA and its substrate. *EMBO J* **13**(20): 4870-4876.

Komine Y, Kitabatake M, Yokogawa T, Nishikawa K, Inokuchi H. 1994. A tRNA-like structure is present in 10Sa RNA, a small stable RNA from *Escherichia coli*. *Proc Natl Acad Sci USA* **91**(20): 9223-9227.

Kurz JC, Fierke CA. 2002. The affinity of magnesium binding sites in the *Bacillus subtilis* RNase P x pre-tRNA complex is enhanced by the protein subunit. *Biochemistry* **41**(30): 9545-9558.

Lee JY, Engelke DR. 1989. Partial characterization of an RNA component that copurifies with *Saccharomyces cerevisiae* RNase P. *Molecular and Cellular Biology* **9**(6): 2536-2543.

Lee JY, Rohlman CE, Molony LA, Engelke DR. 1991. Characterization of RPR1, an essential gene encoding the RNA component of *Saccharomyces cerevisiae* nuclear RNase P. *Molecular and Cellular Biology* **11**(2): 721-730.

Lee Y, Kindelberger DW, Lee JY, McClennen S, Chamberlain J, Engelke DR. 1997. Nuclear pre-tRNA terminal structure and RNase P recognition. *RNA* **3**(2): 175-185.

Li Y, Altman S. 2003. A specific endoribonuclease, RNase P, affects gene expression of polycistronic operon mRNAs. *Proc Natl Acad Sci USA* **100**(23): 13213-13218.

Liu F, Altman S. 1994. Differential evolution of substrates for an RNA enzyme in the presence and absence of its protein cofactor. *Cell* **77**(7): 1093-1100.

Loria A, Niranjanakumari S, Fierke CA, Pan T. 1998. Recognition of a pre-tRNA substrate by the *Bacillus subtilis* RNase P holoenzyme. *Biochemistry* **37**(44): 15466-15473.

Lygerou Z, Mitchell P, Petfalski E, Séraphin B, Tollervey D. 1994. The *POP1* gene encodes a protein component common to the RNase MRP and RNase P ribonucleoproteins. *Genes Dev* **8**(12): 1423-1433.

Lygerou Z, Pluk H, van Venrooij WJ, Séraphin B. 1996. hPop1: an autoantigenic protein subunit shared by the human RNase P and RNase MRP ribonucleoproteins. *The EMBO Journal* **15**(21): 5936-5948.

Miller DL, Martin NC. 1983. Characterization of the yeast mitochondrial locus necessary for tRNA biosynthesis: DNA sequence analysis and identification of a new transcript. *Cell* **34**(3): 911-917.

Muth GW, Ortoleva-Donnelly L, Strobel SA. 2000. A single adenosine with a neutral pKa in the ribosomal peptidyl transferase center. *Science* **289**(5481): 947-950.

Niranjanakumari S, Kurz JC, Fierke CA. 1998a. Expression, purification and characterization of the recombinant ribonuclease P protein component from *Bacillus subtilis*. *Nucleic Acids Res* **26**(13): 3090-3096.

Niranjanakumari S, Stams T, Crary SM, Christianson DW, Fierke CA. 1998b. Protein component of the ribozyme ribonuclease P alters substrate recognition by directly contacting precursor tRNA. *Proc Natl Acad Sci USA* **95**(26): 15212-15217.

Nissen P, Hansen J, Ban N, Moore PB, Steitz TA. 2000. The structural basis of ribosome activity in peptide bond synthesis. *Science* **289**(5481): 920-930.

Pan T, Jakacka M. 1996. Multiple substrate binding sites in the ribozyme from *Bacillus subtilis* RNase P. *The EMBO Journal* **15**(9): 2249-2255.

Pannucci JA, Haas ES, Hall TA, Harris JK, Brown JW. 1999. RNase P RNAs from some Archaea are catalytically active. *Proc Natl Acad Sci USA* **96**(14): 7803-7808.

Peck-Miller KA, Altman S. 1991. Kinetics of the processing of the precursor to 4.5 S RNA, a naturally occurring substrate for RNase P from *Escherichia coli*. *J Mol Biol* **221**(1): 1-5.

Perederina A, Esakova O, Koc H, Schmitt ME, Krasilnikov AS. 2007. Specific binding of a Pop6/Pop7 heterodimer to the P3 stem of the yeast RNase MRP and RNase P RNAs. *RNA*. **13**(10): 1648-1655.

Pfeiffer T, Tekos A, Warnecke JM, Drainas D, Engelke DR, Séraphin B, Hartmann RK. 2000. Effects of phosphorothioate modifications on precursor tRNA processing by eukaryotic RNase P enzymes. *J Mol Biol* **298**(4): 559-565.

Pluk H, van Eenennaam H, Rutjes SA, Pruijn GJ, van Venrooij WJ. 1999. RNA-protein interactions in the human RNase MRP ribonucleoprotein complex. *RNA* **5**(4): 512-524.

Potuschak T, Rossmanith W, Karwan R. 1993. RNase MRP and RNase P share a common substrate. *Nucleic Acids Res* **21**(14): 3239-3243.

Randau L, Schröder I, Söll D. 2008. Life without RNase P. *Nature* **453**(7191): 120-123.

Rossmanith W, Karwan RM. 1998. Characterization of human mitochondrial RNase P: novel aspects in tRNA processing. *Biochem Biophys Res Commun* **247**(2): 234-241.

Salinas K, Wierzbicki S, Zhou L, Schmitt ME. 2005. Characterization and purification of *Saccharomyces cerevisiae* RNase MRP reveals a new unique protein component. *J Biol Chem* **280**(12): 11352-11360.

Samanta MP, Tongprasit W, Sethi H, Chin CS, Stolc V. 2006. Global identification of noncoding RNAs in *Saccharomyces cerevisiae* by modulating an essential RNA processing pathway. *Proc Natl Acad Sci USA* **103**(11): 4192-4197.

Schmitt M, Clayton DA. 1994. Characterization of a unique protein component of yeast RNase MRP: an RNA-binding protein with a zinc-cluster domain. *Genes Dev* **8**(21): 2617-2628.

Schmitt ME, Clayton DA. 1993. Nuclear RNase MRP is required for correct processing of pre-5.8S rRNA in *Saccharomyces cerevisiae*. *Mol Cell Biol* **13**(12): 7935-7941.

Seif ER, Forget L, Martin NC, Lang BF. 2003. Mitochondrial RNase P RNAs in ascomycete fungi: lineage-specific variations in RNA secondary structure. *RNA* **9**(9): 1073-1083.

Shi H, Moore PB. 2000. The crystal structure of yeast phenylalanine tRNA at 1.93 A resolution: a classic structure revisited. *RNA* **6**(8): 1091-1105.

Sidote DJ, Heideker J, Hoffman DW. 2004. Crystal structure of archaeal ribonuclease P protein aRpp29 from *Archaeoglobus fulgidus*. *Biochemistry* **43**(44): 14128-14138.

Smith J, Hsieh J, Fierke CA. 2007. Importance of RNA-protein interactions in bacterial ribonuclease P structure and catalysis. *Biopolymers* **87**(5-6): 329-338.

Srisawat C, Houser-Scott F, Bertrand E, Xiao S, Singer RH, Engelke DR. 2002. An active precursor in assembly of yeast nuclear ribonuclease P. *RNA* **8**(10): 1348-1360.

Stams T, Niranjanakumari S, Fierke CA, Christianson DW. 1998. Ribonuclease P protein structure: evolutionary origins in the translational apparatus. *Science* **280**(5364): 752-755.

Stolc V, Altman S. 1997. Rpp1, an essential protein subunit of nuclear RNase P required for processing of precursor tRNA and 35S precursor rRNA in *Saccharomyces cerevisiae*. *Genes & Development* **11**(21): 2926-2937.

Stribinskis V, Ramos KS. 2007. Rpm2p, a protein subunit of mitochondrial RNase P, physically and genetically interacts with cytoplasmic processing bodies. *Nucleic Acids Res* **35**(4): 1301-1311.

Sun L, Campbell F, Zahler NH, Harris ME. 2006. Evidence that substrate-specific effects of C5 protein lead to uniformity in binding and catalysis by RNase P. *EMBO J* **25**(17): 3998-4007.

Sun L, Harris ME. 2007. Evidence that binding of C5 protein to P RNA enhances ribozyme catalysis by influencing active site metal ion affinity. *RNA* **13**(9): 1505-1515.

Takagi H, Watanabe M, Kakuta Y, Kamachi R, Numata T, Tanaka I, Kimura M. 2004. Crystal structure of the ribonuclease P protein Ph1877p from hyperthermophilic archaeon *Pyrococcus horikoshii* OT3. *Biochem Biophys Res Commun* **319**(3): 787-794.

Thomas BC, Li X, Gegenheimer P. 2000. Chloroplast ribonuclease P does not utilize the ribozyme-type pre-tRNA cleavage mechanism. *RNA* **6**(4): 545-553.

Thurlow DL, Shilowski D, Marsh TL. 1991. Nucleotides in precursor tRNAs that are required intact for catalysis by RNase P RNAs. *Nucleic Acids Res* **19**(4): 885-891.

Tsai HY, Pulukkunat DK, Woznick WK, Gopalan V. 2006. Functional reconstitution and characterization of *Pyrococcus furiosus* RNase P. *Proc Natl Acad Sci USA* **103**(44): 16147-16152.

van Eenennaam H, Lugtenberg D, Vogelzangs JH, van Venrooij WJ, Pruijn GJ. 2001. hPop5, a protein subunit of the human RNase MRP and RNase P endoribonucleases. *J Biol Chem* **276**(34): 31635-31641.

van Eenennaam H, Pruijn GJ, van Venrooij WJ. 1999. hPop4: a new protein subunit of the human RNase MRP and RNase P ribonucleoprotein complexes. *Nucleic Acids Res* **27**(12): 2465-2472.

Walker SC, Engelke DR. 2006. Ribonuclease P: the evolution of an ancient RNA enzyme. *Crit Rev Biochem Mol Biol* **41**(2): 77-102.

Wegscheid B, Condon C, Hartmann RK. 2006. Type A and B RNase P RNAs are interchangeable *in vivo* despite substantial biophysical differences. *EMBO Rep* **7**(4): 411-417.

Welting TJM, van Venrooij WJ, Pruijn GJM. 2004. Mutual interactions between subunits of the human RNase MRP ribonucleoprotein complex. *Nucleic Acids Res* **32**(7): 2138-2146.

Westhof E, Wesolowski D, Altman S. 1996. Mapping in three dimensions of regions in a catalytic RNA protected from attack by an Fe(II)-EDTA reagent. *J Mol Biol* **258**(4): 600-613.

Wilson RC, Bohlen CJ, Foster MP, Bell CE. 2006. Structure of Pfu Pop5, an archaeal RNase P protein. *Proc Natl Acad Sci USA* **103**(4): 873-878.

Wilusz JE, Freier SM, Spector DL. 2008. 3' end processing of a long nuclear-retained noncoding RNA yields a tRNA-like cytoplasmic RNA. *Cell* **135**(5): 919-932.

Xiao S, Scott F, Fierke CA, Engelke DR. 2002. Eukaryotic ribonuclease P: a plurality of ribonucleoprotein enzymes. *Annu Rev Biochem* **71**: 165-189.

Yang L, Altman S. 2007. A noncoding RNA in *Saccharomyces cerevisiae* is an RNase P substrate. *RNA* **13**(5): 682-690.

Yuan Y, Altman S. 1995. Substrate recognition by human RNase P: identification of small, model substrates for the enzyme. *EMBO J* **14**(1): 159-168.

Ziehler WA, Day JJ, Fierke CA, Engelke DR. 2000. Effects of 5' leader and 3' trailer structures on pre-tRNA processing by nuclear RNase P. *Biochemistry* **39**(32): 9909-9916.

CHAPTER 2
BINDING AND CLEAVAGE OF UNSTRUCTURED RNA BY NUCLEAR RNASE P

Introduction

Ribonuclease P (RNase P) is a highly conserved complex of RNA and protein subunits with the well-defined function of processing precursor transfer RNAs (pre-tRNAs) via an endonucleolytic cleavage to create their mature 5′ termini (Frank and Pace 1998; Walker and Engelke 2006). In almost all reported examples, RNase P has a similar catalytic RNA subunit that is responsible for pre-tRNA cleavage (Guerrier-Takada *et al*. 1983; Holzmann *et al*. 2008; Gobert *et al*. 2010). *In vivo*, protein subunit(s) are also required for proper function and they are present in varying numbers with generally 1 in Bacteria, 4-5 in some Archaea, and 9-10 in Eukarya (Hall and Brown 2002; Jarrous 2002; Evans *et al*. 2006; Smith *et al*. 2007). All but one of the eukaryotic nuclear RNase P proteins are also present in a separate enzyme, RNase MRP, which processes a number of RNAs not affected by RNase P, including pre-rRNA, mitochondrial RNA primers, and a cell cycle linked mRNA (Chang and Clayton 1987; Schmitt and Clayton 1993; Lee and Clayton 1998; Gill *et al*. 2004). In addition, RNase P and RNase MRP ribonucleoprotein complexes possess distinct, though related RNA subunits (Walker *et al*. 2010).

The additional proteins that are found in the nuclear enzyme may serve to expand the RNA binding and cleavage potential beyond that of pre-tRNAs (Marvin and Engelke 2009). Many additional substrates have been shown for the bacterial enzyme, which uses only a single small protein *in vivo* to expand its range of substrates (Bothwell *et al*. 1976;

Peck-Miller and Altman 1991; Giegé *et al*. 1993; Alifano *et al*. 1994; Komine *et al*. 1994; Liu and Altman 1994; Hartmann *et al*. 1995; Jung and Lee 1995; Gimple and Schön 2001; Hansen *et al*. 2001; Li and Altman 2003; Altman *et al*. 2005; Wilusz *et al*. 2008). Adding a larger number of protein subunits to RNase P RNA in eukaryotes appears to have further broadened the recognition potential of the complex. Eukaryotic RNase P was shown to bind a diverse set of RNAs *in vivo* and mutations in RNase P subunits affected processing and turnover of other RNAs, including antisense RNAs, certain snoRNAs, and ribosomal RNAs (Chamberlain *et al*. 1996; Ziehler *et al*. 2000; Yang and Altman 2007; Coughlin *et al*. 2008). These observations suggest that one function of the additional protein complexity in nuclear RNase P might be to allow broader substrate recognition, without the need for the strict structural requirements of the bacterial holoenzyme.

The yeast nuclear enzyme has previously been shown to bind homopolymer RNAs with a marked sequence preference for polyU and polyG, which were both potent inhibitors of pre-tRNA cleavage (Ziehler *et al*. 2000). However, the bacterial holoenzyme was not affected by homopolymer RNAs. It is likely that the bacterial and eukaryotic enzymes use alternative strategies to interact with non-tRNA substrates that may be a direct result of their differing subunit compositions. The additional protein subunits in the eukaryotic enzyme may be involved in the selection of additional substrates and we sought to further characterize the interaction of these inhibitory RNAs with the yeast nuclear holoenzyme.

To further explore the interaction of eukaryotic RNase P with potential alternative substrates, we investigated binding and cleavage of a variety of single stranded RNA by nuclear RNase P. Given the diversity of non-tRNA substrates, as outlined above, we

chose to examine how single stranded RNA interacts with yeast nuclear RNase P *in vitro*. We found that the unstructured homopolymer RNA, polyU, bound strongly and in a length-dependent manner to RNase P. Mixed sequence RNAs also bound tightly, but in contrast to polyU, were cleaved by RNase P with no obvious sequence dependence or structural consensus. Crosslinking experiments showed multiple binding sites for polyU with multiple RNase P protein subunits (Rpr2p, Pop4p) and, most prominently, with the RNA subunit (Rpr1r). Pre-tRNA^{Tyr}, mixed sequence RNA, and polyU$_{50}$ RNA form crosslinks with the same conserved region of Rpr1r, which is thought to constitute the catalytic center of RNase P, although not at the exact same positions. These results indicate that single stranded RNA binds in a relatively sequence-independent fashion near the active site, and that this tight binding is independent of whether the bound RNA can be efficiently cleaved.

Materials and Methods

Yeast Strains

Yeast nuclear RNase P was isolated from the *S. cerevisiae* strain SCWY10 (Hsieh *et al*. 2009). For some experiments, this strain contained a C-terminal 6xHis tag (*pop6::6HIS-HYG, pop8::6HIS-HYG*).

Yeast Extract Preparation

The yeast strain *SCWY10*, and its 6xHIS tagged derivatives were prepared as in (Hsieh *et al*. 2009) with the following exceptions: yeast (9-36 L) were lysed in 10 mM Tris-Cl pH 7.5, 150 mM NaCl, 1 mM Mg-acetate, 1 mM imidazole, 2 mM $CaCl_2$, 10 % NP-40, and EDTA free Complete protease inhibitors (Roche) by passing through 200 μm

and 100 μm chambers 10 times each. Extract was centrifuged at 17,000 xg for 30 minutes and stored at -80 ˚C.

RNase P Purification

RNase P was purified using multiple affinity-based methods described below, with extract preparation derived from (Hsieh *et al*. 2009). RNase P purifications did not contain RNase MRP RNA as determined by northern blot, which was also used to determine the amount of RNase P relative to control RNA synthesized *in vitro,* and for RNase P crosslinking controls (Hsieh *et al*. 2009). The RNase P fraction used in crosslinking was highly purified showing only the subunit pattern expected for RNase P in denaturing protein gels (Hsieh *et al*. 2009).

For isolation method 1, yeast extract was bound in batch to 5 μl packed calmodulin resin per 1 ml of extract with constant mixing for 2 hours at 4 ˚C. Calmodulin affinity resin (Stratagene) was washed 3 times with forty column volumes of lysis buffer without protease inhibitors in batch. Two consecutive elutions were carried out with five column volumes of lysis buffer plus 20 mM EGTA (calmodulin elution buffer). Pooled elutions were diluted to 100 mM equivalent NaCl, as measured using a conductivity meter, with calmodulin elution buffer lacking NaCl. Samples were then bound to 250 μl 50 % slurry DEAE cellulose resin (DE52, Whatman) per 1 ml of sample for 1 hour at 4 ˚C with constant mixing. Washes were carried out in batch with five column volumes of calmodulin elution buffer, followed by two washes with a 50 % mix of calmodulin elution buffer and DEAE wash buffer [10 mM HEPES pH 7.5, 10 mM $MgCl_2$, 10 % NP-40], and finally two washes with DEAE wash buffer. Samples were then eluted using

DEAE elution buffer [400 mM NaCl, 10 % glycerol, 10 mM HEPES pH 7.5, 10 mM $MgCl_2$, 10 % NP-40].

For isolation method 2, samples from method 1 were diluted to a monovalent salt equivalent of 150 mM with calmodulin elution buffer (above) and applied to a 1 ml mono-Q column (Amersham-Pharmacia). Bound sample was washed with 0.1 M NaCl buffer (10 mM HEPES pH 7.5, 10 mM $MgCl_2$, 100 mM NaCl, 10 % glycerol). RNase P was eluted using a 15 ml linear gradient of 0.1-0.8 M NaCl. Samples reproducibly eluted between 200 mM and 230 mM equivalent salt.

RNA Preparation

Pre-$tRNA^{Tyr}$ with a 12 nt leader was transcribed from a linearized plasmid using titrated amounts of T7 RNA polymerase (Milligan and Uhlenbeck 1989; Hsieh *et al*. 2009). Mixed sequence RNA from the *PHO84* locus was transcribed using templates generated by PCR products containing T7 promoters from *S. cerevisiae* genomic DNA (Table 2.1) (Ziehler *et al*. 2000). Radiolabeled RNA was transcribed with either [α-P^{32}]UTP (3000 Ci/mmol) or [α -P^{32}]GTP (3000 Ci/mmol) and 0.1 mM UTP or GTP in modified buffer (Milligan and Uhlenbeck 1989). HPLC purified $polyU_{50}$ RNA was purchased from Integrated DNA Technology whereas polyU of various sizes was produced by alkaline hydrolysis and separated by size (see below). Transcribed RNA was treated with Antarctic Phosphatase (NEB), 5′ radiolabeled with [γ-P^{32}]ATP (6000 Ci/mmol) using T4 polynucleotide kinase (NEB), and purified using 6-8 % denaturing polyacrylamide gel electrophoresis (PAGE). $PolyU_{50}$ RNA was 5′ radiolabeled without Antarctic Phosphatase treatment.

Table 2.1. Oligonucleotides used in PCR and primer extension analysis.

Primer Name	Sequence
5′ RNA 1_{AS}*	GCGGCGAACCATAATCAATTGCCGT
5′ RNA 2_{AS}*	GTTAATTAATGAGTAATACGCACGT
5′ RNA 3_{AS}*	CCTGGTGATCTACGAGATGAGGAAA
5′ RNA 4_{AS}*	TCATCGATGGACTCCAAAGCCAATC
5′ RNA 5_{AS}*	AACCAAATTGACCAATAACAGTACC
5′ RNA 6_{AS}*	TTCAGAAGTAATAATAGAAGATAGT
5′ RNA 7_{AS}*	AACCCAATAAGGATTCTCCACATTT
5′ RNA 8_{AS}*	GAGATTCGACGGCAGTAGAAGCTCT
5′ RNA 9_{AS}*	ATACAGTTTCTTGTAAACGTTTTTG
5′ RNA 10_{AS}*	CAAATGACGTAAAGAGCCAACAGAC
5′ RNA 11_{AS}*	GTAACCAACAGTTGGTTGGCTTACC
5′ RNA 12_{AS}*	TTATGCTTCATGTTGAAGTTGAGAT
3′ RNA 1_{AS}	ATGCCAAGAAATGACAGCAATCAGT
3′ RNA 2_{AS}	AACACCCGTTCCTCTCACTGCCGCA
3′ RNA 3_{AS}	TGCCTGCTTATTAGCTAGATTAAAA
3′ RNA 4_{AS}	TCTAAGTTCACTTCTAAATTTTATC
3′ RNA 5_{AS}	ATTGAAGATCCTCTGGAAAGAAGAA
3′ RNA 6_{AS}	CTTGTTGAAGGTTTCCACTTCTGTT
3′ RNA 7_{AS}	GTATTGGTATCGGTGGTGACTACCC
3′ RNA 8_{AS}	GCTAGATGTCAAAAGGCTTGTGACC
3′ RNA 9_{AS}	AGACATGGCAATTAACGGTTTGGAA
3′ RNA 10_{AS}	TGCAAACCATCGGTTATGCCGGTTC
3′ RNA 11_{AS}	GCATACCATAAACTTGGTGACCATG
3′ RNA 12_{AS}	AATCGACCATAACTGTGCTAGAGAC
5′ RNA 1_S*	ATGCCAAGAAATGACAGCAATCAGT
5′ RNA 2_S*	CCAGCACGTGGGGCGGAAATTAGCG
5′ RNA 3_S*	AATTATTATTCCTTTTTGGCAGCAT
5′ RNA 4_S*	TCCACGAATACAATCCAAATGAGTT
5′ RNA 5_S*	ACAAGTTAAGACCATCTCCATTGCT
5′ RNA 6_S*	TTGTTGGTCGTAAGAGAATTTATGG
5′ RNA 7_S*	AGAGGTGCCATCATGGGTGCTGTCT
5′ RNA 8_S*	GGCATGTTTGTATTTCAGATTAACT
5′ RNA 9_S*	AGGCTTCGTTCAAAGATTTCTGCAG
5′ RNA 10_S*	CTGATTTTGATTTGTGCTGGTTCAT
5′ RNA 11_S*	CGGTCCAAACACAACCACCTTTATT
5′ RNA 12_S*	AATCGACCATAACTGTGCTAGAGAC

Primer Name	Sequence
3′ RNA 1_S	GCGGCGAACCATAATCAATTGCCGT
3′ RNA 2_S	TACCGGTGTGCAATGTGGTTGCATC
3′ RNA 3_S	ACATGAATAGTATCTTTATTGACGG
3′ RNA 4_S	AAGAATCTGTCAAGAAACCAACACC
3′ RNA 5_S	GACAATCATGATAATAAGTTCCATA
3′ RNA 6_S	ATTTGACCCCAAGCTTGGTTAGCAA
3′ RNA 7_S	ATTGATATCTAGGAGATTCTGGAAT
3′ RNA 8_S	ACCGTACTTCCATTGACCAAAATGT
3′ RNA 9_S	AAGACGGATACCCAGTAACCAGGTA
3′ RNA 10_S	GAGTTGGGAAACACTCACCAGGAAC
3′ RNA 11_S	TTCTGGGATCAACAAGGTTGTGAAG
3′ RNA 12_S	TTATGCTTCATGTTGAAGTTGAGAT
RPR1_END[a]	GCTGGAACAGCAGCAGTAATCGGTA
RPR1_200[a]	AACGGTCGGTAAAGACTGGTTCCCC

All oligos were ordered from Integrated DNA Technology. 5′ and 3′ pairs of indicated RNA fragments (ex. 5′ RNA 1_{AS}/3′ RNA 1_{AS}) were used to prepare DNA templates for T7 *in vitro* transcription.

*All 5′ oligos have the sequence TAATACGACTCACTATAGG (T7 promoter) added to the 5′ end of the indicated sequences.

[a] Oligos used for primer extension analysis of Rpr1r.

Alkaline Hydrolysis of PolyU RNA

Alkaline hydrolysis of a mix of polyU RNA (Sigma-Aldrich) was done by incubating 10 mg polyU RNA with 20 mM NaOH at 65 °C for 8 minutes. The reaction was quenched by adding 188 mM NaOAc pH 5.2. Samples were separated on a 10 % polyacrylamide gel and regions every 10 cm were eluted out of the gel. Samples were 5′ radiolabeled with [γ-P^{32}]ATP using T4 polynucleotide kinase (NEB) and separated on a 10 % denaturing polyacrylamide gel next to Decade Markers (Ambion).

Inhibition studies

RNase P (17.4 pM) was incubated for 15 minutes at 25 °C with 4 nM both radiolabeled and unlabeled pre-$tRNA^{Tyr}$ in the presence of unlabeled inhibitor RNA (polyU and mixed sequence RNA) in RNase P buffer (10 mM HEPES pH 7.5, 10 mM $MgCl_2$, 100 mM NaCl). For size dependent inhibition with alkaline digested polyU, 100 nM of each size range was used with 17.4 pM RNase P. Higher amounts of RNase P (152 pM) were needed to result in observable cleavage at 107 nM pre-$tRNA^{Tyr}$. Reactions were stopped by adding an equal volume of 2x FEXBS (47.5 % formamide, 7.5 mM EDTA, 0.0125 % SDS, 0.01 % xylene cyanol dye, 0.01 % bromophenol blue dye). Reactions were separated using denaturing 8 % PAGE and visualized with a Typhoon Trio+ imager.

Prism 5.0a (GraphPad Software) was used for nonlinear regression of the fraction of radiolabeled pre-$tRNA^{Tyr}$ produced under increasing concentrations of RNA inhibitors using equation 1.

$$\text{Equation 1:} \quad y=\max+(\min*X)/(1+X/IC_{50}) \qquad (1)$$

In equation 1, max is the initial turnover per minute and min is the final turnover per minute. Turnover per minute was calculated using moles of substrate divided by moles of RNase P per time of the reactions. This method was applied to normalize between the different conditions that were used to obtain IC_{50} values.

Cleavage assays

In vitro cleavage of ~1-2 ng radiolabeled RNA by 2-fold dilutions of RNase P (0.038-0.6 fmoles for pre-$tRNA^{Tyr}$ and $polyU_{50}$; 0.1-0.85 fmoles for RNA $3_{S/AS}$) was carried out for 15 minutes in RNase P buffer at 25 °C. Cleavage of 1 ng 5′ radiolabeled RNA 3_S by RNase P (0.21-0.84 fmoles) was carried out for 20 minutes at 25 °C. Positions of cleavage were mapped for RNA 3_S using 0.2 ng RNase A (Roche) and 0.2 U RNase T1 (Gibco BRL) as shown (Ziehler and Engelke 2001). Reactions were stopped with 2x FEXBS and separated using 8 % denaturing PAGE, then visualized.

Micrococcal Nuclease Digestion

100 U or 200 U micrococcal nuclease (MNase; Worthington Biochemical Corporation) was incubated in 10 mM HEPES pH 7.5, 4 mM $CaCl_2$, and 12 mM $MgCl_2$ with RNase P (1 fmol) at 37 °C for 10 minutes. Some reactions were pre-treated with 40 mM EGTA prior to the addition of RNase P and all MNase reactions were terminated with 40 mM EGTA. RNase P cleavage was then started by the addition of radiolabeled RNA (pre-$tRNA^{Tyr}$ or RNA 3_S) with RNase P buffer containing 12 mM $MgCl_2$ for 20 minutes at 25 °C. Reactions were stopped by EtOH precipitation and separated using 6 % denaturing PAGE in 2x FEXBS and then visualized.

Crosslinking

RNase P (100 fmoles) was crosslinked in the presence of unlabeled RNA (100 nM: polyU$_{50}$, pre-tRNA^{Tyr}, or RNA 3$_S$) or 5′ radiolabeled RNA (1 ng polyU$_{50}$) using 254 nm UV light (Model UVG-11) at a distance of 20 mm for 2 minutes in RNase P buffer with 135 mM NaCl on ice. Crosslinks were EtOH precipitated and resuspended in either 2x FEXBS for separation using 6 % denaturing PAGE or 2x Laemmli buffer (with 2-mercaptoethanol) (Bio-Rad) for separation on a 4-15 % Tris-HCl acrylamide gel (Bio-Rad) with a SeeBlue Plus^2 pre-stained protein ladder (Invitrogen). To determine the nature of the 5′ radiolabeled polyU$_{50}$ crosslinks, 120 fmoles pre-tRNA^{Tyr} was added prior to crosslinking. In addition, some crosslinked samples were treated with 1/10 volume CP stop [2 % SDS, 100 mM EDTA, 1 mg/ml proteinase K (Roche)] for 20 minutes at 42 °C prior to denaturing PAGE and visualization.

Pre-tRNA^{Tyr}, polyU$_{50}$, and RNA 3$_S$ crosslink positions in Rpr1r were determined using a Sensiscript primer extension kit (Qiagen) after CP stop treatment and acid phenol/chloroform treatment followed by EtoH precipitation. Primer extension for 50 minutes at 42 °C was performed using oligonucleotides labeled with [γ-P^{32}]ATP (6000 Ci/mmol) using PNK (NEB) (Table 2.1). Dideoxy sequencing ladders were generated using Rpr1 DNA from a pUC19 plasmid (Hull *et al*. 1991). After EtOH precipitation samples were resuspended in 2x FEXBS and separated on a 6 % denaturing polyacrylamide gel for visualization.

Mass Spectroscopy

Uncrosslinked and UV crosslinked RNase P (1 pmole; (Hsieh *et al*. 2009)), both with 100 nM polyU$_{50}$ RNA, were cut out of a 4-15 % Tris-HCl acrylamide gel (Bio-Rad).

Gel slices were trypsin digested and peptide masses were identified using a LC-MS/MS (nano-UPLC coupled to a Q-Tof premier) at the UMMS Proteomics & Mass Spectrometry Facility (Rosenegger *et al*. 2010).

Results

Binding of Single Stranded RNA to RNase P

Earlier results suggested that nuclear RNase P, but not bacterial RNase P, was strongly inhibited by RNA homopolymers. Although some homopolymers inhibited pre-tRNA cleavage more readily, there was no obvious relationship to structural potential (polyU~polyG>>polyA>>>polyC) (Ziehler *et al*. 2000). PolyU RNA was chosen for further study of length requirements for pre-tRNA cleavage inhibition due to the predicted lack of secondary and tertiary structure (Kankia 2003; Davis 2004).

A range of polyU sizes from 25-60 nucleotides (nt) (+/- 2 nt) were isolated by alkaline hydrolysis of polyU RNA and denaturing electrophoretic separation as shown in Fig. 2.1. The polyU sizes were tested for size-dependent inhibition of pre-tRNA^{Tyr} cleavage catalyzed by purified yeast nuclear RNase P (Fig. 2.2 A). Larger polyU RNA (>40 nt) was required for substantial inhibition of pre-tRNA cleavage, though there was not a sharp cutoff in size dependence. This size dependence is not straightforward however as our data do not indicate if smaller polyU RNA is bound to RNase P and not inhibiting. What is clear is that only the larger polyU is inhibiting pre-tRNA cleavage and so that was used in additional studies to analyze binding to RNase P as estimated by inhibition of pre-tRNA cleavage.

For further analysis of inhibition by polyU RNA, a chemically synthesized 50 nt polyU, polyU$_{50}$, was used to characterize single stranded RNA binding by RNase P.

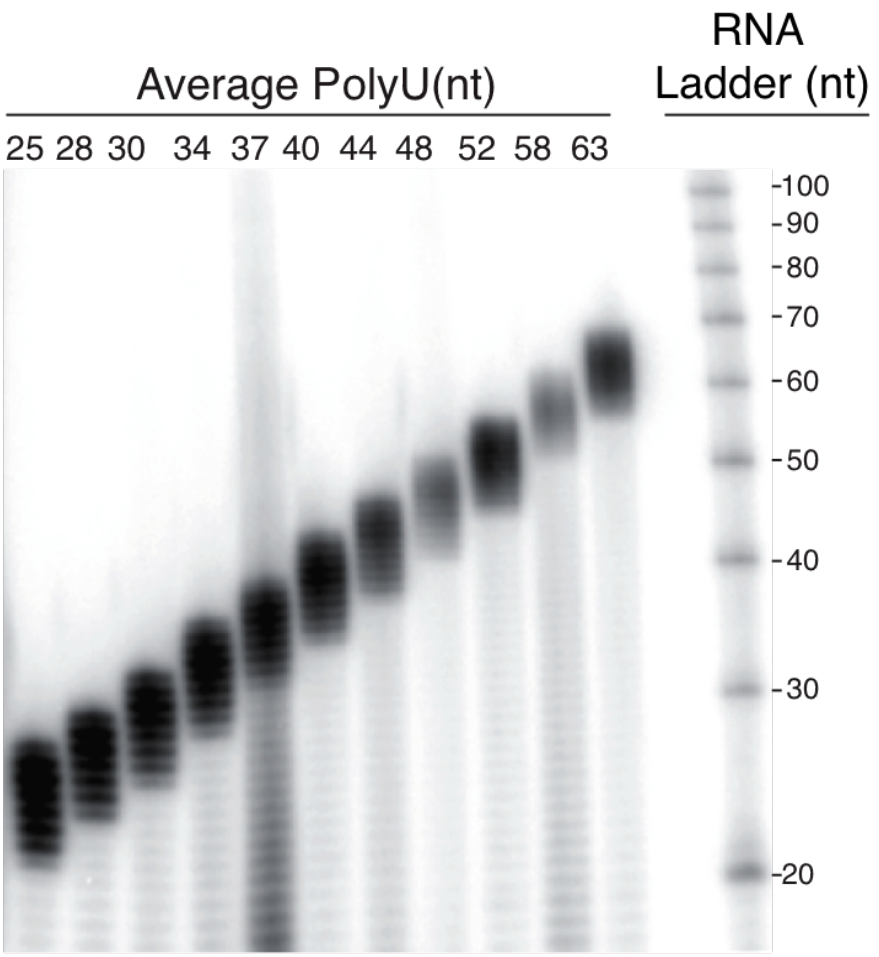

Figure 2.1. Size determination of alkaline hydrolyzed polyU RNA.
A mix of polyU RNA was partially degraded at high pH and isolated by size on polyacrylamide gels. 5′ radiolabeled RNA fragment pools, indicated by average size, are shown separated on a 10 % denaturing polyacrylamide gel with average sizes determined by comparison to a Decade RNA ladder (Ambion).

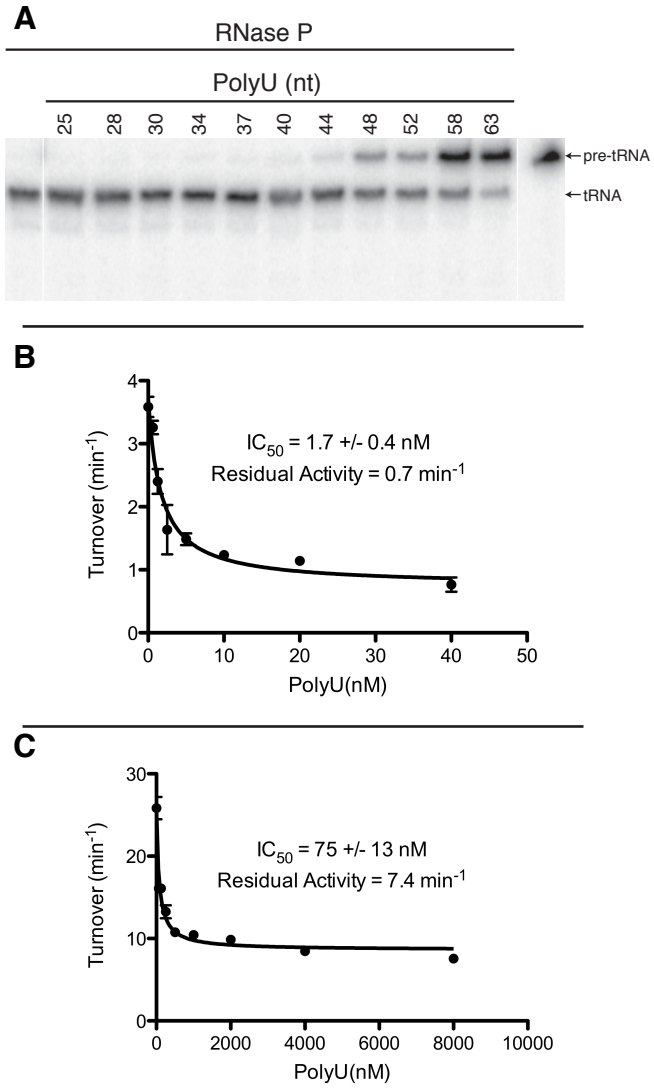

Figure 2.2. PolyU RNA inhibition of RNase P-catalyzed pre-tRNA^{Tyr} cleavage.
A) Denaturing polyacrylamide gel electrophoresis of radiolabeled pre-tRNA^{Tyr} cleavage products was used to monitor RNase P activity in the presence of 100 nM increasing sizes of competitor polyU RNA. B,C) PolyU$_{50}$ RNA inhibition of RNase P-catalyzed cleavage of radiolabeled pre-tRNA^{Tyr} when [pre-tRNA^{Tyr}] = 4 nM (< K_m) B) or [pre-tRNA^{Tyr}] = 107 nM (> K_m) C) was measured in triplicate. The data are curve fit using a binding isotherm with a nonzero activity at saturating inhibitor; both the value of the IC_{50} and the residual activity are indicated with error from curve fitting shown as standard error (S.E.M.). The K_m for this pre-tRNA was previously determined to be 55 nM (Ziehler *et al*. 2000).

Relative IC_{50} values for $polyU_{50}$ were obtained for conditions where the concentration of pre-$tRNA^{Tyr}$ was both below (Fig. 2.2 B) and above (Fig. 2.2 C) the K_m value (Ziehler *et al*. 2000). The relative IC_{50} values for $polyU_{50}$ are in the nanomolar range, indicative of potent inhibition; furthermore, the IC_{50} value increases at the higher substrate concentration indicating that the inhibitor and substrate are at least partially competitive for binding to RNase P. However, even high concentrations of RNA do not result in complete inhibition of RNase P cleavage, demonstrating that RNase P is capable of binding and cleaving substrate in the presence of bound inhibitor. These data are consistent with $polyU_{50}$ binding to one or more sites in RNase P that directly or indirectly interfere with pre-tRNA binding, but is not fully consistent with binding solely at the pre-tRNA cleavage site (see discussion for model). Our crosslinking studies, outlined below, further characterize how $polyU_{50}$ interacts with purified RNase P.

Mixed Sequence RNA Binding Can Lead to RNase P Cleavage

Given the previously observed sequence preference for homopolymer binding by RNase P, we wanted to determine if mixed sequence RNA bound strongly to RNase P. With the diversity of RNA that has been previously identified to both co-purify with RNase P and change in abundance in strains with RNase P temperature sensitive mutations, we chose multiple *in vitro* transcripts from both strands of the *PHO84* locus as a representative region for potential RNase P non-tRNA substrates (Coughlin *et al*. 2008). Both strands were tested because this locus has been shown to have physiologically relevant antisense RNA (Camblong *et al*. 2007). Both sense and antisense RNA transcripts (250 nt) comprising the entire locus were tested for inhibition of RNase P-catalyzed pre-$tRNA^{Tyr}$ cleavage. At a concentration of 100 nM inhibitor using a pre-

tRNA substrate concentration $<K_m$, all 24 sense and antisense RNAs inhibited RNase P, though there was variability in the extent of inhibition (Fig. 2.3 A; Fig. 2.4). This variability in inhibition is consistent with sequence preferences observed with homopolymer RNA inhibition. It is also possible that the inhibitory properties of bound RNAs may depend on how well they block the RNase P active site (see crosslinking data below).

To assess the strength of mixed sequence RNA inhibition, IC_{50} values were obtained for one pair of sense and antisense RNAs: RNA 3_S and RNA 3_{AS} (Fig. 2.3 B,C). IC_{50} values for these RNAs were essentially equivalent and in the same range as $polyU_{50}$ RNA. In addition, as was the case with $polyU_{50}$ these RNAs did not completely inhibit RNase P. We interpret these data as showing that nuclear RNase P has a broad ability to bind mixed sequence RNA in a way that partially conflicts with pre-tRNA cleavage. These data, combined with the diversity of RNA both bound to and affected by RNase P, suggest that *in vivo* RNA interactions with RNase P are determined primarily by factors other than the sequence of the RNA ligands.

Next, we determined if RNase P could cleave any of these RNA molecules *in vitro*. At all levels of RNase P tested, $polyU_{50}$ RNA showed no detectable cleavage products (Fig. 2.5 A), consistent with results from longer polyU homopolymers (Ziehler *et al*. 2000). However, both of the mixed sequence RNAs (RNA 3_S and RNA 3_{AS}) used in the IC_{50} experiments were cleaved (Fig. 2.5 A). Pre-treatment of highly purified RNase P with micrococcal nuclease (MNase) prior to adding mixed sequence RNA resulted in the loss of cleaved product (Fig. 2.6). This loss is consistent with the requirement for the nucleic acid subunit of RNase P, Rpr1r, for cleavage. We conclude that nuclear RNase P,

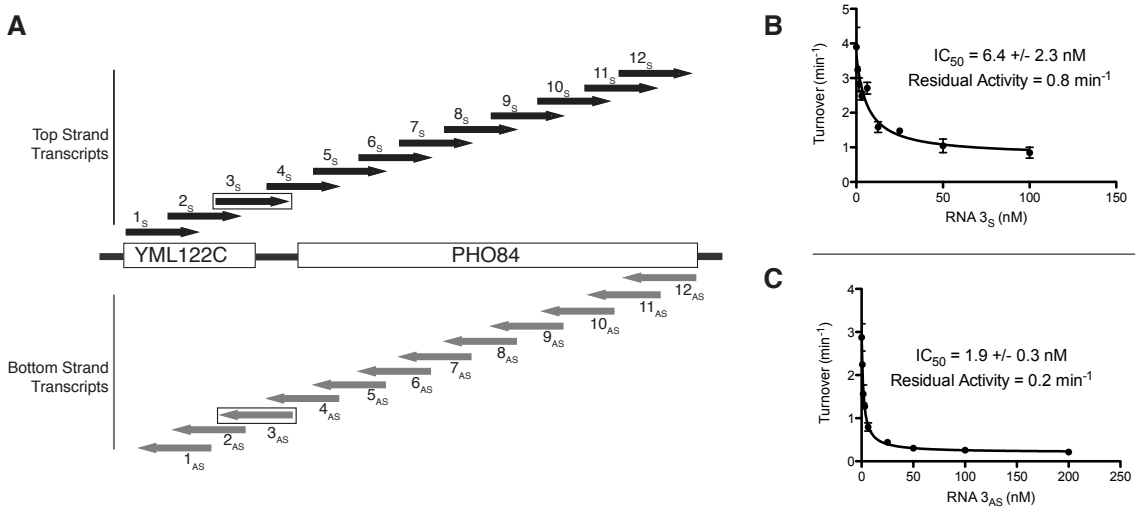

Figure 2.3. Inhibition of pre-tRNA^{Tyr} cleavage by mixed sequence RNA.
A) 100 nM, 250 nt partially overlapping transcripts from both the top strand (1_S-12_S) and bottom strand (1_{AS}-12_{AS}) of *S. cerevisiae PHO84* locus and neighboring YML122C, were tested for inhibition of RNase P-catalyzed pre-tRNA^{Tyr} cleavage. B,C) Inhibition of radiolabeled pre-tRNA^{Tyr} cleavage when [pre-tRNA^{Tyr}] = 4 nM (< K_m) by RNA 3_S B) titrated in triplicate or RNA 3_{AS} C) titrated in duplicate. The residual activity indicates the catalytic activity at saturating inhibitor and the apparent IC_{50} value is indicated with error from curve fitting (S.E.M). Curve fitting was done as in Fig. 2.2 B,C.

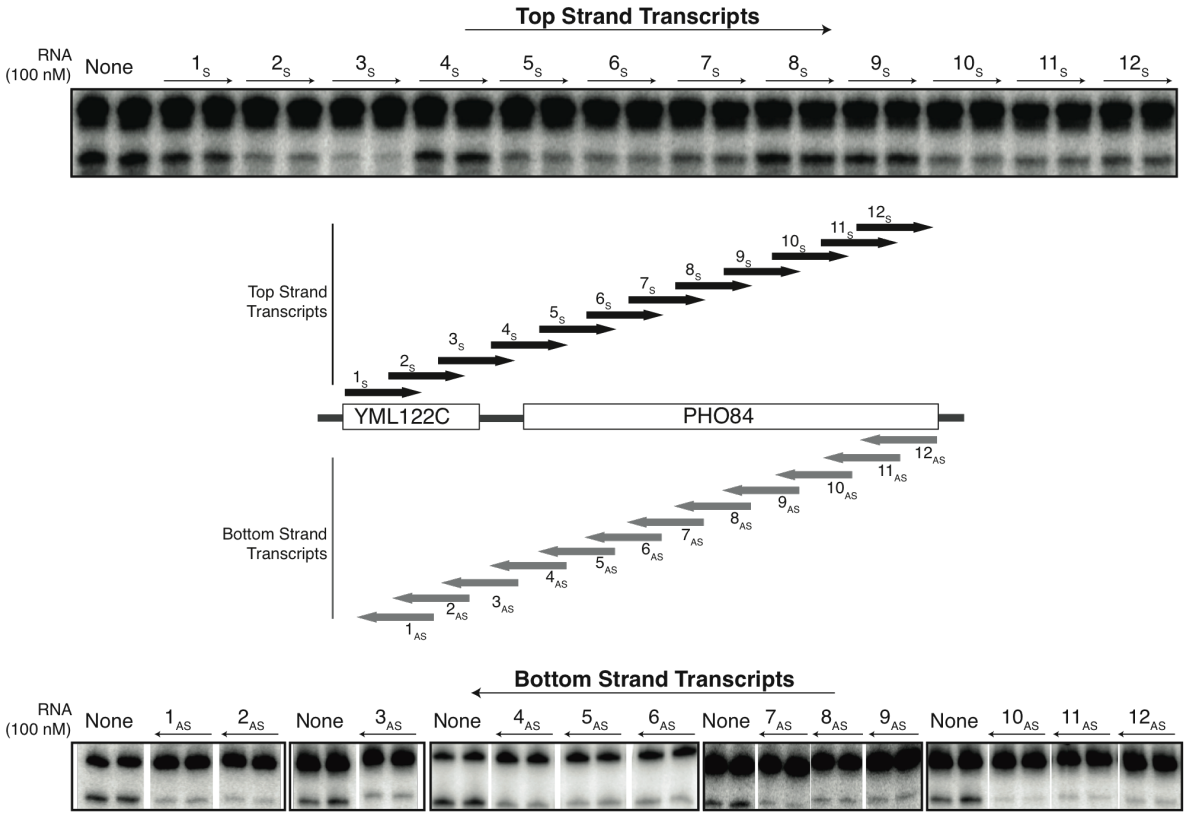

Figure 2.4. Mixed sequence RNA inhibition of RNase P.
RNase P cleavage of radiolabeled pre-tRNA^{Tyr} is shown in duplicate incubated with 24 different 100 nM mixed sequence RNAs (250 nt). Radiolabeled pre-tRNA^{Tyr} cleavage products are shown separated on 8 % denaturing polyacrylamide gels. Reactions are grouped with appropriate no inhibitor controls, indicated by "none" designation, in order to compare levels of inhibition with added mixed sequence RNA. Fig. 2.3A is reproduced for visualization of RNAs tested here with arrows indicating the relative direction of transcription.

and not a minor nuclease contaminant, is directly responsible for the cleavage of this mixed sequence RNA.

In order to determine if there was a sequence preference for cleavage of RNA by RNase P we mapped the multiple cleavage sites from RNase P-catalyzed cleavage of one of the many mixed sequence RNAs (Fig. 2.5 B). As is shown in Figure 2.7, there was no strong sequence specificity for the cleavage sites that were identified nor evidence of predicted structural consensus in the area surrounding the position of cleavage (Zuker 2003). In addition, upon comparison of regions surrounding the cleavage site with other previously identified RNAs cleaved by nuclear RNase P, we did not see any sequence specificity for cleavage (Figure 2.7 B, (Chamberlain *et al*. 1996; Coughlin *et al*. 2008)). However, it is possible that local RNA structure might play a role in cleavage that we do not currently understand given that polyU RNA, which is predicted to lack stable secondary and tertiary structures, was not cleaved (Fig. 2.5 A).

Further, consistent with our data, we only observe a small fraction of the mixed sequence RNA being cleaved by RNase P (Fig. 2.5 A). Increasing the RNase P concentration by as much as eightfold only increases cleavage by a small fraction. It therefore appears that RNase P can bind strongly to RNA even if it cannot always cleave it, as observed with our polyU data. Also, when RNase P cleaves the mixed sequence RNA it cleaves at multiple positions, which indicates that slow cleavage could be due to suboptimal positioning of RNA in the active site. It therefore appears that RNase P can bind RNA in multiple positions with some of this binding leading to low levels of cleavage.

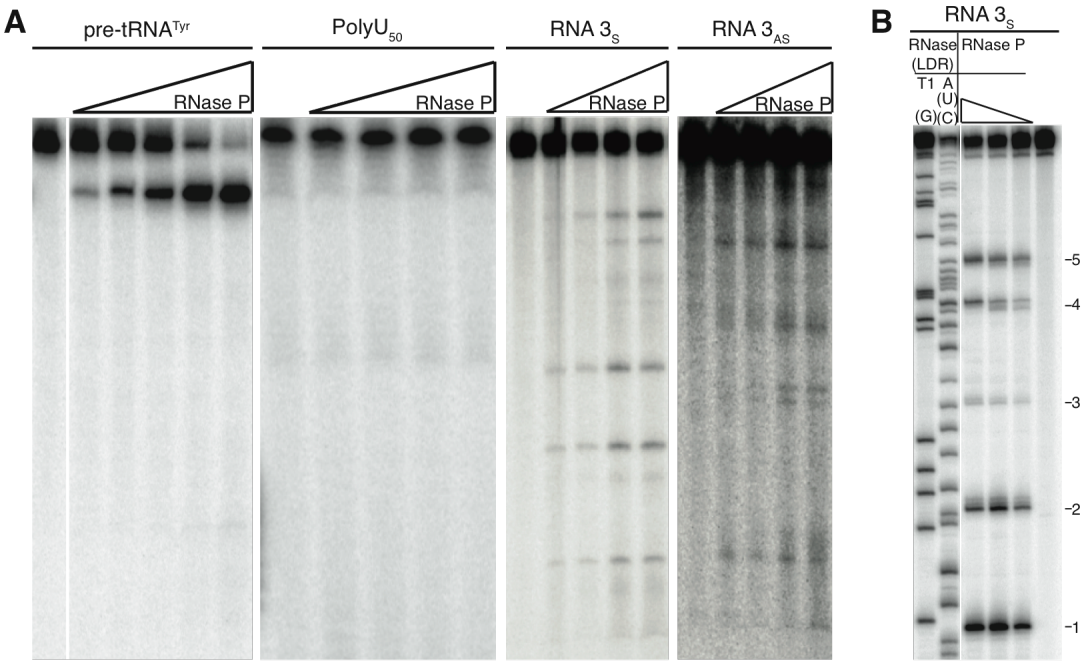

Figure 2.5. Cleavage of various RNA by RNase P.
A) Two-fold increasing concentrations of RNase P (3.8 pM-60 pM for pre-tRNA^{Tyr}; 10 pM-85 pM for all other RNA) were used for testing cleavage of radiolabeled RNAs (pre-tRNA^{Tyr}, RNA 3$_S$, and RNA 3$_{AS}$) and 5′ radiolabeled polyU$_{50}$ after incubation for 15 min. Cleavage products are shown separated on 8 % denaturing polyacrylamide gels. B) The cleavage sites in 5′ radiolabeled RNA 3$_S$ at increasing amounts of RNase P were identified by comparison to cleavage of mixed sequence RNA by RNases with known specificity. Nucleotide specificity of RNases used for mapping is indicated. 5 major sites of RNase P cleavage are indicated numbered 1-5. Cleavage products are shown separated on 8 % denaturing polyacrylamide gels.

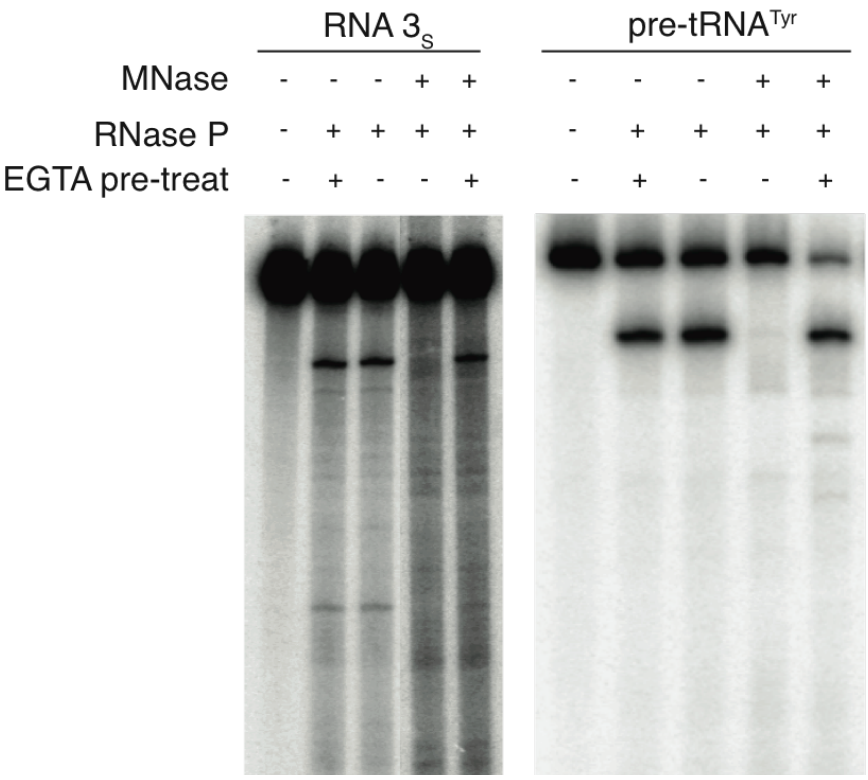

Figure 2.6. RNase P cleavage of RNA 3_S and pre-tRNA^{Tyr} is sensitive to micrococcal nuclease (MNase) pre-treatment.
8 % denaturing polyacrylamide gel separation of radiolabeled pre-tRNA^{Tyr} and RNA 3_S cleavage products are shown under conditions where RNase P was treated with MNase prior to addition of radiolabeled substrates. MNase treatment inactivates RNase P cleavage of both radiolabeled RNA 3_S and, shown as a control, pre-tRNA^{Tyr}. Specifically inhibiting MNase treatment by pre-treating the MNase with excess EGTA prevents this result as expected. EGTA pre-treatment does not prevent cleavage by RNase P.

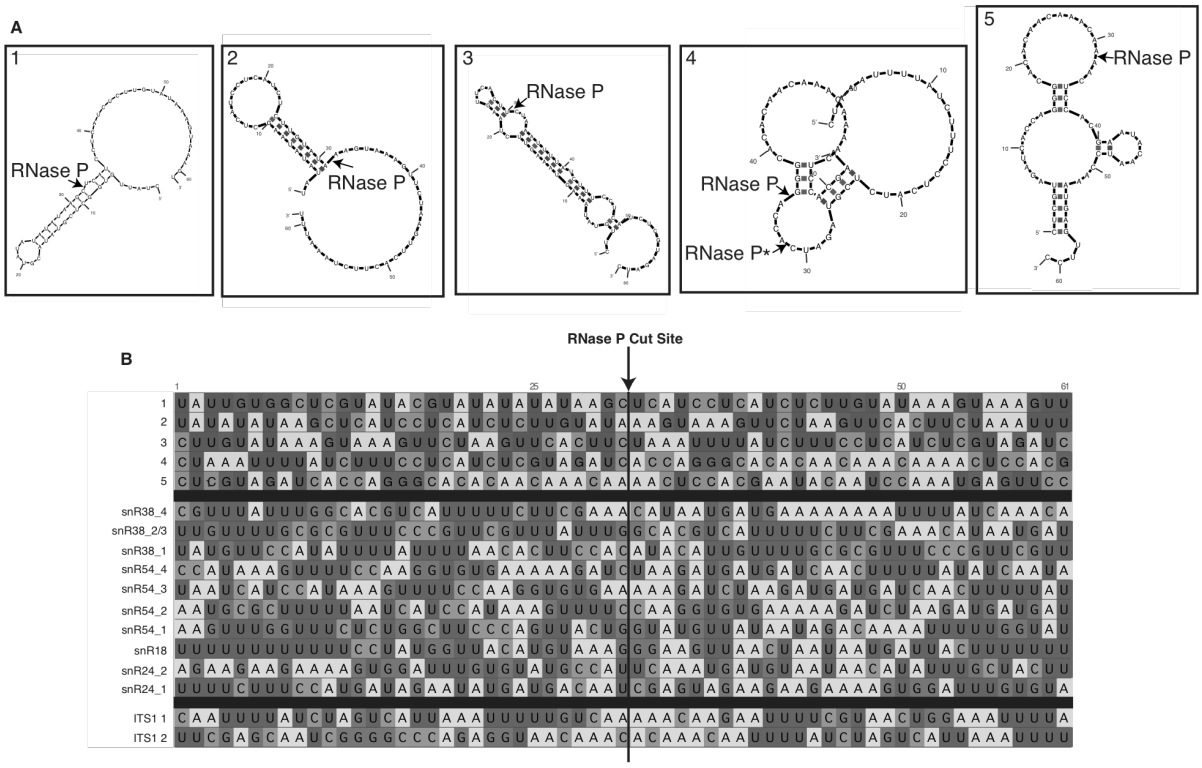

Figure 2.7. RNA 3_S does not fold into predicted tRNA-like structures and RNase P cleavage sites do not show strong consensus sequences.

A) mFold (http://www.bioinfo.rpi.edu/applications/mfold) was used to predict RNA secondary structures at cleavage sites (1-5) and the surrounding RNA 3_S sequence. 61 nt RNA fragments were used for folding to examine regions in close proximity to the cleavage sites. Arrows indicate sites of RNase P cleavage. B) Cleavage site alignment of RNA 3_S (cleavage sites 1-5; Fig. 2.5 B) is shown with previously identified preferential cleavage sites for yeast nuclear RNase P in snoRNAs and pre-ribosomal RNA ITS1 (Chamberlain *et al.* 1996; Coughlin *et al.* 2008). Multiple cleavages from the same RNA are indicated by numbers after the name. Cleavage sites are centered and indicated by an arrow and a bold line. Only a very weak consensus was obtained using EDNAFULL alignment matrix ($XNNANAUN_5UN_{16}UU$) with X indicating the cleavage site.

Identification of RNA Contact Sites in RNase P

We used crosslinking to investigate contacts with highly purified RNase P, comparing un-cleavable polyU$_{50}$ RNA with cleavable RNAs (pre-tRNA^{Tyr} and RNA 3$_S$). Covalently linked complexes were separated by denaturing polyacrylamide gel electrophoresis (Fig. 2.8 A). We tested multiple crosslinking reagents, but only ultraviolet light irradiation (UV, 254 nm) provided discrete, reproducible crosslinked complexes between RNA and RNase P. Treatment with either formaldehyde or glutaraldehyde resulted in extremely heterogeneous or high molecular weight migration on gels, consistent with multiple crosslinking events per complex (data not shown). The major UV crosslinks were found to be between polyU and the RNA subunit, Rpr1r, as initially judged by insensitivity of the major shifted band to proteinase K on denaturing gels containing 7 M urea (Fig. 2.8 A). Unlabeled pre-tRNA^{Tyr} could compete with polyU$_{50}$ for all RNase P-dependent shifts, indicating that substrate pre-tRNAs can compete for binding to at least some of the crosslinking contacts.

To clarify if polyU$_{50}$, RNA 3$_S$, and pre-tRNA^{Tyr} bound to similar site(s) in Rpr1r, we identified crosslinking positions in purified RNase P. After UV crosslinking and deproteinization, crosslinked sites were identified by primer extension analysis (Fig. 2.8 B). For each of the RNA ligands, primer extensions were done to examine the entire sequence of Rpr1r, minus only the extreme 3′ end for technical reasons (primer hybridization), and the only significant crosslinks to all three RNA ligands were found in a single region. Each of the identified crosslinks to polyU$_{50}$, pre-tRNA^{Tyr}, or RNA 3$_S$ were found within ”Critical Region I” (CR-I) (Fig. 2.8 B,C). This region is an absolutely

Figure 2.8. Single stranded RNAs and pre-tRNA crosslink to RNase P RNA.
A) 5′ radiolabeled polyU$_{50}$ is shown on a denaturing polyacrylamide gel. A crosslink dependent shift is observed with UV light and RNase P, which is also shown to be resistant to deproteinization by proteinase K. Unlabeled pre-tRNA^{Tyr} is shown to compete for the RNase P-polyU$_{50}$ crosslinks with crosslinking also observed to polyU$_{50}$ in the absence of RNase P regardless of deproteinization. B) RNA ligands (pre-tRNA^{Tyr}, RNA 3$_S$, polyU$_{50}$) crosslink to the CR-I region of Rpr1 RNA. After deproteinization, primer extension stops were compared from uncrosslinked and crosslinked RNase P to RNase P crosslinked in the presence of various RNA ligands. Unique extension stops in the presence of RNA ligands represent sites of crosslinking between RNase P RNA Rpr1 and the RNA ligand. The primer extensions are mapped using the indicated dideoxy sequencing ladder lanes. Only the Rpr1r sequence where ligands crosslink is shown with ligand type indicated. Rpr1r sequence where the crosslinks occur is shown next to the primer extension data. C) Secondary structure of Rpr1 RNA showing positions of crosslinking by polyU, RNA 3$_S$ and pre-tRNA^{Tyr}, as identified in B). Conserved stems are indicated (P1 etc.) along with eukaryotic specific helixes (eP8 etc.). In addition, the five universally conserved sequence regions, conserved regions (CR), are shown (CRI-CRV).

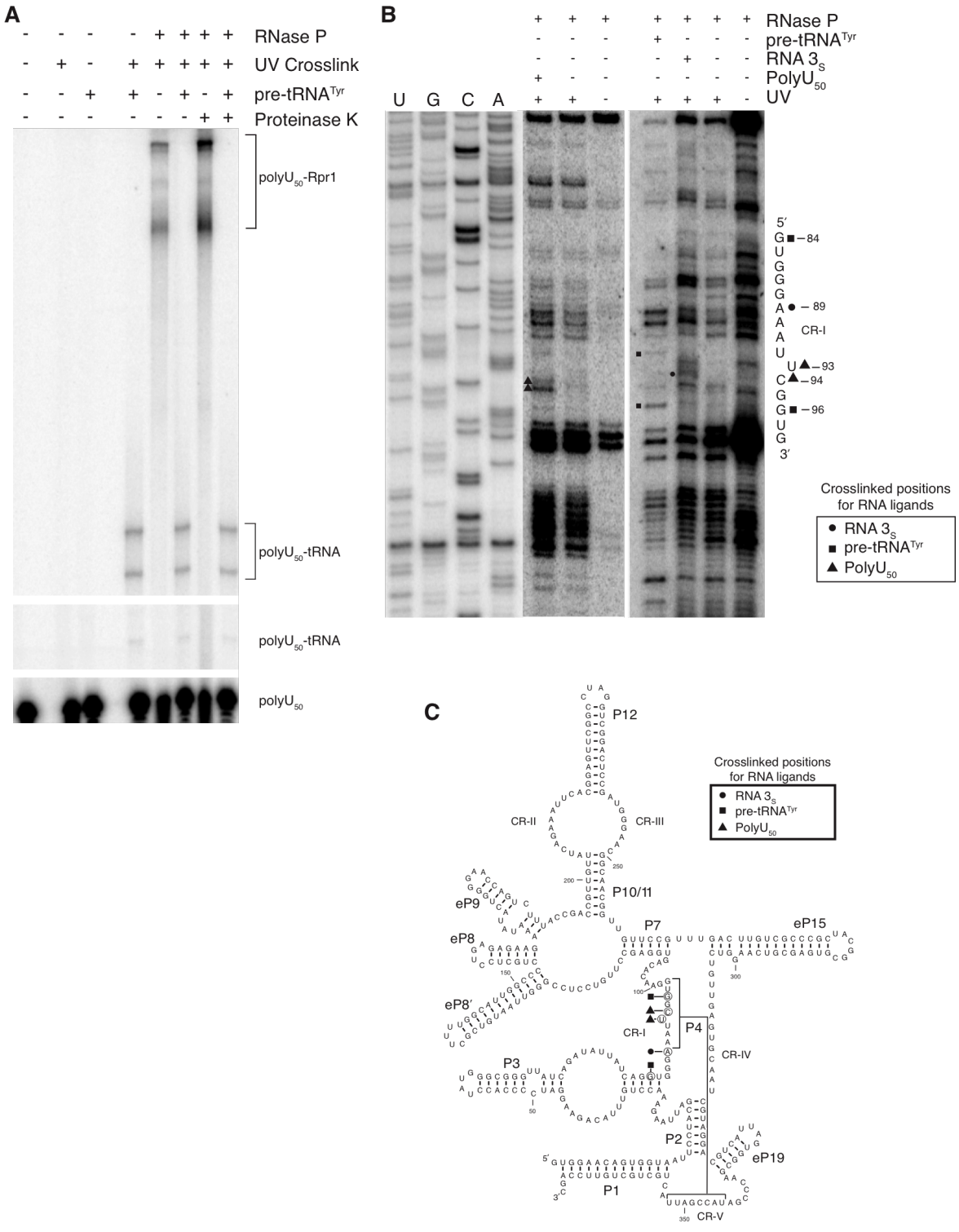
A
RNase P
UV Crosslink
pre-tRNA^Tyr
Proteinase K
polyU50-Rpr1
polyU50-tRNA
polyU50-tRNA
polyU50
B
RNase P
pre-tRNA^Tyr
RNA 3S
PolyU50
UV
U G C A
5′
G ■ – 84
U
G
G
G
A ● – 89
A
A CR-I
U
U ▲ – 93
C ▲ – 94
G
G ■ – 96
U
G
3′
Crosslinked positions for RNA ligands
● RNA 3S
■ pre-tRNA^Tyr
▲ PolyU50
C
P12
CR-II
CR-III
P10/11
eP9
eP8
eP8′
P7
eP15
CR-I
P4
CR-IV
P3
P2
eP19
P1
CR-V
Crosslinked positions for RNA ligands
● RNA 3S
■ pre-tRNA^Tyr
▲ PolyU50

conserved feature of all known RNase P RNAs and is thought to comprise part of the catalytic core of the ribozyme (Chen and Pace 1997).

Although the major UV-induced crosslinks to the RNA ligands were shown to occur with the Rpr1 RNA subunit, we also investigated whether crosslinks could be detected with protein subunits. Multiple crosslinked RNase P proteins were identified, though possible approaches were limited by inefficiency of crosslinking and the small amounts of the low-copy and unstable holoenzyme that could be purified to homogeneity (Hsieh *et al*. 2009). When separated on SDS-polyacrylamide gels to observe denatured protein migration (Fig. 2.9), polyU$_{50}$-RNase P crosslinks were visible as multiple discrete shifted bands. The smaller of these bands was not identified previously using 7 M urea gels (Fig. 2.8 A), possibly because these protein-containing complexes were part of insoluble aggregates that routinely failed to enter the urea gels. The two upper-shifted bands are consistent with crosslinking of polyU$_{50}$ to the Rpr1 RNA subunit since they were proteinase K-resistant (data not shown). Further, this large doublet is consistent with internally crosslinked Rpr1r, which gives two or more distinct bands on urea gels (Fig. 2.10). However, the two lower shifted bands were sensitive to proteinase K treatment indicating probable protein subunit crosslinks (data not shown).

LC-MS/MS analysis of gel slices from equivalent positions containing the polyU$_{50}$ RNA with or without crosslinking indicated the crosslinking-dependent association of several proteins with polyU (Fig. 2.9, Table 2.2). Pop4p and Rpr2p associated with shifted polyU$_{50}$ only in the crosslinked lanes, and we interpret this as being in close contact with the single stranded RNA. Although tested extensively, we did

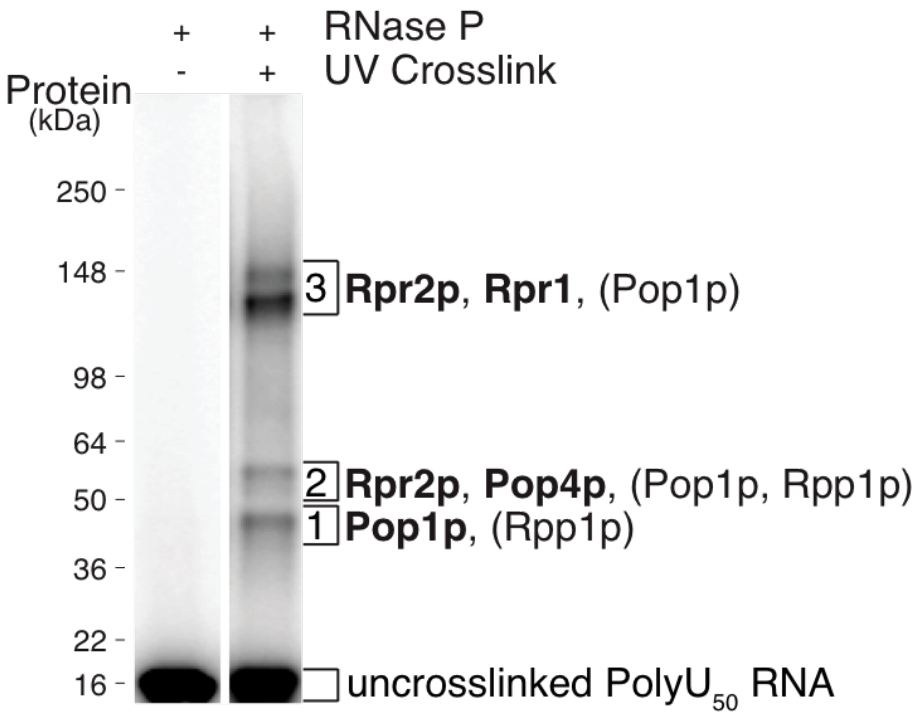

Figure 2.9. PolyU$_{50}$ RNA crosslinks to RNase P proteins.
5′ radiolabeled polyU$_{50}$ is shown with RNase P separated on a 4-15 % SDS polyacrylamide gel. A crosslink dependent shift is observed with polyU$_{50}$ and RNase P. Indicated regions (gel slices 1,2,3) were analyzed by mass spectrometry in crosslinked and uncrosslinked lanes (Table 2.2). Proteins that are interpreted to crosslink to polyU$_{50}$ (found only in crosslinked gel slices) are in bold type while ambiguous proteins (found in both crosslinked and uncrosslinked gel slices) are in parenthesis. Relative migration of a protein ladder (SeeBlue Plus[2]) is shown. Only RNase P proteins are indicated, see table 2.2 for full mass spectrometry results.

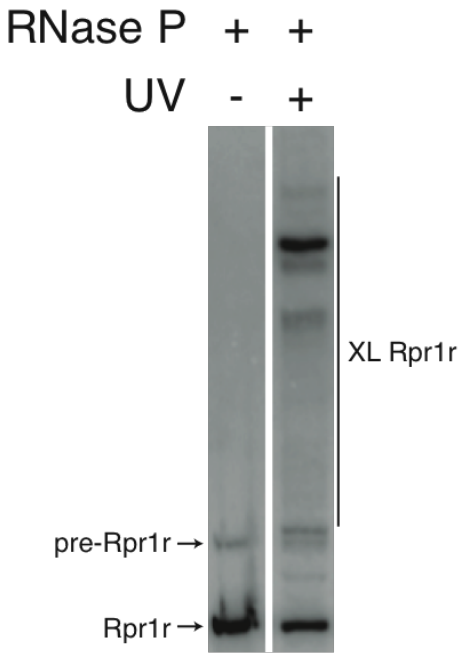

Figure 2.10. Rpr1r shows a UV dependent shift when RNase P is crosslinked without added RNA ligands.
Total RNA is was separated on a 6 % denaturing polyacrylamide gel and subjected to northern blot analysis. The blot was probed for Rpr1r and is shown comparing positions of uncrosslinked RNase P (Rpr1r and pre-Rpr1r) to crosslinked RNase P (XL Rpr1r). UV crosslinked RNase P, under the same conditions used for crosslinking polyU RNA (Figs. 2.8; 2.9), has multiple shifts that indicate internal crosslinking in RNase P. Most importantly, the presence of unshifted Rpr1r after UV crosslinking indicates that samples are not over-crosslinked under these conditions.

Table 2.2. RNase P proteins crosslink to polyU RNA

		1[a]		1XL[b]		2[a]		2XL[b]		3[a]		3XL[b]	
Name (Accession)	Size kDa	Unique Peptides	PLGS Score	Unique Peptides	PLGS Score	Unique Peptides	PLGS Score	Unique Peptides	PLGS Score	Unique Peptides	PLGS Score	Unique Peptides	PLGS Score
Rpr2 (P40571)	16.3	-	-	-	-	-	-	3	300	-	-	3	185
Pop4 (P38336)	32.9	-	-	-	-	-	-	3	346	-	-	-	-
Pop1 (P41812)	100.5	-	-	3	86	15	226	21	374	55	2090	42	1903
Rpp1 (P38786)	32.2	19	1974	18	1535	3	381	10	938	-	-	-	-

Data from gel slices indicated and numbered in Fig. 2.9. Yeast protein nomenclature (http://www.yeastgenome.org) and accession number for SwissProt database (http://expasy.org/sprot) are indicated. PLGS score is calculated by Protein Lynx Global Server (Waters) from all available mass spectrometry data and is a statistical measure of peptide assignment accuracy (Rosenegger *et al*. 2010). Data was also searched against a randomized database to determine the false positive cut off rate with data below the cut off eliminated. Though the purity of the RNase P used in this experiment has been shown in a prior study (Hsieh *et al*. 2009), there were some minor contaminating peptides found in the gel slices. The following yeast proteins were identified and are shown with protein name and accession, as above, in parenthesis: Yp115 (Q06108), Hsp76 (P40150), Eno1 (P00924), Act (P60010), Ef1a (P02994), H4 (P02309), Rpn2 (P32565), Yl419 (Q06698), Prs8 (Q01939), Rga2 (Q06407), and Prs6a (P33297). The following minor human contaminant proteins were also identified: K1c10 (P13645.6), K2c1 (P04264.6), K22e (P35908.2), K1c14 (P02533.4), Albu (P02768.2), and K1c10 (P13645.6) along with *Sus. scrofa* Tryp (P00761.1) peptides leftover from in-gel digestion of gel slices.

[a.] Gel slices from uncrosslinked RNase P and polyU RNA.

[b.] Gel slices from UV crosslinked RNase P and polyU RNA.

not detect UV crosslinks between pre-tRNA substrate and RNase P protein subunits. However, given that pre-tRNA was shown to compete for crosslink shifts with radiolabeled polyU_{50} separated on SDS-polyacrylamide gels (data not shown), the identified RNase P proteins (Pop4p, Rpr2p) that crosslink to polyU_{50} RNA could also directly contact the pre-tRNA substrate.

It is possible that the largest protein, Pop1p, is also bound to the PolyU_{50}, though the data are ambiguous. Peptides from the C-terminus of Pop1p are found migrating in the smallest shifted band in a UV-dependent fashion, as well as throughout the gel at larger (slower migrating) positions in a UV-independent fashion (Fig. 2.9, Table 2.2). Full length Pop1p would be expected to more substantially retard the migration of the crosslinked PolyU_{50} due to its 100 kDa size. Since Pop1 is known to be particularly susceptible to proteolysis the data are consistent with proteolysis prior to UV induced crosslinking (Lygerou *et al*. 1994; Chamberlain *et al*. 1998). The only other RNase P protein identified by mass spectrometry was Rpp1p, which migrates at analyzed gel positions whether or not UV crosslinking takes place, so if there were an Rpp1p-dependent shift it would be masked (Table 2.2).

Discussion

Broad RNA Recognition Potential for Yeast Nuclear RNase P

Previous work indicated strong sequence preference when polynucleotide homopolymers were tested as inhibitors of the yeast nuclear RNase P (Ziehler *et al*. 2000). These RNAs did not similarly affect the simpler bacterial enzyme and it is proposed that the additional proteins found in the eukaryotic enzyme may have a direct

influence on substrate interactions. Here we have observed that many mixed sequence RNAs have the potential to bind to the yeast nuclear RNase P and inhibit cleavage of pre-tRNAs. Although we observe some variability in the binding of different RNAs we find no obvious sequence preferences suggesting that yeast nuclear RNase P can bind a broad set of mixed sequence RNA.

We also observe that RNase P cleaves mixed sequence RNAs at multiple sites, whereas polyU RNA is not cleaved despite also being a potent inhibitor (Fig. 2.5; Fig. 2.7). Our crosslinking data indicate that polyU RNA is very close to the active site and is positioned similarly to the cleaved substrates pre-tRNA and mixed sequence RNA (Fig. 2.8 B). Given that polyU RNA is not predicted to form stable secondary structure, these observations are consistent with a model where RNA sequence or structure is a determinant for the cleavage of an RNA by RNase P, even though the initial binding and blockage of the active site is a relatively sequence-independent event (Fig. 2.4).

It is also noted that only a small fraction of a particular mixed sequence RNA was cleaved, despite increasing levels of RNase P. This would be consistent with only a defined fraction of RNA existing in the correct conformation for cleavage at any given moment. However, this does not mean that this cleavage might not be important as *in vivo* non-tRNA substrates might be correctly positioned for cleavage by protein cofactors that assist the folding of the RNA into a more fully cleavable form (Chamberlain *et al*. 1996; Coughlin *et al*. 2008). This could explain why multiple positions of the RNA are cleaved and why cleavage is slow (Fig. 2.5).

Model of Single-Stranded RNA Binding RNase P

As expected, polyU RNA inhibits pre-tRNA cleavage by RNase P (Ziehler *et al*. 2000). However, even at high levels of polyU RNA complete inhibition was not attained (Fig. 2.2 B,C). This residual activity is not explained by a simple competitive inhibition model with the formation of an E•I complex that is in direct competition with E•S, with substrate and inhibitor competing for the same binding pocket. A model that is consistent with our data is the formation of a ternary complex E•S•I where RNase P retains a small amount of cleavage activity at high levels of inhibitor (Scheme 1). Alternatively, our data does not preclude a model where there is an inactive E•I complex that is competitive with E•S or the formation of any sort of ternary complex such as E•P•I that is in equilibrium with E•S. Finally, although there is no indication that our purification of RNase P is not homogenous, there could also be two forms of RNase P where one binds non-tRNA and the other does not. All of these possibilities indicate that there are two types of RNA binding sites in RNase P with one type that is competitive for binding tRNA structure and the other that binds RNA independently of tRNA structure.

Scheme 1

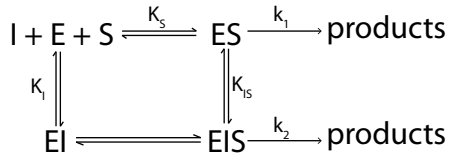

In addition, calculation of the apparent IC_{50} for mixed sequence RNA was estimated using the same equation for polyU even though at high levels of RNase P some mixed sequence RNA was cleaved (Fig. 2.5). As we titrated the IC_{50} for the mixed

sequence RNAs at levels of RNase P below those showing significant cleavage, the same scheme (Scheme 1) as polyU can be applied to mixed sequence RNA.

The Catalytic RNA Core of RNase P Can Interact With a Diverse Set of RNAs

The catalytic core of RNase P (helix P4) is formed by sequences from CR-I and CR-V and makes only limited contacts with pre-tRNA^{Tyr} substrates within the CR-I region (Fig. 2.8). Earlier crosslinking results with the deproteinized *Schizosaccharomyces pombe* RNase P RNA subunit and mature tRNA found multiple crosslinks throughout the RNA subunit (Marquez *et al*. 2006). However, we find all of the tested pre-tRNA and single stranded RNA ligands exclusively crosslink in the RNA active site of the *S. cerevisiae* holoenzyme. This could be due to more precise positioning of the RNAs in the holoenzyme, protection of inappropriate sites in the RNA subunit by protein coverage, or both.

The precise positioning of RNA crosslinked in the RNase P active site was shown via primer extension although there were differences in the exact nucleotides within Rpr1r that were in contact with the pre-tRNA^{Tyr}, polyU$_{50}$, and RNA 3$_S$ ligands (Fig. 2.8 B). This could be consistent with differences in cleavage competence among the RNA ligands (Fig. 2.5). The lack of complete congruence of the crosslinking sites is also consistent with the inhibition curves for polyU and the mixed sequence RNAs, which suggest that they do not completely block the active site (Fig. 2.2 B,C; Fig. 2.3 B,C).

RNase P Protein Subunits Interact With Single Stranded RNA

Although yeast nuclear RNase P and bacterial RNase P have been shown to have similar kinetic behavior with pre-tRNA substrates, the significantly increased content of

basic proteins of the nuclear enzyme and the ability to be inhibited by homopolymer RNA argued for a broadened ability to bind single stranded RNAs (Hsieh *et al*. 2009). We strove to understand how single stranded RNA bound to the complex in order to identify eukaryotic specific modes of interaction (Ziehler *et al*. 2000). The size dependence of unstructured polyU inhibition suggests multiple interactions with the holoenzyme are required for tight binding in a way that obscures the pre-tRNA cleavage site (Fig. 2.2 A). Many of the protein subunits are potential candidates for RNA binding, given that 7 of the 9 RNase P proteins are highly basic and several studies have shown that most of the proteins can bind RNA *in vitro* (Walker and Engelke 2006). In addition, structural studies have shown that Pop6p and Pop7p bind specifically to the P3 region of Rpr1r (Perederina *et al*. 2010). Consistent with this, we do not find Pop6p and Pop7p crosslinked with the substrate, but rather at least two other proteins (Pop4p and Rpr2p), and possibly more (including Pop1p) are in close contact with $polyU_{50}$ RNA (Fig. 2.9; Table 2.2). The proposal that these two proteins bind RNA is consistent with the finding that archaeal homologs of yeast Rpr2p and Pop4p, RPP21 and RPP29, decrease K_m, but not k_{cat} for pre-tRNA cleavage in reconstituted enzymes (Chen *et al*. 2010). Future studies of RNase P should examine the mechanism(s) of how the extensive protein complement of nuclear RNase P helps to capture and control the cleavage of physiological substrates.

In summary, our results show that yeast nuclear RNase P can bind and cleave a diverse set of RNAs *in vitro* and suggests that future studies of non-tRNA RNase P substrates will need to identify determinants other than intrinsic RNA sequence for investigating non-tRNA substrates *in vivo*. In addition, we have shown that both pre-

tRNAs and diverse single stranded RNAs bind to the active site of the Rpr1r RNA subunit. These data provide a model of nuclear RNase P in which the increased protein content allows binding of non-tRNA substrates in such a way as to allow positioning of RNA within the same catalytic site used by the ancient ribozyme for pre-tRNA 5′ end removal.

Acknowledgements

Dr. Scott Walker provided highly purified RNase P for mass spectrometry identification of crosslinked protein and critically read the manuscript. I thank Dr. Carol Fierke for critical reading of the manuscript and advice on interpretation and analysis of kinetic data. Also thanks to Dr. Goldstrohm for helpful discussions and mentioning the UMMS Proteomics & Mass Spectrometry Facility at UMASS medical school which was critical to successful protein crosslink identification. Also May Tsoi for preparation of large volumes of yeast media. This work was supported by grants GM034869 to (to D.R.E.), UM Cellular Biotechnology Training Grant T32-GM08353, and a fellowship from Horace H. Rackham Graduate School (both to M.C.M.).

References

Alifano P, Rivellini F, Piscitelli C, Arraiano CM, Bruni CB, Carlomagno MS. 1994. Ribonuclease E provides substrates for ribonuclease P-dependent processing of a polycistronic mRNA. *Genes Dev* **8**(24): 3021-3031.

Altman S, Wesolowski D, Guerrier-Takada C, Li Y. 2005. RNase P cleaves transient structures in some riboswitches. *Proc Natl Acad Sci USA* **102**(32): 11284-11289.

Bothwell AL, Stark BC, Altman S. 1976. Ribonuclease P substrate specificity: cleavage of a bacteriophage phi80-induced RNA. *Proc Natl Acad Sci USA* **73**(6): 1912-1916.

Camblong J, Iglesias N, Fickentscher C, Dieppois G, Stutz F. 2007. Antisense RNA stabilization induces transcriptional gene silencing via histone deacetylation in *S. cerevisiae*. *Cell* **131**(4): 706-717.

Chamberlain JR, Lee Y, Lane WS, Engelke DR. 1998. Purification and characterization of the nuclear RNase P holoenzyme complex reveals extensive subunit overlap with RNase MRP. *Genes Dev* **12**(11): 1678-1690.

Chamberlain JR, Pagán-Ramos E, Kindelberger DW, Engelke DR. 1996. An RNase P RNA subunit mutation affects ribosomal RNA processing. *Nucleic Acids Res* **24**(16): 3158-3166.

Chang DD, Clayton DA. 1987. A novel endoribonuclease cleaves at a priming site of mouse mitochondrial DNA replication. *EMBO J* **6**(2): 409-417.

Chen JL, Pace NR. 1997. Identification of the universally conserved core of ribonuclease P RNA. *RNA* **3**(6): 557-560.

Chen W-Y, Pulukkunat DK, Cho I-M, Tsai H-Y, Gopalan V. 2010. Dissecting functional cooperation among protein subunits in archaeal RNase P, a catalytic ribonucleoprotein complex. *Nucleic Acids Research*. Published online August 12, 2010: 1-12.

Coughlin DJ, Pleiss JA, Walker SC, Whitworth GB, Engelke DR. 2008. Genome-wide search for yeast RNase P substrates reveals role in maturation of intron-encoded box C/D small nucleolar RNAs. *Proc Natl Acad Sci USA* **105**(34): 12218-12223.

Davis JT. 2004. G-quartets 40 years later: from 5'-GMP to molecular biology and supramolecular chemistry. *Angew Chem Int Ed Engl* **43**(6): 668-698.

Evans D, Marquez SM, Pace NR. 2006. RNase P: interface of the RNA and protein worlds. *Trends Biochem Sci* **31**(6): 333-341.

Frank DN, Pace NR. 1998. Ribonuclease P: unity and diversity in a tRNA processing ribozyme. *Annu Rev Biochem* **67**: 153-180.

Giegé R, Florentz C, Dreher TW. 1993. The TYMV tRNA-like structure. *Biochimie* **75**(7): 569-582.

Gill T, Cai T, Aulds J, Wierzbicki S, Schmitt ME. 2004. RNase MRP cleaves the CLB2 mRNA to promote cell cycle progression: novel method of mRNA degradation. *Mol Cell Biol* **24**(3): 945-953.

Gimple O, Schön A. 2001. *In vitro* and *in vivo* processing of cyanelle tmRNA by RNase P. *Biol Chem* **382**(10): 1421-1429.

Gobert A, Gutmann B, Taschner A, Gößringer M, Holzmann J, Hartmann RK, Rossmanith W, Giegé P. 2010. A single Arabidopsis organellar protein has RNase P activity. *Nat Struct Mol Biol* **17**(6): 740-744.

Guerrier-Takada C, Gardiner K, Marsh T, Pace N, Altman S. 1983. The RNA moiety of ribonuclease P is the catalytic subunit of the enzyme. *Cell* **35**(3 Pt 2): 849-857.

Hall TA, Brown JW. 2002. Archaeal RNase P has multiple protein subunits homologous to eukaryotic nuclear RNase P proteins. *RNA* **8**(3): 296-306.

Hansen A, Pfeiffer T, Zuleeg T, Limmer S, Ciesiolka J, Feltens R, Hartmann RK. 2001. Exploring the minimal substrate requirements for trans-cleavage by RNase P holoenzymes from *Escherichia coli* and *Bacillus subtilis*. *Mol Microbiol* **41**(1): 131-143.

Hartmann RK, Heinrich J, Schlegl J, Schuster H. 1995. Precursor of C4 antisense RNA of bacteriophages P1 and P7 is a substrate for RNase P of *Escherichia coli. Proc Natl Acad Sci USA* **92**(13): 5822-5826.

Holzmann J, Frank P, Löffler E, Bennett KL, Gerner C, Rossmanith W. 2008. RNase P without RNA: identification and functional reconstitution of the human mitochondrial tRNA processing enzyme. *Cell* **135**(3): 462-474.

Hsieh J, Walker SC, Fierke CA, Engelke DR. 2009. Pre-tRNA turnover catalyzed by the yeast nuclear RNase P holoenzyme is limited by product release. *RNA* **15**(2): 224-234.

Hull MW, Thomas G, Huibregtse JM, Engelke DR. 1991. Protein-DNA interactions *in vivo*: examining genes in *Saccharomyces cerevisiae* and *Drosophila melanogaster* by chromatin footprinting. *Methods Cell Biol* **35**: 383-415.

Jarrous N. 2002. Human ribonuclease P: subunits, function, and intranuclear localization. *RNA* **8**(1): 1-7.

Jung YH, Lee Y. 1995. RNases in ColE1 DNA metabolism. *Mol Biol Rep* **22**(2-3): 195-200.

Kankia BI. 2003. Mg^{2+}-induced triplex formation of an equimolar mixture of poly(rA) and poly(rU). *Nucleic Acids Res* **31**(17): 5101-5107.

Komine Y, Kitabatake M, Yokogawa T, Nishikawa K, Inokuchi H. 1994. A tRNA-like structure is present in 10Sa RNA, a small stable RNA from *Escherichia coli*. *Proc Natl Acad Sci USA* **91**(20): 9223-9227.

Lee DY, Clayton DA. 1998. Initiation of mitochondrial DNA replication by transcription and R-loop processing. *J Biol Chem* **273**(46): 30614-30621.

Li Y, Altman S. 2003. A specific endoribonuclease, RNase P, affects gene expression of polycistronic operon mRNAs. *Proc Natl Acad Sci USA* **100**(23): 13213-13218.

Liu F, Altman S. 1994. Differential evolution of substrates for an RNA enzyme in the presence and absence of its protein cofactor. *Cell* **77**(7): 1093-1100.

Lygerou Z, Mitchell P, Petfalski E, Séraphin B, Tollervey D. 1994. The *POP1* gene encodes a protein component common to the RNase MRP and RNase P ribonucleoproteins. *Genes Dev* **8**(12): 1423-1433.

Marquez SM, Chen JL, Evans D, Pace NR. 2006. Structure and function of eukaryotic Ribonuclease P RNA. *Mol Cell* **24**(3): 445-456.

Marvin MC, Engelke DR. 2009. Broadening the mission of an RNA enzyme. *J Cell Biochem* **108**(6): 1244-1251.

Milligan JF, Uhlenbeck OC. 1989. Synthesis of small RNAs using T7 RNA polymerase. *Meth Enzymol* **180**: 51-62.

Peck-Miller KA, Altman S. 1991. Kinetics of the processing of the precursor to 4.5 S RNA, a naturally occurring substrate for RNase P from *Escherichia coli*. *J Mol Biol* **221**(1): 1-5.

Perederina A, Esakova O, Quan C, Khanova E, Krasilnikov AS. 2010. Eukaryotic ribonucleases P/MRP: the crystal structure of the P3 domain. *EMBO J* **29**: 761-769.

Rosenegger D, Wright C, Lukowiak K. 2010. A quantitative proteomic analysis of long-term memory. *Mol Brain* **3**(1): 9.

Schmitt ME, Clayton DA. 1993. Nuclear RNase MRP is required for correct processing of pre-5.8S rRNA in *Saccharomyces cerevisiae*. *Mol Cell Biol* **13**(12): 7935-7941.

Smith JK, Hsieh J, Fierke CA. 2007. Importance of RNA-protein interactions in bacterial ribonuclease P structure and catalysis. *Biopolymers* **87**(5-6): 329-338.

Walker SC, Engelke DR. 2006. Ribonuclease P: the evolution of an ancient RNA enzyme. *Crit Rev Biochem Mol Biol* **41**(2): 77-102.

Walker SC, Marvin MC, Engelke DR. 2010. Eukaryote RNase P and RNase MRP. In *Protein Reviews: Ribonuclease P*, Vol 10 (ed. F. Liu, S. Altman), pp. 173-202. Springer.

Wilusz JE, Freier SM, Spector DL. 2008. 3' end processing of a long nuclear-retained noncoding RNA yields a tRNA-like cytoplasmic RNA. *Cell* **135**(5): 919-932.

Yang L, Altman S. 2007. A noncoding RNA in *Saccharomyces cerevisiae* is an RNase P substrate. *RNA* **13**(5): 682-690.

Ziehler WA, Day JJ, Fierke CA, Engelke DR. 2000. Effects of 5' leader and 3' trailer structures on pre-tRNA processing by nuclear RNase P. *Biochemistry* **39**(32): 9909-9916.

Ziehler WA, Engelke DR. 2001. Probing RNA structure with chemical reagents and enzymes. *Current Protocols in Nucleic Acid Chemistry*: 6.1.1-6.1.21.

Zuker M. 2003. Mfold web server for nucleic acid folding and hybridization prediction. *Nucleic Acids Res* **31**(13): 3406-3415.

CHAPTER 3
IN VIVO ROLES FOR RNASE P

Introduction

Nuclear ribonuclease P (RNase P) in *Saccharomyces cerevisiae* plays an essential role in maturing the 5′ end of pre-tRNA via catalysis of an endonucleolytic cleavage (Frank and Pace 1998; Walker and Engelke 2006). All of the nine protein subunits and the RNA subunit, Rpr1r, are essential (Chamberlain *et al*. 1998). In addition to pre-tRNA, other substrates have been identified or implicated in yeast. Further, the affinity of RNase P *in vitro* for single stranded RNA implicates many other cellular RNAs as potential substrates for RNase P *in vivo* (CHAPTER 2).

A previous study indicated that yeast RNase P co-purifies with a diverse set of RNA (Coughlin *et al*. 2008). In addition, RNase P temperature sensitive mutants in either the RNA subunit or one of the protein subunits has been previously used to identify the accumulation of potential RNase P substrates (Samanta *et al*. 2006; Coughlin *et al*. 2008). These earlier studies agree with the model of an increased set of substrates for nuclear RNase P in yeast. However, they were carried out with earlier methods that were not of sufficient resolution to distinguish between introns, coding regions, intergenic regions, and which strand of the genome corresponded to specific RNA. Our current study investigates the effect of the RNase P temperature sensitive mutation on the levels of RNA in *S. cerevisiae* using updated tools that provide a more comprehensive analysis of the role of RNase P *in vivo*. Two distinct classes of non-tRNA transcripts were found to

broadly accumulate in an RNase P mutant including recently characterized non-coding RNAs of unknown function and pre-mRNAs containing introns.

It was previously shown using a high density, strand-specific microarray that as much as 85 % of the yeast genome is transcribed, with many novel non-coding RNAs of unknown function identified (David *et al*. 2006). These recently identified transcripts have been shown to fall into two broad categories of RNA that either exist stably in cells (Stable Unannotated Transcripts, SUTs), or are normally degraded rapidly by RNA surveillance pathways (Cryptic Unstable Transcripts, CUTs) (reviewed in (Jacquier 2009)). These two classes were differentiated using a deletion mutant of a catalytic component of the nuclear exosome, *RRP6*, with CUTs generally stabilized in the knockout strain (reviewed in (Vanacova and Stefl 2007)). Both of these RNA classes are transcribed by RNA polymerase II, with many of them transcribed in the opposite direction of associated gene promoters (Neil *et al*. 2009; Xu *et al*. 2009). CUTs are typically ~200-600 nucleotides, 5′-capped, and have heterologous 3′ ends (reviewed in (Jacquier 2009)). SUTS are usually longer then CUTs with an average length of 761 nucleotides (Xu *et al*. 2009). The two classes are not rigidly differentiated since there are conflicting results from two studies that show overlap between the two (Neil *et al*. 2009; Xu *et al*. 2009. Inclusion of probes specific to CUTs and SUTs on the microarray used in this study showed a broad accumulation of both types of non-coding RNA with RNase P mutation.

In addition to CUTs and SUTs, introns of pre-mRNA were also probed using the microarray as outlined below and the broad accumulation of intron containing pre-mRNA was observed. Splicing of pre-mRNA in *S. cerevisiae* is atypical of eukaryotes in that

introns are only present in ~5 % of genes (Spingola *et al*. 1999; Juneau *et al*. 2006; Roy and Gilbert 2006). Of this small percentage of genes that have introns, ribosomal genes dominate with 71 % containing one or more introns (Planta and Mager 1998). Pre-mRNA splicing in yeast is mechanistically similar to other eukaryotes, requiring five small nuclear ribonucleoprotein particles (snRNPs): U1, U2, U4, U5, U6 (Patel and Bellini 2008). These snRNPs associate with pre-mRNA and a large number of splicing factors to form the spliceosome (reviewed in (Brow 2002; Wahl *et al*. 2009)). The small nuclear RNAs (snRNA) that are specific to these snRNPs are variably capped, modified, and processed on the 3′-end (Will and Lührmann 2001; Patel and Bellini 2008). In addition, only U6 snRNA, which is the most highly conserved snRNA, is transcribed by RNA polymerase III while the other spliceosome snRNA are transcribed by RNA polymerase II.

The assembly of the spliceosome is a complex process involving sequential assembly of snRNPs (Will and Lührmann 2001). Spliceosomal snRNAs U1, U2, U4, U5 are bound by seven common "Sm" proteins: B, D1, D2, D3, E, F, G along with snRNA specific proteins to form snRNPs (Brow 2002). U6 snRNA is bound first by the yeast La protein, Lhp1, then later by seven "Sm-like" proteins Lsm2-8 along with specific proteins to form U6 snRNP (Pannone *et al*. 2001). Some of the proteins that make up the U6 snRNP also bind to other RNAs such as Rpr1r and pre-tRNA. Specifically, the La protein has been shown to bind the oligo uridine 3′ end of newly RNA polymerase III transcribed pre-tRNA and associate with the precursor to RNase P RNA, pre-Rpr1r (Pannone *et al*. 1998). In addition Lsm2-8 has been shown to bind pre-Rpr1r (Salgado-Garrido *et al*. 1999). The complex process of spliceosomal assembly and the relatively unknown role

that some of these proteins also play in binding both pre-Rpr1r and the RNase P substrate pre-tRNA indicates possible overlap of RNase P and pre-mRNA splicing associated factors.

The goal of this study was to identify non-tRNA RNase P substrates in yeast that were not detected previously. Monitoring the accumulation of RNA in strains with an RNase P mutation led to the identification of two main classes of RNase P substrates: SUTs/CUTs and mRNA containing introns. These results expanded the previous identification of one specific class of intron containing pre-mRNA, intron encoded box C/D snoRNA, and indicated that general splicing is disrupted with RNase P temperature sensitive mutation. We further show that a defect in U4/U6 snRNA assembly coincides with RNase P mutation. However, we do not know if this is a direct effect from RNase P or due to the general accumulation of pre-tRNA in the RNase P mutant strain. In addition, we found that a large number of SUTs and CUTs accumulate in the RNase P mutant with some accumulating antisense to coding regions. Also, the accumulation of multiple large antisense transcripts could implicate some of these largely uncharacterized RNAs as RNase P substrates. This work expands on previous studies in order to provide a more complete understanding of the extent of RNase P's influence on a variety of RNA in the cell.

Materials and Methods

Yeast Strains

S. cerevisiae strain JLY1 (*MATa ade2-1 his3-11,15 leu2-3,112 trp1-1 ura3-1 can1-100 RPR1::HIS3*), with a background of W3031A, was the parent strain with *RPR1*

on a *LEU2*-marked plasmid. We investigated the effect of a temperature sensitive mutation in Rpr1r at position $G_{207}G_{211}$ (Pagán-Ramos *et al*. 1996). Recently it has come to our attention that another mutation in the P3 region of *RPR1* (position 69-75: ATCAGAT::CAGGACG) is present in both the wild type control strain and the temperature sensitive mutant strain $G_{207}G_{211}$.

Yeast Growth

The synthetic dropout media (SD-His) was used for growth of JLY1 strains. For temperature sensitive shifts of $G_{207}G_{211}$ previous studies have identified the optimal growth conditions to observe RNase P defects (Coughlin *et al*. 2008). Both wild type and temperature sensitive yeast were grown into mid-log phase then diluted and shifted to 37 °C in pre-warmed SD-His media for 2 hours.

Total RNA/Genomic DNA Preparation

RNA was extracted from yeast pellets prepared as outlined above from 500 ml liquid culture. Cells were re-suspended in 10 ml AE buffer [50 mM NaOAc pH 5.2, 10 mM EDTA] and 1.7 ml 10 % SDS. 10 ml acid phenol [pH 4.3] was added and samples were incubated at 65 °C for 10 minutes with vortexing every minute. 10 ml of chloroform was added and samples were spun down for 5 minutes at 14,000 RPM. The top layer was taken off and 10 ml of a 50:50 mix of chloroform and acid phenol was added. Samples were spun for 5 minutes at 14,000 RPM. This was repeated two more times followed by 10 ml of chloroform. Samples were ethanol (EtOH) precipitated [3x volume 100 % EtOH and 1/10 volume 3 M NaOAc pH 5.2], spun at 14,000 RPM for 30 minutes, and pellets were washed with 70 % EtOH. RNA was resuspended in H_20 and incubated with 1x final

20x CP-stop mix [0.05 mg/ml proteinase K, 0.1% SDS, 5 mM EDTA] for 20 minutes at 42 °C. Samples were then extracted three times with acid-phenol:chloroform followed with chloroform as outlined above. After EtOH precipitation and 70 % EtOH wash as outlined above, samples were resuspended in H_20 and stored in -80 °C.

Genomic DNA (gDNA) was prepared from the same background strain W3031A that was used for total RNA preparation above. Yeast pellets from 100 ml liquid culture grown to mid-log phase were resuspended in 0.5 ml 1 M sorbitol and 0.1 M EDTA (pH 7.5). 250 μg Zymolyase 20T [Seikagaku] was added and samples were incubated at 37 °C for 1 hour. Cells were spun down at 10,000 RPM briefly then resuspended in 0.5 ml 50 mM Tris-Cl (pH 7.4) and 20 mM EDTA (pH 7.5) along with 0.05 ml 10 % SDS and incubated at 65 °C for 30 minutes. 0.2 ml 5 M potassium acetate was then added and samples were incubated on ice for 60 minutes. After centrifugation at 14,000 RPM for 5 minutes nucleic acid was precipitated using equal volume 100 % isopropanol. Samples were spun at 14000 RPM for 5 minutes then resuspended in H_20.

Microarray Analysis

400 μg total RNA, as prepared above, was treated with 12 U Turbo DNase I [Ambion] at 37 °C for 30 minutes. 10 μl inactivation reagent [Ambion] was added for 2 minutes at 25 °C to inactivate the DNase. Supernatant was analyzed using UV/Vis spectroscopy to determine the nucleic acid concentration after DNase treatment. Figure

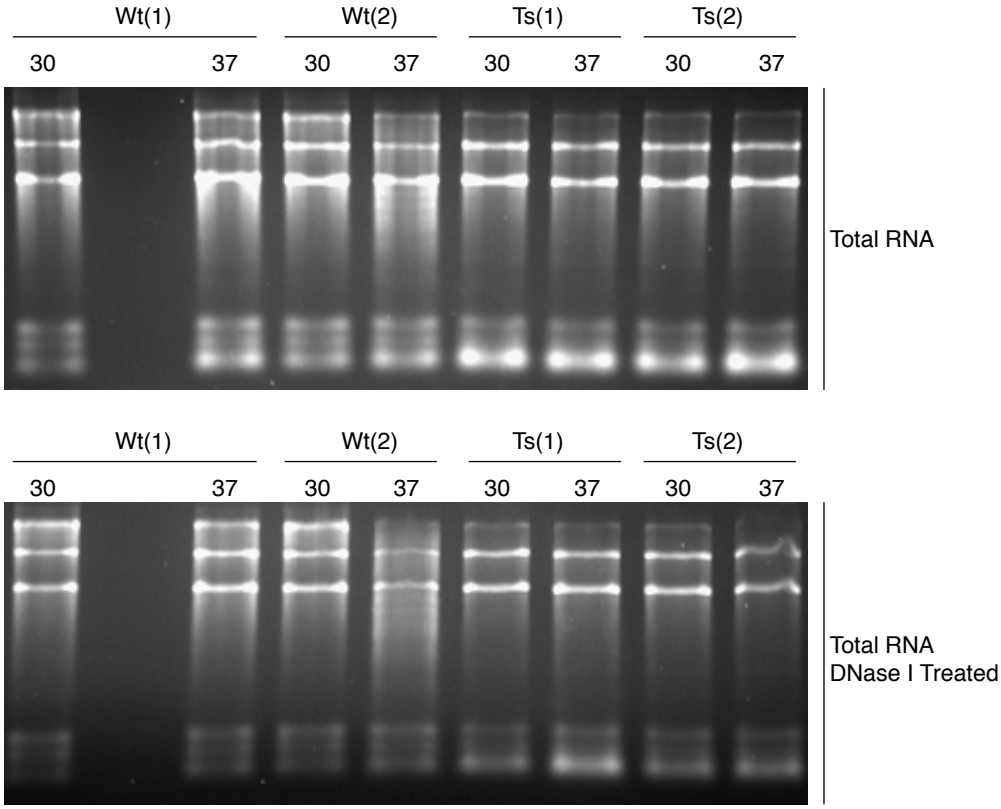

Figure 3.1. Total RNA with and without DNase I treatment.
Total RNA was separated on a 1 % agarose gel and stained with ethidium bromide. Wild type (WT) and temperature sensitive (TS) RNA samples were isolated from biological replicates indicated by number. The temperature that the samples were grown at, 30 °C or 37 °C, is also indicated. DNase I treated samples are indicated and these were samples used for microarray analysis.

3.1 shows total RNA used in the microarray analysis with and without DNase I treatment. Samples were EtOH precipitated as above and shipped to collaborators for further preparation as outlined below [Dr. Lars Steinmetz].

The laboratory of Dr. Lars Steinmetz prepared complementary cDNA for hybridization as follows. cDNA first strand synthesis was carried out using random hexamer primers [Invitrogen] at a ratio of RNA:hexamer of 1:0.086 using the SuperScript II reverse transcriptase [Invitrogen]. Hexamers were annealed to RNA in the presence of oligo dT 12-18 primers [Invitrogen] by heating at 70 °C for 10 minutes followed by incubation on ice. Primer extension was then carried out per Superscript II protocol at 42 °C but with the addition of 20 μg/ml final concentration of actinomycin D (ActD). ActD, which inhibits DNA but not RNA dependent polymerase activity, was added during reverse transcription in order to prevent spurious synthesis of second strand cDNA that often occurs during primer extension, which could produce false antisense signal (Perocchi *et al*. 2007). RNA was digested with an RNase cocktail (RNase A & RNase T1 [Ambion] and RNase H [Epicentre] to leave cDNA. cDNA was purified with Affymetrix Genechip cleanup module [Affymetrix] per manufacturers directions.

cDNA was fragmented and biotinylated using the Affymetrix GeneChip WT Terminal labeling kit [Affymetrix]. Prior to biotinylation, fragmentation was done using 10 U uracil DNA glycosylase (UDG) and 1000 U apurinic/apyrimidinic endonuclease (APE) at 37 °C for 1 hour. Samples were then labeled on the 3′ end for 1 hour at 37 °C with a proprietary biotinylated compound using terminal deoxynucleotidyl transferase (TdT) per Affymetrix's protocol.

Samples were hybridized to arrays using Affymetrix GeneChip hybridization, wash, and stain kit [Affymetrix]. Biological duplicate samples were hybridized twice and duplicate results were used for further analysis. As a further control, genomic DNA, which was prepared as outlined above, was also prepared and hybridized to the array. This was used to minimize probe specific effects (Huber *et al*. 2006).

The hybridization data were normalized and segmented using the Bioconductor package 'tilingArray (Huber *et al*. 2006). The database found on the website: http:// steinmetzlab.embl.de/engelkeArray/index.html provides further information as well as an interface to visualize array expression data. Details of the array design can be found in previous work by the Steinmetz lab (David *et al*. 2006).

Northern Blots of RNA

Northern blots were carried out using both denaturing and native polyacrylamide and denaturing agarose gel systems. For denaturing polyacrylamide northern blots, RNA was either EtOH precipitated as above or dried down using a speed vacuum system prior to re-suspending in 5 µl 2x FEXBS [95 % formamide, 15 mM EDTA, 0.025 % SDS, 0.02 % xylene cyanol, 0.02 % bromophenol blue]. Samples were heated at 95 °C for 5 minutes prior to loading on a freshly poured and fully polymerized (6-10%) polyacrylamide gel [SequaGel-UreaGel System, National Diagnostics] that had been pre-run for at least 30 minutes at 50 mA in 1x TBE [Tris/Borate/EDTA] running buffer. RNA was separated using 40 mA for varying time depending on the size of the RNA being analyzed. The RNA was then electro-transferred to a Nytran Supercharge membrane for 2 hours [Schleicher & Schuell Biosciences].

For native polyacrylamide northern blots to determine the interaction of U4/U6 snRNPs the indicated protocol was followed (Pannone *et al*. 2001). Briefly, 4 % 80:1 acrylamide:bis-acrylamide was mixed with 25 mM Tris-HCl pH 7.5, 25 mM boric acid, and 1 mM EDTA. Lysate that was isolated from yeast by bead beating using acid washed glass beads was loaded in this same gel buffer with 4 % glycerol and 0.02 % bromophenol blue dye. Samples were separated on a pre-run gel (250 V for 30 minutes) at 4 °C running at 300 V until the dye reached the bottom of the gel. RNA was electro-transferred as above to Nytran membrane.

Denaturing agarose gels were used for larger RNA and were carried out as follows. RNA was mixed with an equal volume of 2x northern sample buffer [1x MOPS buffer pH 7.0, 20 % formaldehyde, 50 % formamide]. MOPS buffer was prepared as a 20x pH 7.0 stock [400 mM MOPS, 60 mM NaOAc, 20 mM EDTA]. Also, 1/10 volume 10x northern loading dye [50 % glycerol, 1 mM EDTA pH 8.0, 0.25 % bromophenol blue, 0.25 % xylene cyanol] and 0.5 μg ethidium bromide was added to the RNA. An RNA ladder [Lonza] was loaded in the same way as total RNA and run for size estimation. 1-1.4 % agarose gels were prepared using 1x MOPS buffer and 640 mM formaldehyde. Gel dimensions were 1 cm thick, 150 cm long, and 120 cm wide. RNA was heated at 95 °C for 5 minutes then loaded on gels and separated in 1x MOPS buffer at 120 V. RNA was transferred to Nytran Supercharge membrane using 20x SSPE for 3 hours using a TurboBlotter apparatus for passive downward transfer of RNA to the blot [Schleicher & Schuell Biosciences].

Specific oligonucleotide probes outlined in table 3.1 were designed to hybridize to RNA under analysis (IDT). Probes were labeled with [γ-P^{32}]ATP using 1000 U

Table 3.1. Northern blot and primer extension analysis oligonucleotides.

Primer Name	Sequence
$tRNA^{Leu3}$	TGCTAAGAGATTCGAACTCTTGCA
Hnm1	TCAAAGGTACACCAGTGTGTGGGT
Sut428_1	GAGGAGTGGAAGAGATTGGTTGACTTGGAGGACTTGGATTCAAAA GAGGGG
Sut428_2	CCATCAGGGGCAGAAAGTATGGTATCAATATCGATAAACCATGGAC CCAAA
Opt2	TTGGCATGACTGTTGGCCATAGTGCA
Sut116_1	CCGCATATCCGCACGCCGGTGGTCAGTTTTGGTGGTCTTTGAAGCTT GCCC
Sut116_2	GGCAAGGTTATGTTGGTCATTTGCCAGGGACAATGGTCTTCCATTAT CCCG
Rps15	GCTGGCTTGGAAGTCATACCACGGGC
Rpl31A/B	AACACCCTTGACACCTCTCTTCCAG
Ubc13_CDS	GCTTCCATTGGATAGTCGTCAGGCA
Rps29A_CDS	GCCGTACTTTCTGATCAAACCGGTG
Scr1	AGAACGGACTCTCCCGCCTCCGGGC
U1	CGTCAGCAAACACGCCTTCCGCGCCG
U2	GAGCGCCCCATCCGCACTAGCACCCC
U4	AGGTATTCCAAAAATTCCCTAC
U5	CCACAGTTCTTGATGTTGACC
U6	CGAAATAAATCTCTTTGTAAAACGG

All oligonucleotides were ordered from Integrated DNA Technology.

polynucleotide kinase [NEB] for 1 hour at 37 °C. Samples were then desalted using Qiagen nucleotide removal kits and eluted from columns in provided buffer EB [Qiagen]. Membranes were pre-hybridized for 1 hour at 40 °C, which was 5 °C below the hybridization temperature (45 °C), in pre-hybridization buffer [5.25x SSPE, 0.5 % SDS, 5.25x Denhardts (Amresco)]. 20x SSPE buffer pH 7.4 contains [3 M NaCl, 200 mM sodium phosphate monobasic, 25 mM EDTA]. ~$40x10^6$ CPM of kinased oligo was then added to the membrane and incubated in hybridization buffer [6.3x SSPE, 1 % SDS] for at least 12 hours at 45 °C.

After hybridization blots were washed 4 times with buffer A [6x SSPE, 1 % SDS] at either room temperature or 37 °C for 15 minutes each. One final wash was carried out with 6x SSPE for 15 minutes at 37 °C. Blots were exposed to phosphor screen and visualized using a Typhoon Trio+ imager. Quantization of bands was done using ImageJ software [http://rsbweb.nih.gov/ij/].

Primer Extension Analysis of U4 and U6

Primer extension was carried out with total RNA isolated from wildtype control yeast and temperature sensitive yeast prepared as above. Omniscript reverse transcriptase was used per manufacturer's protocol [Qiagen]. 4 U of Omniscript reverse transcriptase was used to synthesize cDNA from 1 μg total RNA for 50 minutes at 42 °C. 20 U Superasin RNase inhibitor was also added [Ambion]. ~200,000 CPM of kinased U4 and U6 oligos, see Table 3.1, were used for primer extension. After primer extension, samples were precipitated using EtOH as above then resuspended in 2x FEXBS, heated at 95 °C for 3 minutes, and loaded on an a pre-run [50 mA for 30 minutes] 8 % denaturing polyacrylamide gel [SequaGel-UreaGel System, National Diagnostics]. Samples were

separated with 40 mA then the gel was dried down using a gel drying vacuum system and exposed to a phosphor screen with visualization using a Typhoon Trio+ imager.

Results

High-Density, Strand-Specific Identification of RNAs that Accumulate in Temperature-Sensitive Mutants

We have previously identified several RNase P temperature sensitive (TS) mutations that result in the accumulation of pre-tRNA (Pagán-Ramos *et al*. 1996; Xiao *et al*. 2005; Xiao *et al*. 2006). Some of the TS mutations in Rpr1r, the RNA subunit of RNase P, were in a region that had been implicated in magnesium coordination, which is important for cleavage. Mutations were also shown to primarily affect the k_{cat} for tRNA substrates (Pagán-Ramos *et al*. 1996). Using these TS mutants in the past we have identified RNAs that are enriched after temperature shift to 37 °C, indicating that RNase P could be involved in the processing of these accumulated RNAs (Coughlin *et al*. 2008). As would be expected, the severity of the mutations varied, indicated by the time it took growing at 37 °C to observe the accumulation of pre-tRNA. In one mutation in Rpr1r where the wild type adenosine nucleotides where replaced with guanosine nucleotides at the indicated positions, $G_{207}G_{211}$, pre-tRNA processing defects were observed after 2 hour incubation at 37 °C and therefore this mutant was used in this study. To control for temperature induced changes that were independent of RNase P mutation, we also grew both wild type (WT) and the TS yeast at 30 °C for 2 hours. As seen in Figure 3.2, pre-$tRNA^{Leu}$, is accumulating strongly in the TS strain. It is also worth noting that a defect is observed even at 30 °C, consistent with severely defective RNase P activity.

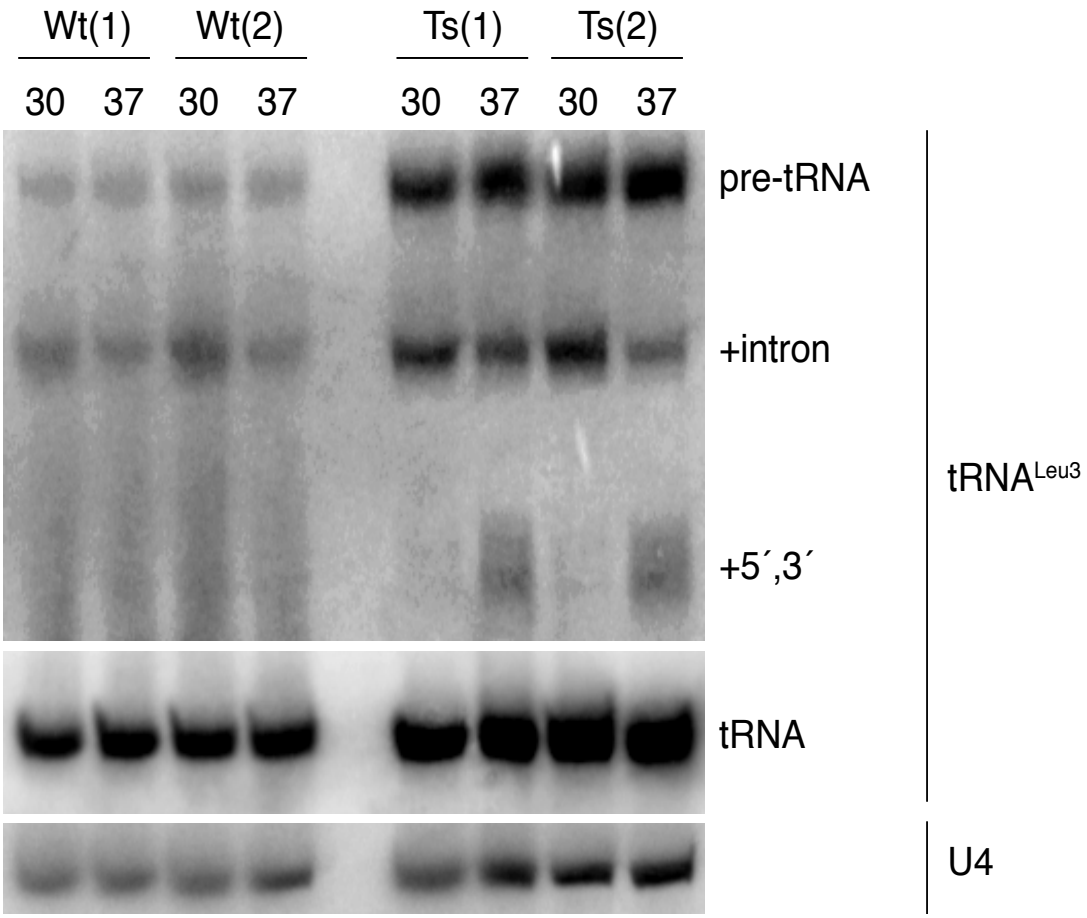

Figure 3.2. Pre-tRNA accumulates with RNase P temperature sensitive mutation ($G_{207}G_{211}$).

Samples were separated on an 8 % denaturing polyacrylamide gel and subjected to northern blot analysis. Northern blots probed with an oligonucleotide specific to the 3´ non-coding exon region of $tRNA^{Leu3}$ are shown with biological replicates of total RNA from wild type (WT) and temperature sensitive (TS) strains grown at 30 °C or 37 °C. Identity of precursor tRNA is indicated with identification due to relative size of accumulated RNA. Pre-tRNA precursor species were previously characterized (Lee *et al.* 1991). U4 RNA is probed as a loading control. Panels are shown separated from the same blot due to the varying amounts of different RNA species.

Table 3.2. Top nuclear-encoded RNAs that enrich with temperature sensitive mutation.

Ribosomal small subunit mRNAs (from Top 250)	*RPS10A* (13.81), *RPS29A* (7.80), *RPS10B* (6.79), *RPS25A* (6.48), *RPS18B* (5.40), *RPS4A* (4.88), *RPS6B* (4.80), *RPS30A* (4.04), *RPS19A* (3.78), *RPS19B* (3.53), *RPS26B* (3.31), *RPS21B* (3.16), *RPS16A* (3.09), *RPS23B* (2.91), *RPS29B* (2.84), *RPS24B* (2.82), *RPS30B* (2.75), *RPS27B* (2.46), *RPS8A* (2.43), *RPS24A* (2.41), *RPS11B* (2.26)
Ribosomal large subunit mRNAs (from Top 250)	*RPL39* (15.05), *RPL27B* (14.45), *RPL34B* (13.62), *RPL37A* (13.47), *RPL26B* (11.19), *RPL13B* (9.37), *RPL34A* (8.50), *RPL37B* (7.69), *RPL19B* (7.39), *RPL31A* (5.73), *RPL23B* (5.11), *RPL36A* (4.54), *RPL40B* (4.51), *RPL14A* (4.26), *RPL29* (4.24), *RPL27A* (4.08), *RPL40A* (4.02), *RPL43A* (3.75), *RPL35B* (3.49), *RPL33B* (3.45), *RPL7A* (3.00), *RPL21A* (2.88), *RPL26A* (2.65), *RPL6A* (2.40), *RPL14B* (2.38)
Cryptic Untranslated Transcripts (CUTs) (from Top 250)	*CUT324* (5.43), *CUT526* (5.34), *CUT680* (4.93), *CUT843* (4.20), *CUT008* (4.00), *CUT249* (3.42), *CUT846* (3.14), *CUT128* (3.13), *CUT073* (3.12), *CUT149* (3.05), *CUT732* (3.04), *CUT009* (2.99), *CUT791* (2.94), *CUT595* (2.89), *CUT523* (2.80), *CUT347* (2.75), *CUT339* (2.67), *CUT572* (2.63), *CUT306* (2.61), *CUT447* (2.60), *CUT376* (2.60), *CUT461* (2.60), *CUT168* (2.57), *CUT894* (2.56), *CUT190* (2.51), *CUT734* (2.47), *CUT085* (2.44), *CUT055* (2.42), *CUT456* (2.39), *CUT012* (2.37), *CUT325* (2.35), *CUT689* (2.33), *CUT125* (2.33), *CUT432* (2.32), *CUT238* (2.29), *CUT830* (2.27), *CUT676* (2.27)
Stable Unannotated Transcripts (SUTs) (from Top 250)	*SUT582* (5.32), *SUT741* (3.90), *SUT116* (3.83), *SUT677* (3.74), *SUT074* (3.53), *SUT139* (3.49), *SUT248* (3.48), *SUT625* (3.27), *SUT279* (3.26), *SUT517* (3.23), *SUT814* (3.10), *SUT631* (3.08), *SUT699* (3.04), *SUT008* (3.02), *SUT205* (3.00), *SUT617* (2.96), *SUT101* (2.96), *SUT771* (2.95), *SUT542* (2.93), *SUT045* (2.89), *SUT346* (2.79), *SUT343* (2.78), *SUT129* (2.78), *SUT249* (2.73), *SUT691* (2.68), *SUT035* (2.67), *SUT519* (2.66), *SUT553* (2.65), *SUT636* (2.64), *SUT200* (2.62), *SUT287* (2.59), *SUT827* (2.58), *SUT442* (2.54), *SUT535* (2.53), *SUT700* (2.48), *SUT411* (2.45), *SUT844* (2.44), *SUT278* (2.43), *SUT404* (2.41), *SUT313* (2.39), *SUT273* (2.37), *SUT482* (2.34), *SUT497* (2.33), *SUT056* (2.32), *SUT114* (2.32), *SUT001* (2.30), *SUT756* (2.29), *SUT808* (2.28), *SUT652* (2.27), *SUT250* (2.27), *SUT288* (2.26), *SUT526* (2.25), *SUT593* (2.25)
Core Sm Transcripts (from Top 250)	*SMD3* (3.00), *SMX3* (2.27)
Transcripts Containing Introns (from Top 250)	*DYN2* (2.75), *YNL050C* (2.27)
Dubious or Unknown Transcripts (from Top 250)	*YOR053W* (3.70), *COS12* (2.99), *YIL127C* (2.96), *YGR169C-A* (2.70), *YGR121W-A* (2.69), *YJL144W* (2.51), *YNL162W-A* (2.46), *YNL050C* (2.27)
Miscellaneous Transcripts (from Top 250)	*AIF1* (3.97), *SPG4* (3.20), *YCL058W-A* (2.85), *ATG8* (2.74), *SNR9* (2.51), *MAG1* (2.50), *JID1* (2.25)

Accumulation values are indicated in parenthesis for 37 °C only. Full listing can be found in Appendix. Underlined RNAs have one or more intron(s).

Using high-density, double stranded microarrays we determined how RNA levels change with RNase P TS mutation. The 250 most highly enriched RNAs indicated by the microarray are listed in the Appendix. Table 3.2 shows a summary of these RNAs organized by type of gene product. Two classes of RNA that were the most affected by RNase P mutation were ribosomal protein mRNA, both large and small subunit, and CUTs/SUTs. In addition, we also observed two mRNA transcripts, Smd3 and Smx3, accumulating, which encode core proteins of the Sm complex and associate with four of the five spliceosome snRNAs (U1, U2, U4, U5). Further we observe two additional transcripts that have introns, Dyn2 and Ynl050c. Dyn2 is a cytoplasmic light chain dynein that is thought to be involved in assembly of the nuclear pore complex and Ynl050c is an uncharacterized ORF. We also see a number of dubious/unknown transcripts along with miscellaneous transcripts that do not easily fit into a category.

Using a transcript map that visually indicates the change in abundance of RNAs across the microarray, it was clear that the introns of ribosomal protein mRNAs were enriched (Fig. 3.3 A,B). Further, other introns of non-ribosomal mRNA were also enriched (Fig. 3.3 C). Figure 3.3 F-H shows a representative sample of regions corresponding to CUTs and SUTs that are enriched in the temperature sensitive mutant at the non-permissive temperature. These RNAs could not be distinguished in our previous study because double-stranded, whole ORF probe arrays were used (Coughlin *et al*. 2008).

Intron Containing mRNA

We used northern blot analysis of total RNA to confirm microarray results for selected mRNA intron regions and to determine the nature of the RNAs that were

Figure 3.3. Transcript heat-maps.
Expression data along various positions of the indicated chromosomes (x-axis) for the Watson (W, top) and the Crick (C, bottom) strands. The whole genome is found in a searchable online database (see methods). Normalized signal intensities are shown for indicated samples (y-axis): biological replicates for either wild type (WT) or temperature sensitive (TS) strains grown at either 30 °C or 37 °C in synthetic media. Vertical red lines show inferred positions of transcription boundaries. Genome annotations are shown in the center with annotated open reading frames (ORFs) in blue and untranslated regions (UTRs) and introns represented by gray lines. SUTs are represented by orange boxes and CUTs by purple boxes while a dubious ORF is indicated by a light blue box. Arrows indicate direction of transcription. Coordinates are indicated in base pairs in the center. A-C) show representative examples of introns accumulating in mRNA with RNase P TS mutation, either ribosomal mRNA A,B) or non-ribosomal mRNA C) with a ribosomal mRNA not containing an intron D) shown as a control. E-H) show representative examples of SUTs E,G,H) and CUTs F,H) accumulating with RNase P TS mutation. Some examples show reciprocal trends of ORFs de-enriching with RNase P TS mutation while antisense RNA accumulates E,H).

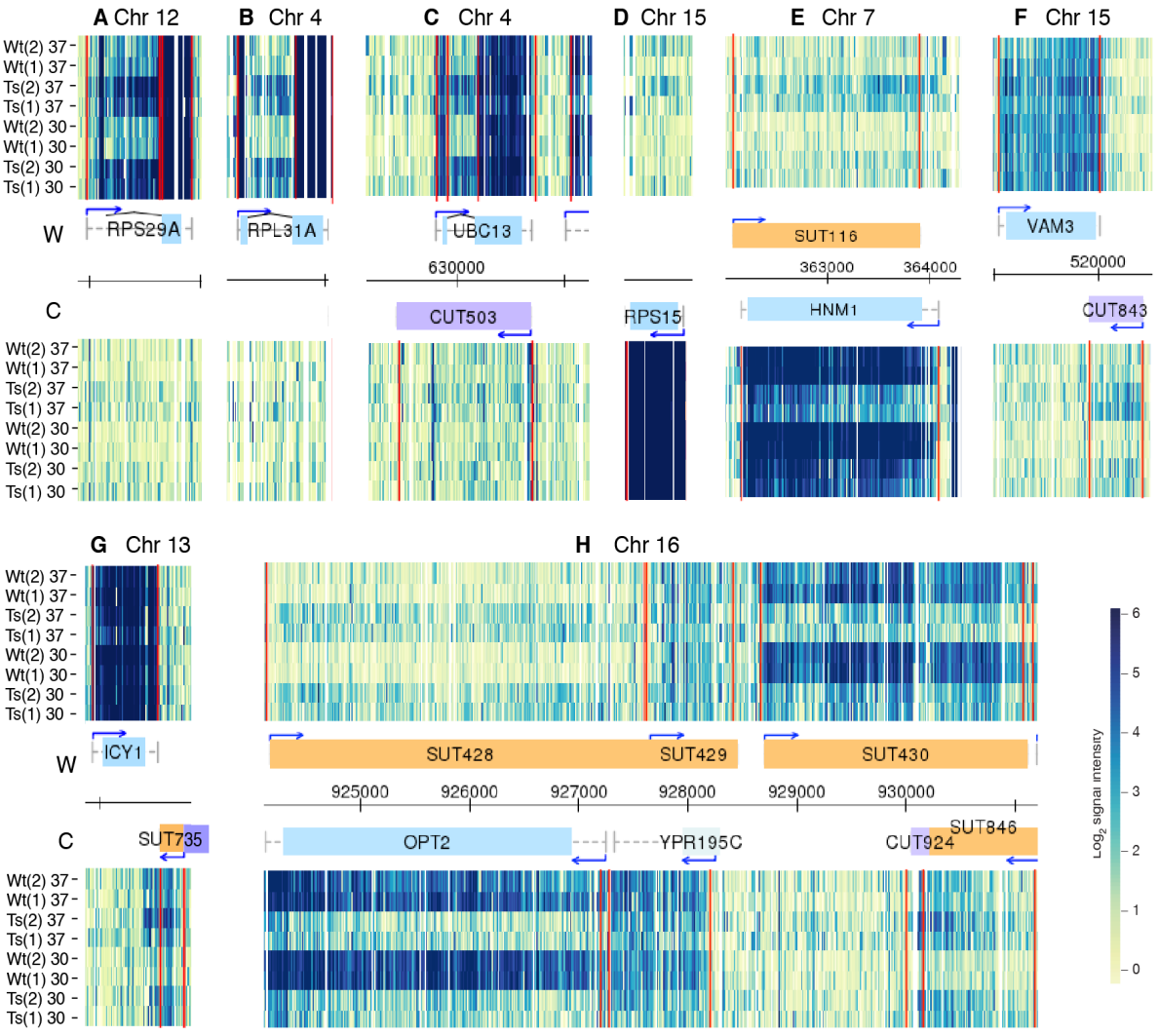
A Chr 12
B Chr 4
C Chr 4
D Chr 15
E Chr 7
F Chr 15
Wt(2) 37
Wt(1) 37
Ts(2) 37
Ts(1) 37
Wt(2) 30
Wt(1) 30
Ts(2) 30
Ts(1) 30
W
RPS29A
RPL31A
UBC13
SUT116
VAM3
630000
363000
364000
520000
C
CUT503
RPS15
HNM1
CUT843
G Chr 13
H Chr 16
ICY1
SUT428
SUT429
SUT430
925000
926000
927000
928000
929000
930000
SUT735
OPT2
YPR195C
CUT924
SUT846
Log2 signal intensity
6
5
4
3
2
1
0

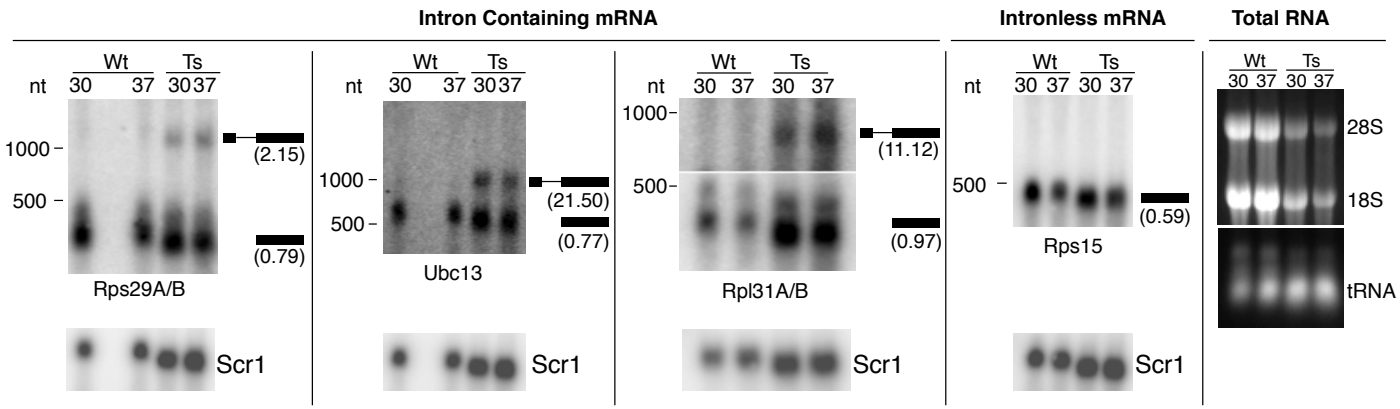

Figure 3.4. Pre-mRNA accumulates with RNase P temperature sensitive mutation.
Total RNA was separated using 1.4 % denaturing agarose gels and subjected to northern blot analysis. Indicated RNAs, intron containing or intron-less mRNA, were probed on blots with oligos specific to 3´-exon regions. Total RNA is shown for wild type (WT) and temperature sensitive (TS) total RNA isolated from yeast grown at either 30 °C or 37 °C. An RNA ladder was used to estimate sizes (nt) of probed RNA and is indicated next to each blot. In addition, a schematic of inferred RNA identity with pre-mRNA and mature mRNA is indicated next to the bands. Fold-enrichment levels for TS compared to WT samples (average of both temperatures) normalized to loading control Scr1 RNA are shown for both mature mRNA and accumulating pre-mRNA as indicated below schematics in parenthesis next to each band. Both intron containing ribosomal and non-ribosomal mRNA along with a ribosomal mRNA without an intron are shown. One representative sample of the total RNA used for indicated northern blots is shown separated on a 1.4 % denaturing agarose gel with staining using ethidium bromide along with major RNA species indicated along the side (28S, 18S, tRNA).

accumulating in RNase P TS samples. Figure 3.4 shows northern blots of RNA from both WT and TS yeast that were shifted to 30 °C or 37 °C for 2 hours. We probed RNA for two ribosomal mRNAs containing introns, as well as a non-ribosomal mRNA and one non-ribosomal mRNA as a control using an oligonucleotide primer specific for the coding sequence (CDS). We observe accumulation of pre-mRNA in all intron-containing mRNAs tested. Using the Scr1 RNA as a loading control, we normalized the signals and the ratios of TS/WT for both pre-mRNA and mature mRNA with results shown in Figure 3.4. There is a slight decrease in the amount of the mature mRNA when comparing the ratio of TS to WT in most cases once loading differences are accounted for. In addition, the ethidium stained ribosomal bands shown in Figure 3.4 indicate that the ribosomal bands, 28S and 18S, are decreasing in abundance also. As a further control we carried out semi-quantitative RT-PCR with primers specific to the 5′ exon and the intron of Rpl31a and Ubc13 pre-mRNA from total RNA isolated from both WT and TS yeast. These experiments confirmed that pre-splicing precursor pre-mRNA is accumulating in the TS samples and not a splicing intermediate mRNA (data not shown).

In probing the U6 snRNA as a loading control we noticed that there was a small size difference in U6 in the TS strain relative to the WT strain. We subsequently analyzed all of the spliceosome snRNAs and found that there was a slight size decrease in the ones that were small enough for a 2-4 nt difference to be resolved (Fig. 3.5). It appears that the overall sizes of the RNAs get smaller in the temperature sensitive strain even at 30 °C. As these size changes suggested terminal exonuclease trimming, we used primer extension to determine if the 5′ ends of U4 and U6 RNAs were changing in size. Figure 3.5 C shows

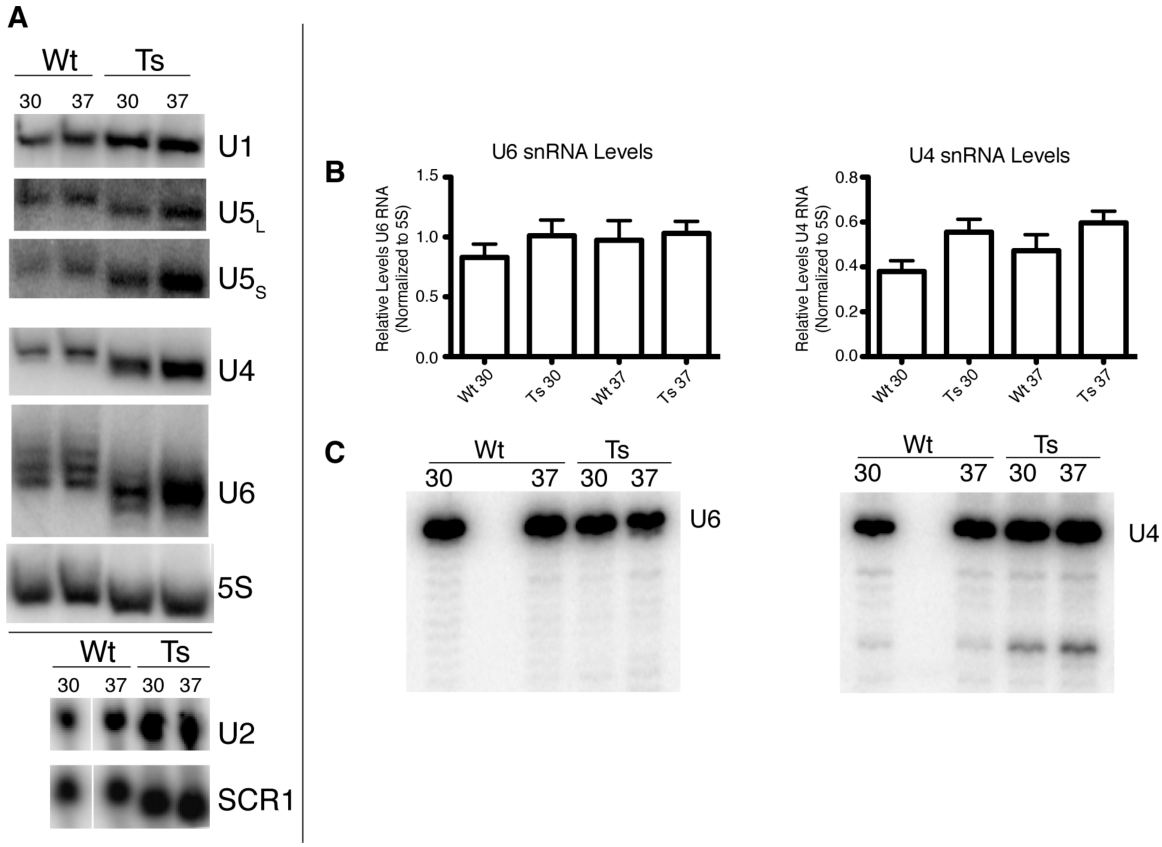

Figure 3.5. Spliceosome RNA in RNase P temperature sensitive mutant samples.
A) Total RNA was separated on either a 10 % denaturing polyacrylamide gel (U1, U5, U4, U6) or a 1.4 % denaturing agarose gel (U2) then subjected to northern blot analysis. Spliceosome RNA is shown probed with oligos on a northern blot in samples isolated from biological replicates of either wild type (WT) or RNase P temperature sensitive (TS) samples grown at either 30 °C or 37 °C. Apparent size change in most spliceosome RNA is observed with identity of probed RNA shown along the side of the blots. B) Quantification of U4 and U6 RNA levels relative to 5S RNA loading control. RNA was loaded twice from biological triplicate samples on the same gel. Error bars indicate S.E.M. C) Primer extension analysis of U4 and U6 RNA is shown with total RNA isolated from WT and TS samples grown at either 30 °C or 37 °C. Reactions were separated on an 8 % denaturing polyacrylamide gel.

that the primer extension is not different between WT and TS. The fact that the 5′-ends of U6 and U4 are not changing in these samples suggests that the 3′-end is slightly shorter. This suggests that the 3′-end is slightly more exposed to 3′ exonuclease attack. Since RNA polymerase III transcribed snRNA U6 and the other spliceosomal snRNAs, which are transcribed by RNA polymerase II, are not known to have common modifications, or common proteins bound to the 3′ termini, this could be an indicator of general disruption of RNP complex formation that otherwise sequesters the 3′ ends from attack by nucleases (Brow 2002).

The size change in spliceosome RNA as well as the splicing defect that we observed led us to investigate spliceosome assembly. One early step for assembly of the spliceosome is the formation of the U4/U6 snRNP (Brow 2002). Using native gel electrophoresis we analyzed the association between U4 RNA and U6 RNA (Fig. 3.6; (Pannone *et al*. 1998)). In biological replicates of WT and TS yeast grown at either 30 °C or shifted to 37 °C we observe a significant depletion of U4/U6 complexes, relative to loading controls. However, free levels of U4 and U6 snRNA do not appear to significantly decrease in level when total RNA is probed (Fig. 3.5 A,B). It is not clear at this time whether the loss of U4/U6 complexes is the cause of, or a result of defective spliceosome assembly. Also, it is currently not known how the RNase P mutation could result in the observed spliceosome defect, since there is no indication that any of the snRNAs are direct substrates for RNase P. One interesting possibility is that pre-tRNA accumulation due to lack of RNase P cleavage is competing for some component essential for proper snRNP assembly. A reasonable candidate for this was the La protein, which binds to the 3′ polyU sequences of both pre-tRNA and U6 RNA, but

overexpression of La did not seem to correct the U6 defect (data not shown). Multiple additional explanations are possible that will require extended testing.

Sense/Antisense RNA Effected by RNase P Depletion

A second major class of RNAs that appears to be affected by the RNase P mutation was the general class of non-coding RNAs of unknown function, CUTs and SUTs (Table 3.2, Fig. 3.3 E-H). Many non-coding RNAs, 73 out of 925 total annotated CUTs and 75 out of 847 total annotated SUTs, were shown to be in the top 250 enriched transcripts with the RNase P TS mutation. Upon inspection of the transcript map results, which can be found at: (http://steinmetzlab.embl.de/engelkeArray/index.html), it became apparent that many of these enriched RNAs (Table 3.2) did not visibly accumulate, possibly because the affected regions were too small to visualize changes. However, some interesting visual changes were evident with larger transcripts (Fig. 3.3 E-H). Out of these changes a subclass of accumulated RNA was further confirmed. Antisense RNA that visibly accumulated while corresponding sense RNA from ORFs was de-enriched was confirmed by northern blots (Fig. 3.7). These results also indicated that the SUT RNA was accumulating in multiple larger forms. Most of the annotations of the boundaries of CUTs and SUTs were mapped using a segmentation algorithm and manually curated (Xu *et al*. 2009). The exact length of most of these RNAs is not known. Thus, it is interesting that my northern blot confirmation of these SUTs indicated multiple larger sizes, as large as 6000 nt (Figure 3.7). These larger sizes appear to result in a reciprocal loss of overlapping mRNA signal on the northern. The exact nature of these extended RNAs and how they might be related to loss of transcripts from the opposing strand remains to be determined.

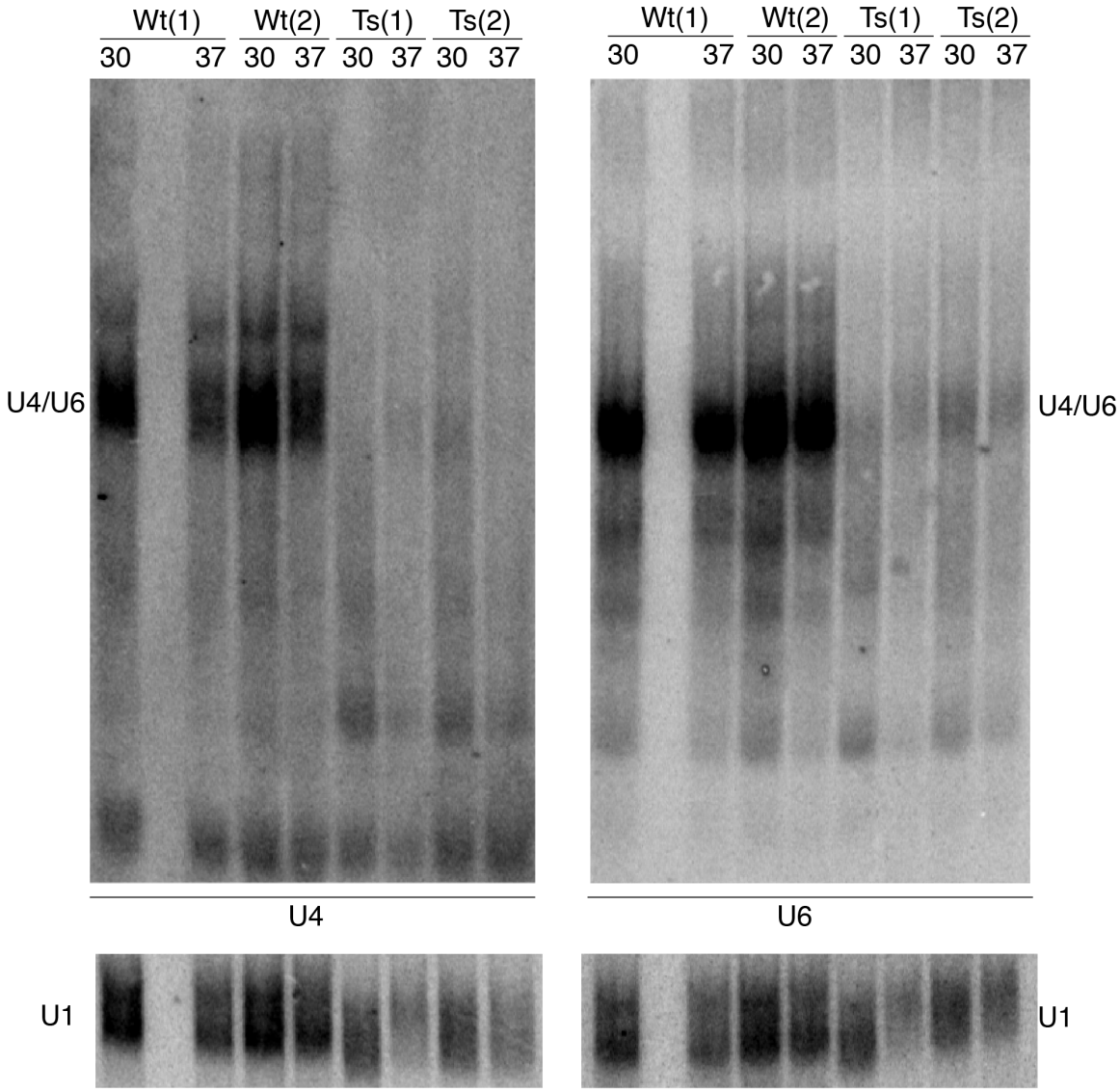

Figure 3.6. U4/U6 assembly in RNase P temperature sensitive strain.
Extracts from WT or TS cells grown in biological replicate at either 30 °C or 37 °C were loaded on a 4 % native polyacrylamide gel and subject to northern blot analysis. U4 and U6 containing complexes were detected using specific radiolabeled oligos. Blots were re-probed for U1 RNA as a loading control for the samples. Successive probing of blots indicates that the major band observed contains U4 associated with U6, with blots originating from the same gel.

Figure 3.7. Large antisense RNA accumulation and overlapping mRNA de-enrichment with RNase P temperature sensitive mutation.
Biological replicates of total RNA isolated from wild type (WT) or RNase P temperature sensitive (TS) samples grown at either 30 °C or 37 °C are shown separated on 1.4 % denaturing agarose gels with subsequent northern blot analysis. Sizes (nt) were estimated from an RNA ladder. A) Northern blots probed for Sut428 or Opt2 with re-probing for Scr1 as a loading control. Two large RNAs accumulate that are observed when probing for Sut428 (1,2). The schematic of Sut428 and Opt2 genes is shown with estimated RNA species indicated by numbered lines over Sut428. Direction of transcription is indicated with arrows. Watson (W) and Crick (C) strands are indicated. B) Three large RNAs accumulate that are observed when probing for Sut116 (1,2,3) while Hnm1 RNA is shown de-enriched. Blots were re-probed for Scr1 as a loading control. A diagram indicating organization of Sut116 and Hnm1 is shown with estimated RNA from Sut116 indicated.

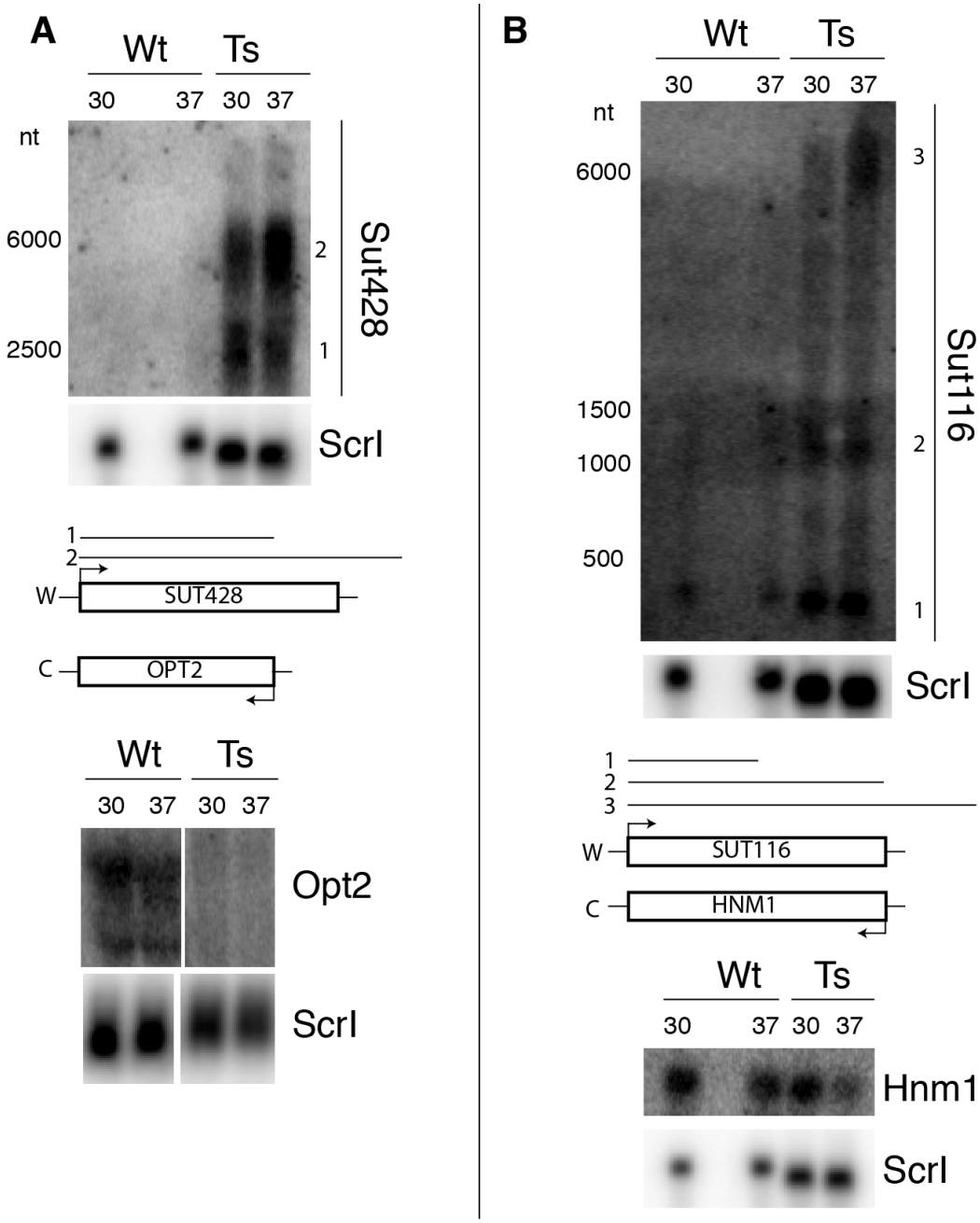
A
Wt
Ts
30
37
30
37
nt
6000
2500
2
1
Sut428
ScrI
1
2
W
SUT428
C
OPT2
Wt
Ts
30
37
30
37
Opt2
ScrI
B
Wt
Ts
30
37
30
37
nt
6000
1500
1000
500
3
2
1
Sut116
ScrI
1
2
3
W
SUT116
C
HNM1
Wt
Ts
30
37
30
37
Hnm1
ScrI

Discussion

Recent work has indicated that RNase P can bind and cleave most RNAs *in vitro* (CHAPTER 2) and possibly cleave RNA *in vivo* (Samanta *et al*. 2006; Coughlin *et al*. 2008). The *in vitro* results showing strong binding to most RNA and cleavage at many sites indicate the potential for very broad substrate recognition, with specificity provided by RNP structure and other parameters that control access *in vivo*. Given the accumulation of broad RNA classes in the RNase P mutant *in vivo*, it seems possible that the catalytic site of the ancient RNase P ribozyme has been adapted to participate in turnover of RNAs as well as structure-specific cleavage of tRNAs.

One major type of RNA that was shown to accumulate with RNase P temperature sensitive mutation in this study was intron-containing pre-mRNA. A previous study indicated accumulation of intron-encoded box C/D snoRNA (Coughlin *et al*. 2008). The current results indicate that this previous result might have been part of much broader effects on intron-containing mRNA accumulation, leading to increased alternative excisions of snoRNAs whether or not RNase P was directly involved. The co-isolation of intron-containing mRNAs with affinity-tagged RNase P continues to suggest that RNase P could play some direct role, but there are reasons to believe that indirect effects are also plausible (Coughlin *et al*. 2008).

Two key observations help to form an alternative model of why un-spliced mRNA is accumulating in my RNase P temperature sensitive strain. One is that a key precursor element of the spliceosome complex (U4/U6 snRNP) is greatly depleted in the RNase P mutant strain compared to the wild type (Fig. 3.6). Given this defect it appears that pre-mRNA could be accumulating due to a defect in spliceosome assembly. Second,

we observe a size change in most of the snRNAs in the temperature sensitive strain (Fig. 3.5 A). This could either contribute to the splicing defect or result from inability to form spliceosomes or be a reflection of a broad disruption in stability of splicing snRNPs. Both of these results suggest that RNase P might not be directly involved with removal of pre-mRNA introns, but rather affect splicing through unknown indirect mechanisms. Possibilities include competition for key proteins by accumulated pre-tRNAs, disruption of nucleolar pathways leading to compromised snRNP biogenesis, and/or other currently obscure intersections between RNA processing pathways in the nucleus.

We made a preliminary attempt to see if overexpression of one of the proteins that intersects both the pre-tRNA and pre-mRNA pathways had an affect on the shortening of U6 snRNA (Pannone *et al*. 1998; Mayes *et al*. 1999). The yeast La protein, Lhp1, is required for correct assembly of U6 snRNP, and also binds pre-tRNA where it is required for the endonucleolytic cleavage of their 3′ ends (Pannone *et al*. 1998). If Lhp1 is not present, the 3′-trailer of pre-tRNA is removed by exonucleases (Yoo and Wolin 1997). The accumulation of pre-tRNA in an RNase P mutant leads to precursors with both 5′ leaders and 3′ trailers still attached, which could effectively compete Lhp1 from U6 RNA and therefore result in 3′-shortened U6 RNA. However, over-expression of Lhp1 protein on a high-copy yeast plasmid did not result in a reversal of the shortened U6 RNA, (data not shown) and in any case Lhp1 depletion is not expected to affect the other snRNPs. The Lsm 2-8 complex of proteins also interacts both with U6 RNA at its 3′ end, pre-tRNA and precursor RNase P RNA pre-Rpr1 (Mayes *et al*. 1999; Salgado-Garrido *et al*. 1999; Beggs 2005). It is possible that simultaneous overexpression of all the subunits of the Lsm complex, or the multiple other protein components of the snRNP complexes

might correct this defect. It is interesting to note that deleting or depleting the Lsm 2-8 complex results in reduced levels of free U6 RNA and a mild splicing defect, which is similar to the defect observed in the RNase P TS strain (Mayes *et al*. 1999; Beggs 2005), so that the Lsm complex might be a particularly attractive target for explaining the apparently indirect effects of the RNase P mutation on splicing.

The other major class of RNA that accumulates with the RNase P temperature sensitive mutation is a diverse set of noncoding RNA (CUTs/SUTs). Earlier studies have attempted to differentiate between stable (SUTs) and unstable (CUTs) transcripts via deleting part of the nuclear exosome (Jacquier 2009; Xu *et al*. 2009). The present results mirror this study, but we observe accumulation of many different CUTs and SUTs with RNase P mutation, indicating that RNase P could either be directly or indirectly involved with general RNA turnover of these RNAs. General RNA quality control in the nucleus of yeast is currently known to involve various components of the exosome (reviewed in (Houseley and Tollervey 2009)). The nuclear exosome is fundamentally different from RNase P in that its major role has been primarily characterized as an exonuclease that degrades RNA from the 3′ to the 5′ direction (3′-5′) (Lebreton *et al*. 2008). One possibility that could theoretical be compatible with my results showing that noncoding RNA accumulates is that RNase P could play either a directly or indirect role with RNA degradation pathways in yeast such as nuclear or cytoplasmic 3′-5′ degradation, 5′-3′ degradation, or affecting complexes that trigger RNA degradation such as the TRAMP (Trf4/5-Air1/2-Mtr4 polyadenylation) complex (Houseley and Tollervey 2009). Further study is needed to clarify the role of RNase P in degrading CUTs and SUTs.

If RNase P is involved with the turnover of noncoding RNA then it appears that it does not directly or stably associate with exosome components or other known nuclease activities. Using Multidimensional Protein Identification Technology (MudPIT) we do not observe obvious strong association between purified RNase P and exosome components (Scott C. Walker, personal communication). Thus, if RNase P does play a role in degradation of these accumulating noncoding RNAs then it does so at an independent location from the primary exosome or does not stably associate with the exosome, or other characterized RNA degradation components. Another possibility is that there could be later steps that are required for complete degradation of RNA that is initially cleaved by RNase P so there might not be close association with other complexes. Further work will have to be carried out to determine RNase P's precise role with these accumulating noncoding RNA.

RNase P has evolved to recognize the structure of pre-tRNA and cleave at a precise position relative to the tertiary structure (Frank and Pace 1998; Walker and Engelke 2006). However, it appears that nuclear RNase P has gained additional RNA binding capability due to increased protein content of the RNA core (see CHAPTER 2). This work shows that RNase P's roles in nuclei affect both the splicing of pre-mRNA and the degradation of SUT/CUT RNA. Previous studies have indicated that RNase P RNA is present primarily in the nucleolus (Bertrand *et al*. 1998), where the majority of the tRNA genes and pre-tRNAs are also found. The related complex that processes pre-rRNAs, RNase MRP, has been shown to also be primarily in the nucleolus, but also in the cytoplasm where it might be involved in mRNA turnover (Gill *et al*. 2006). Our data implicate RNase P in either directly or indirectly affecting the levels of a diverse set of

RNA. The *in vitro* activity of the enzyme suggests that it is certainly capable of initiating cleavage and turnover of unprotected RNA. If indeed RNase P were involved directly in degrading some of these RNAs then it would indicate a novel form of RNA turnover in the nucleolus.

Acknowledgments

I would like to thank the Lars Steinmetz lab, particularly Sandra Clauder and Zhenyu Xu for carrying out the microarray analysis. Also I would like to thank the John Yates Lab particularly Ian McRae for the Mudpit analysis of samples prepared by Scott Walker and Scott's communication of unpublished data. This work was supported by grants GM034869 (to D.R.E.), UM Cellular Biotechnology Training Grant T32-GM08353, and a fellowship from Horace H. Rackham Graduate School (both to M.C.M.).

References

Beggs JD. 2005. Lsm proteins and RNA processing. *Biochem Soc Trans* **33**(Pt 3): 433-438.

Bertrand E, Houser-Scott F, Kendall A, Singer RH, Engelke DR. 1998. Nucleolar localization of early tRNA processing. *Genes Dev* **12**(16): 2463-2468.

Brow DA. 2002. Allosteric cascade of spliceosome activation. *Annu Rev Genet* **36**: 333-360.

Chamberlain JR, Lee Y, Lane WS, Engelke DR. 1998. Purification and characterization of the nuclear RNase P holoenzyme complex reveals extensive subunit overlap with RNase MRP. *Genes Dev* **12**(11): 1678-1690.

Coughlin DJ, Pleiss JA, Walker SC, Whitworth GB, Engelke DR. 2008. Genome-wide search for yeast RNase P substrates reveals role in maturation of intron-encoded box C/D small nucleolar RNAs. *Proc Natl Acad Sci USA* **105**(34): 12218-12223.

David L, Huber W, Granovskaia M, Toedling J, Palm CJ, Bofkin L, Jones T, Davis RW, Steinmetz LM. 2006. A high-resolution map of transcription in the yeast genome. *Proc Natl Acad Sci USA* **103**(14): 5320-5325.

Frank DN, Pace NR. 1998. Ribonuclease P: unity and diversity in a tRNA processing ribozyme. *Annu Rev Biochem* **67**: 153-180.

Gill T, Aulds J, Schmitt ME. 2006. A specialized processing body that is temporally and asymmetrically regulated during the cell cycle in *Saccharomyces cerevisiae*. *The Journal of Cell Biology* **173**(1): 35-45.

Houseley J, Tollervey D. 2009. The many pathways of RNA degradation. *Cell* **136**(4): 763-776.

Huber W, Toedling J, Steinmetz LM. 2006. Transcript mapping with high-density oligonucleotide tiling arrays. *Bioinformatics* **22**(16): 1963-1970.

Jacquier A. 2009. The complex eukaryotic transcriptome: unexpected pervasive transcription and novel small RNAs. *Nature Reviews Genetics* **10**(12): 833-844.

Juneau K, Miranda M, Hillenmeyer ME, Nislow C, Davis RW. 2006. Introns regulate RNA and protein abundance in yeast. *Genetics* **174**(1): 511-518.

Lebreton A, Tomecki R, Dziembowski A, Séraphin B. 2008. Endonucleolytic RNA cleavage by a eukaryotic exosome. *Nature* **456**(7224): 993-996.

Lee JY, Rohlman CE, Molony LA, Engelke DR. 1991. Characterization of RPR1, an essential gene encoding the RNA component of *Saccharomyces cerevisiae* nuclear RNase P. *Molecular and Cellular Biology* **11**(2): 721-730.

Mayes AE, Verdone L, Legrain P, Beggs JD. 1999. Characterization of Sm-like proteins in yeast and their association with U6 snRNA. *The EMBO Journal* **18**(15): 4321-4331.

Neil H, Malabat C, d'Aubenton-Carafa Y, Xu Z, Steinmetz LM, Jacquier A. 2009. Widespread bidirectional promoters are the major source of cryptic transcripts in yeast. *Nature* **457**(7232): 1038-1042.

Pagán-Ramos E, Lee Y, Engelke DR. 1996. A conserved RNA motif involved in divalent cation utilization by nuclear RNase P. *RNA* **2**(11): 1100-1109.

Pannone BK, Kim SD, Noe DA, Wolin SL. 2001. Multiple functional interactions between components of the Lsm2-Lsm8 complex, U6 snRNA, and the yeast La protein. *Genetics* **158**(1): 187-196.

Pannone BK, Xue D, Wolin SL. 1998. A role for the yeast La protein in U6 snRNP assembly: evidence that the La protein is a molecular chaperone for RNA polymerase III transcripts. *EMBO J* **17**(24): 7442-7453.

Patel SB, Bellini M. 2008. The assembly of a spliceosomal small nuclear ribonucleoprotein particle. *Nucleic Acids Res* **36**(20): 6482-6493.

Perocchi F, Xu Z, Clauder-Münster S, Steinmetz LM. 2007. Antisense artifacts in transcriptome microarray experiments are resolved by actinomycin D. *Nucleic Acids Res* **35**(19): e128.

Planta RJ, Mager WH. 1998. The list of cytoplasmic ribosomal proteins of *Saccharomyces cerevisiae*. *Yeast* **14**(5): 471-477.

Roy SW, Gilbert W. 2006. The evolution of spliceosomal introns: patterns, puzzles and progress. *Nature Reviews Genetics* **7**(3): 211-221.

Salgado-Garrido J, Bragado-Nilsson E, Kandels-Lewis S, Séraphin B. 1999. Sm and Sm-like proteins assemble in two related complexes of deep evolutionary origin. *The EMBO Journal* **18**(12): 3451-3462.

Samanta MP, Tongprasit W, Sethi H, Chin C-S, Stolc V. 2006. Global identification of noncoding RNAs in *Saccharomyces cerevisiae* by modulating an essential RNA processing pathway. *Proc Natl Acad Sci USA* **103**(11): 4192-4197.

Spingola M, Grate L, Haussler D, Ares M. 1999. Genome-wide bioinformatic and molecular analysis of introns in *Saccharomyces cerevisiae*. *RNA* **5**(2): 221-234.

Vanacova S, Stefl R. 2007. The exosome and RNA quality control in the nucleus. *EMBO Rep* **8**(7): 651-657.

Wahl MC, Will CL, Lührmann R. 2009. The spliceosome: design principles of a dynamic RNP machine. *Cell* **136**(4): 701-718.

Walker SC, Engelke DR. 2006. Ribonuclease P: the evolution of an ancient RNA enzyme. *Crit Rev Biochem Mol Biol* **41**(2): 77-102.

Will CL, Lührmann R. 2001. Spliceosomal UsnRNP biogenesis, structure and function. *Curr Opin Cell Biol* **13**(3): 290-301.

Xiao S, Day-Storms JJ, Srisawat C, Fierke CA, Engelke DR. 2005. Characterization of conserved sequence elements in eukaryotic RNase P RNA reveals roles in holoenzyme assembly and tRNA processing. *RNA* **11**(6): 885-896.

Xiao S, Hsieh J, Nugent RL, Coughlin DJ, Fierke CA, Engelke DR. 2006. Functional characterization of the conserved amino acids in Pop1p, the largest common protein subunit of yeast RNases P and MRP. *RNA* **12**(6): 1023-1037.

Xu Z, Wei W, Gagneur J, Perocchi F, Clauder-Münster S, Camblong J, Guffanti E, Stutz F, Huber W, Steinmetz LM. 2009. Bidirectional promoters generate pervasive transcription in yeast. *Nature* **457**(7232): 1033-1037.

Yoo CJ, Wolin SL. 1997. The yeast La protein is required for the 3' endonucleolytic cleavage that matures tRNA precursors. *Cell* **89**(3): 393-402.

CHAPTER 4
SUMMARY, CONCLUSIONS, AND FUTURE DIRECTION

Understanding of RNase P structure and function has expanded greatly as more and more complexes are discovered with varying amounts of protein and RNA components. In eukaryotes with the presence of nine protein subunits and an RNA subunit RNase P still cleaves pre-tRNA with a kinetic mechanism that is highly similar to the much less proteinaceous bacterial RNase P (Chamberlain *et al*. 1998; Gössringer *et al*. 2006; Hsieh *et al*. 2009). However, given the similarity in substrate cleavage between these RNase P complexes it was also known that they interact with single stranded RNA in very different ways (Ziehler *et al*. 2000). This variation in RNA recognition combined with the fact that RNase P has been shown to cleave non-tRNA substrates led us to hypothesize that this eukaryotic specific binding ability could lead to eukaryotic specific non-tRNA substrates. The work presented here used a combination of *in vitro* and *in vivo* investigations to establish that eukaryotic RNase P does have unique RNA binding abilities and to indicate the presence of additional non-tRNA substrates.

In vitro binding of RNA by RNase P

The fact that RNase P from *Saccharomyces cerevisiae* could be strongly inhibited by single stranded RNA in a sequence specific manner, while *Bacillus subtilis* RNase P could not, suggested that yeast RNase P might have specific RNA binding capabilities not found with bacterial RNase P (Ziehler *et al*. 2000). The work in CHAPTER 2 focused on characterizing this RNA binding and its implications for substrate cleavage. Initial

experiments showed that single stranded RNA inhibited pre-tRNA cleavage by RNase P in a size dependent manner, with a minimal length needed for strong inhibition (Fig. 2.1 A-C). The interpretation of this inhibition was complex, since even at high amounts of polyU, residual activity was still present. Given the basic nature of the protein subunits in yeast RNase P it would be consistent with my results if polyU bound to one or more protein sites away from the active site. This would fit with both the length dependent inhibition of pre-tRNA cleavage and with the lack of complete inhibition. The strong inhibition and the large increase in apparent IC_{50} at increased pre-tRNA levels (Fig. 2.1 C) also suggested that at least some sites showed inhibition of a partial competitive nature.

Given that inhibition of pre-tRNA cleavage by different homopolymer RNA was dramatically different (polyG~polyU>>polyA>>polyC) the investigation of mixed sequence RNA inhibition was tested to see if this sequence specificity was retained (Ziehler *et al*. 2000). All of the mixed sequence RNAs that were tested showed strong inhibition of pre-tRNA cleavage (Fig. 2.2 A). Detailed titrations of two of these RNAs that inhibited as well as polyU RNA showed that they also failed to completely inhibit pre-tRNA cleavage (Fig. 2.2 B,C). This indicated that RNase P could bind most mixed sequence RNA without strong differences in affinity. However, when tested for cleavage by RNase P mixed sequence RNA but not polyU RNA could be cleaved (Fig. 2.3 A). This suggests that selected sites in the mixed sequence RNA bind more appropriately at the active site while polyU cannot. Also, exclusion of a particular sequence at the cleavage site is not apparent as was shown by aligning mixed sequence RNA cleavage sites with previously identified ones. Uridine was not excluded from the RNase P

cleavage site when in the context of mixed sequence RNA (Fig. 2.4 A). What is also clear from cleavage site sequence alignment is that the sequence that RNase P cleaves is not apparently conserved. Thus, it appears that RNase P substrates cannot be predicted from primary sequence.

It seemed possible that a local structure in the RNA might be required for fit into the active site, but in predicting the structure around the cleavage site there was not an obvious trend that emerged (Fig. 2.4 B). Structural predictions of RNA are complicated though, especially when using algorithms that predict folding based on energy minimization due to the presence of multiple folding alternatives that yield the same minimal energy (Zuker 2003; Simmonds *et al*. 2008). In addition, neither tertiary structure nor folding induced by RNA binding proteins is taken into account when predicting folding. The structures that were presented in (Fig. 2.4 B) are therefore a simplification and most likely do not reflect *in vivo* structures. Thus there could be some *in vivo* structure that is recognized by nuclear RNase P that cannot be predicted accurately by current methods.

Binding of RNA to RNase P was more directly investigated by crosslinking to identify the location of contact sites. Until this study the RNA contact sites with natively purified and active nuclear RNase P had not been known. The most striking observation of the study was that a variety of RNA made contacts near the active site of the RNA subunit of RNase P (Fig. 2.5). Upon testing polyU RNA, mixed sequence RNA, and pre-tRNA, even though polyU was not able to be cleaved, they all crosslinked within a few nucleotides of each other near the RNase P RNA active site. It is also striking that other crosslinks with the RNase P RNA were not obtained for any of the RNAs tested. RNA

contacts with two and possibly three protein subunits were also obtained for polyU RNA (Fig. 2.6). Until this point most of the studies of RNA binding with RNase P proteins had been done with reconstitution experiments and did not use active RNase P holoenzyme (Jarrous *et al*. 2001; Marquez *et al*. 2006). The results of the crosslinking further indicate that RNA interacts with RNase P at multiple sites, with some in the protein subunits and limited sites in the RNA subunit.

Although my work made progress with the understanding of how RNase P recognizes and sometimes cleaves RNA, both non-tRNA and pre-tRNA, several important questions concerning RNA recognition still remain. One major question is how high in affinity are the protein binding sites compared to the RNA subunit binding sites and which sites determine whether or not cleavage can take place. Does binding at the proteins hold the RNA in place to bind to the RNA active site or is it that the RNA binds the RNA active site and then is positioned to available protein binding sites? In addition, if protein interactions could be determined for other RNAs in addition to polyU, especially pre-tRNA, then an understanding of how sequence specific the protein binding is would emerge. If the positioning of the protein subunits in the RNase P complex was known in more detail, as is currently under investigation, or a crystal structure of the eukaryotic complex were obtained, then a more complete model of substrate interaction with RNase P in yeast could be produced. This additional information combined with my initial RNA binding results would further refine the model of how eukaryotic RNase P binds and cleaves many different RNAs and possibly help predict other RNase P substrates.

In vivo Roles for RNase P

Although previous studies have identified possible non-tRNA substrates for RNase P, current experimental techniques have enabled a much more detailed analysis of cellular RNA (David *et al*. 2006; Xu *et al*. 2009). CHAPTER 3 is the first study that has used high density, strand-specific microarrays to analyze the identity of RNAs that change in abundance with RNase P temperature sensitive mutation. Results from this study indicated that a much larger and diverse set of RNAs were changing in abundance with RNase P mutation then previously identified (Coughlin *et al*. 2008). Ribosomal protein mRNA was among the most highly enriched RNA (Table 3.2). This result was previously observed but not fully characterized (Coughlin *et al*. 2008). With the high-density microarray and with the results visualized with transcript maps, it became apparent that mRNA introns were accumulating with RNase P mutation (Fig. 3.3 A-C). In addition, the accumulated RNA was indicated to be pre-mRNA containing 5′ exons and not a splicing intermediate (Fig. 3.4; data not shown).

Defects in intron removal led to the investigation of possible defects in spliceosome function. Results indicated that much less of the necessary U4/U6 snRNP was assembled with RNase P mutation (Fig. 3.6). Although it is not yet clear whether the U4/U6 deficit is the cause of reduced splicing or a result of a broader defect in spliceosome assembly, this result suggested that the RNase P effect on splicing was indirectly affecting the splicing apparatus rather than directly involved in cleavage and turnover of the pre-mRNA introns. Thus far RNase P has only been localized to the nucleolus (Bertrand *et al*. 1998). Unless a small portion of RNase P is also found in the nucleoplasm, this suggests any direct effect of RNase P takes place in the nucleolus. One

possibility is that RNase P helps to mature spliceosomal RNA components in an unknown step that is required for spliceosome assembly (Brow 2002). However, the slight reduction in snRNA sizes, presumably from 3´-end exonuclease action, is not really consistent with any known direct cleavage activity by RNase P. Therefore a variety of indirect effects by the RNase P defect are also possible. As discussed in CHAPTER 3, one possible indirect effect is that pre-tRNA accumulation could be indirectly responsible for affecting splicing by sequestering proteins that are required for spliceosomal RNA maturation and/or assembly.

Many questions as to how exactly RNase P mutation results in the observed mRNA splicing defect still remain. For example, the slight size change in most spliceosomal RNA has not been fully characterized and has not been shown to be functionally connected to splicing, however the exact nature of the 3' end of these RNAs will be determined in the near future as that is the probable site of shortening (Fig. 3.5 A). Full characterization of these size changes could shed light on the splicing defect or indicate that the size change is not affecting function. Once the identity of these shortened RNAs is known, *in vitro* reconstitution experiments using both WT and TS RNase P yeast extract that can be depleted for specific snRNA using a primer and RNase H treatment followed by addition of shortened snRNA back to the extract, would indicate if this shortening is what causes reduced activity of the spliceosome (Fabrizio *et al*. 1989). In addition, the U4/U6 snRNP assembly (Fig. 3.6) is an important step but there are earlier steps in intron splicing that could be investigated (Brow 2002). Also, it is possible that the spliceosome is assembled but that recycling of the spliceosome is impaired (Raghunathan and Guthrie 1998). A more detailed analysis of the exact nature

of the splicing defect would provide important information as to why the pre-mRNA is accumulating and could also clarify the possible connection with RNase P.

Previous studies have indicated that 85 % of the yeast genome is transcribed with many more noncoding RNA produced then previously known (David *et al*. 2006; Berretta and Morillon 2009). Exactly how these RNAs function in the cell is not understood. Studies have indicated that many of these noncoding RNAs are rapidly degraded by the exosome but determinants for this degradation are not known (Xu *et al*. 2009). Given results with the *in vitro* RNA binding and cleavage by RNase P in CHAPTER 2, there was a high probability that RNase P could cleave many additional RNAs *in vivo*. Recent annotation of the *S. cerevisiae* noncoding RNA CUTs and SUTs along with the strand specific nature of the microarray that was used in CHAPTER 3 helped to more formally define which noncoding RNA was accumulating with RNase P temperature sensitive mutation (David *et al*. 2006; Huber *et al*. 2006; Samanta *et al*. 2006; Coughlin *et al*. 2008; Xu *et al*. 2009).

As postulated, a large set of noncoding RNA accumulated with RNase P mutation (CUTs/SUTs) (Table 3.2). Out of the many noncoding RNA that were shown to accumulate with RNase P mutation, experiments focused on a select few that were antisense to coding regions of mRNA that were de-enriched (Fig. 3.3 E, H; Fig. 3.7 A, B). In these cases it appeared that multiple large transcripts of the noncoding RNA were accumulating. Whether or not this accumulation caused the de-enrichment of the overlapping mRNA is not clear. To determine if the expression of the noncoding RNA is interfering with the overlapping mRNA, mutants in the antisense promoter region that prevent transcription could be tested in the RNase P mutant strain to see if the

overlapping mRNA is then expressed. This would indicate if the expression of the antisense RNA is what caused the decrease in overlapping mRNA.

Indeed, the CUTs and SUTs that were identified to accumulate with RNase P mutation potentially implicate RNase P in the normal degradation of some of these noncoding RNA (Table 3.2). The divergent levels of mRNA overlapped by noncoding RNA that is observed in multiple cases with RNase P mutation indicates that RNase P could play a role in regulating these regions by cleaving the noncoding RNA (Fig. 3.7 A, B). This would be a novel role for RNase P that was not known until strand specific microarrays could distinguish between overlapping RNAs and annotations of CUTs/SUTs were available.

Further, the nature of accumulated noncoding RNA could also provide information key to understanding if these RNAs are RNase P substrates or how RNase P might be indirectly involved in their accumulation (Fig. 3.7). The largest noncoding RNAs that accumulate are approximately 6000 nt. Transcripts that large would overlap neighboring annotated open reading frames, however existing transcription maps from other studies do not indicate that this is the case (Fig. 3.3, online database [http://steinmetzlab.embl.de/engelkeArray/index.html]). Determining the sequence of accumulating RNA would determine which end of the RNA is extended beyond the annotated region. This would indicate if the extended region overlaps the promoter of the mRNA on the opposite strand, which could point towards a possible transcriptional interference mechanism with accumulated RNA. In addition to possible transcriptional interference there are many other ways in which noncoding RNA could affect gene expression that have been discovered in *S. cerevisiae* that could also account for the

changes observed with RNase P mutation (Martens *et al*. 2004; Berretta and Morillon 2009; Jacquier 2009).

The broad spectrum of RNA that was shown to accumulate with RNase P mutation suggests that RNase P might affect the function of some RNA turnover pathway. However, no physical interaction of RNase P with known RNA turnover pathway gene products was found by our studies or previously shown in interaction databases (data not shown; www.yeastgenome.org). In addition, the enzyme systems for RNA interference (RNAi) in *S. cerevisiae* are not present, so if these noncoding RNAs are regulatory RNAs that are normally turned over or have an affect on gene expression, the pathways by which they function are not currently known (Drinnenberg *et al*. 2009). Additionally, RNase P has been shown in previous studies and in CHAPTER 2 to endonucleolytically cleave a diverse set of RNA besides pre-tRNA at multiple sites *in vitro*. It is possible that RNase P cleavage is guided by interactions with protein cofactors that could interact with potential RNA substrates, forming ribonucleoprotein (RNP) substrates that could guide more specific cleavage, but so far we have been unable to identify the nature of these RNPs.

If RNase P substrate were indeed a RNP *in vivo* then identifying what protein or proteins associates with accumulated RNA would be of great importance. One method to determine if these RNAs are in an RNP is to UV crosslink yeast and then detect shifted RNA using radiolabeled primers on a native gel. Shifted complexes could be analyzed using mass spectrometry to identify protein. In addition, extract could be passed through a column with immobilized RNA of interest and eluted protein could be analyzed. Once the protein component of the RNP is identified then *in vitro* cleavage with RNase P could

be tested on purified RNP rather then just *in vitro* transcribed RNA. Another method would be to take RNase P TS extract and add back large quantities of highly purified RNase P and analyze the cleavage of suspected RNase P substrates. The limitation with this technique would be the probable rapid degradation of the RNase P added to the extract.

Finally, a more direct connection between RNase P and the various accumulating RNAs could be obtained using high throughput sequencing technology to analyze the RNA that co-purifies with RNase P. Co-purification of RNA with RNase P was analyzed in the past by low resolution microarray but obtaining the sequences of co-purified RNA would greatly increase the value of the results (Coughlin *et al*. 2008). Combining results of co-purification data with current RNA accumulation data would implicate these RNAs as direct RNase P substrates *in vivo* and guide future work on RNase P substrate selection.

Acknowledgements

This work was supported by grants from the Cellular Biotechnology Training Grant NIH T32-GM08353, and grants GM034869 and GM082875-01A1 (both to DRE) from the NIH. Further funding and support was provided from the Horace H. Rackham School of graduate studies at the University of Michigan.

References

Berretta J, Morillon A. 2009. Pervasive transcription constitutes a new level of eukaryotic genome regulation. *EMBO Rep* **10**(9): 973-982.

Bertrand E, Houser-Scott F, Kendall A, Singer RH, Engelke DR. 1998. Nucleolar localization of early tRNA processing. *Genes Dev* **12**(16): 2463-2468.

Brow DA. 2002. Allosteric cascade of spliceosome activation. *Annu Rev Genet* **36**: 333-360.

Chamberlain JR, Lee Y, Lane WS, Engelke DR. 1998. Purification and characterization of the nuclear RNase P holoenzyme complex reveals extensive subunit overlap with RNase MRP. *Genes Dev* **12**(11): 1678-1690.

Coughlin DJ, Pleiss JA, Walker SC, Whitworth GB, Engelke DR. 2008. Genome-wide search for yeast RNase P substrates reveals role in maturation of intron-encoded box C/D small nucleolar RNAs. *Proc Natl Acad Sci USA* **105**(34): 12218-12223.

David L, Huber W, Granovskaia M, Toedling J, Palm CJ, Bofkin L, Jones T, Davis RW, Steinmetz LM. 2006. A high-resolution map of transcription in the yeast genome. *Proc Natl Acad Sci USA* **103**(14): 5320-5325.

Drinnenberg IA, Weinberg DE, Xie KT, Mower JP, Wolfe KH, Fink GR, Bartel DP. 2009. RNAi in budding yeast. *Science* **326**(5952): 544-550.

Fabrizio P, McPheeters DS, Abelson J. 1989. *In vitro* assembly of yeast U6 snRNP: a functional assay. *Genes Dev* **3**(12B): 2137-2150.

Gössringer M, Kretschmer-Kazemi Far R, Hartmann RK. 2006. Analysis of RNase P protein (rnpA) expression in *Bacillus subtilis* utilizing strains with suppressible rnpA expression. *J Bacteriol* **188**(19): 6816-6823.

Hsieh J, Walker SC, Fierke CA, Engelke DR. 2009. Pre-tRNA turnover catalyzed by the yeast nuclear RNase P holoenzyme is limited by product release. *RNA* **15**(2): 224-234.

Huber W, Toedling J, Steinmetz LM. 2006. Transcript mapping with high-density oligonucleotide tiling arrays. *Bioinformatics* **22**(16): 1963-1970.

Jacquier A. 2009. The complex eukaryotic transcriptome: unexpected pervasive transcription and novel small RNAs. *Nature Reviews Genetics* **10**(12): 833-844.

Jarrous N, Reiner R, Wesolowski D, Mann H, Guerrier-Takada C, Altman S. 2001. Function and subnuclear distribution of Rpp21, a protein subunit of the human ribonucleoprotein ribonuclease P. *RNA* **7**(8): 1153-1164.

Marquez SM, Chen JL, Evans D, Pace NR. 2006. Structure and function of eukaryotic Ribonuclease P RNA. *Mol Cell* **24**(3): 445-456.

Martens JA, Laprade L, Winston F. 2004. Intergenic transcription is required to repress the *Saccharomyces cerevisiae SER3* gene. *Nature* **429**(6991): 571-574.

Raghunathan PL, Guthrie C. 1998. A spliceosomal recycling factor that reanneals U4 and U6 small nuclear ribonucleoprotein particles. *Science* **279**(5352): 857-860.

Samanta MP, Tongprasit W, Sethi H, Chin CS, Stolc V. 2006. Global identification of noncoding RNAs in *Saccharomyces cerevisiae* by modulating an essential RNA processing pathway. *Proc Natl Acad Sci USA* **103**(11): 4192-4197.

Simmonds P, Karakasiliotis I, Bailey D, Chaudhry Y, Evans DJ, Goodfellow IG. 2008. Bioinformatic and functional analysis of RNA secondary structure elements among different genera of human and animal caliciviruses. *Nucleic Acids Res* **36**(8): 2530-2546.

Xu Z, Wei W, Gagneur J, Perocchi F, Clauder-Münster S, Camblong J, Guffanti E, Stutz F, Huber W, Steinmetz LM. 2009. Bidirectional promoters generate pervasive transcription in yeast. *Nature* **457**(7232): 1033-1037.

Ziehler WA, Day JJ, Fierke CA, Engelke DR. 2000. Effects of 5' leader and 3' trailer structures on pre-tRNA processing by nuclear RNase P. *Biochemistry* **39**(32): 9909-9916.

Zuker M. 2003. Mfold web server for nucleic acid folding and hybridization prediction. *Nucleic Acids Res* **31**(13): 3406-3415.

APPENDIX
TOP 250 NUCLEAR-ENCODED RNAS THAT ENRICH WITH TEMPERATURE SENSITIVE (TS) MUTATION IN RPR1

Values are provided for the fold enrichment (TS/WT) of indicated RNA with RNase P mutation grown at 37 °C and indicated as Rpr1 TS. The presence of either one (+) or two (++) introns and whether they are 5´-untranslated region (UTR) introns (5´UTR intron) is shown. In some cases multiple names are listed for one enrichment value. This is due to overlapping or closely spaced regions that were effectively analyzed as a single species. In future publication of this list of top enriched RNA data will be in $\log_2$ rather then first taking the anti-log then looking for enriched RNA, which is how the data is presented here.

Name	Intron	Rpr1 TS
RPL39	+	15.05
RPL27B	+	14.45
RPS10A	+	13.81
RPL34B	+	13.62
RPL37A	+	13.47
RPL26B	+	11.20
RPL13B	+	9.37
RPL34A	+	8.50
RPS29A	5´UTR intron	7.80
RPL37B	+	7.69
RPL19B	+	7.39
RPS10B	+	6.79
RPS25A	5´UTR intron	6.48
RPL31A	+	5.73

Name	Intron	Rpr1 TS
CUT324		5.43
RPS18B	+	5.40
CUT526		5.34
SUT582		5.32
RPL23B	+	5.11
CUT680		4.93
RPS4A	+	4.88
RPS6B	+	4.80
RPL36A	+	4.54
RPL40B	+	4.51
RPL14A	+	4.26
RPL29, YFR032C-B	5´UTR intron	4.24
CUT843		4.20
RPL27A	+	4.08
RPS30A	+	4.04
RPL40A	+	4.02
CUT008		4.00
AIF1		3.97
SUT741		3.90
SUT116		3.83
RPS19A	+	3.78
RPL43A	+	3.75
SUT677		3.74
YOR053W		3.70
RPS19B	+	3.53
SUT074		3.53
RPL35B	+	3.49
SUT139		3.49

Name	Intron	Rpr1 TS
SUT248		3.48
RPL33A	+	3.45
SOM1		3.43
CUT249		3.42
RPL33B	+	3.41
RPS26B	5´UTR intron	3.31
SUT625		3.27
SUT279		3.26
SUT517		3.23
SPG4		3.20
RPS21B	+	3.16
CUT846		3.14
CUT128		3.13
CUT073		3.12
SUT814		3.10
RPS16A	+	3.09
SUT631		3.08
CUT149		3.05
CUT732		3.04
SUT699		3.04
SUT008		3.02
RPL7A	++	3.00
SUT205		3.00
SMD3		3.00
CUT009		2.99
COS12		2.99
SUT617		2.96
YIL127C		2.96
SUT101		2.96
SUT771		2.95
CUT791		2.94
SUT542		2.93
RPS23B	+	2.91
SUT045		2.89

Name	Intron	Rpr1 TS
CUT595		2.89
YBR190W, RPL21A, YBR191W-A	+	2.88
YCL058W-A		2.85
RPS29B	5´UTR intron	2.84
RPS24B	+	2.82
CUT523		2.80
SUT346		2.79
SUT343		2.78
SUT129		2.78
DYN2	++	2.75
CUT347		2.75
RPS30B	+	2.75
ATG8		2.74
SUT249		2.73
YGR169C-A		2.70
YGR121W-A		2.69
SUT691		2.68
SUT035		2.67
CUT339		2.67
SUT519		2.66
SUT553		2.65
RPL26A	+	2.65
SUT636		2.64
CUT572		2.63
SUT200		2.62
CUT306		2.61
CUT447		2.60
CUT376		2.60
CUT461		2.60
SUT287		2.59
SUT827		2.58
CUT168		2.57
CUT894		2.56
SUT442		2.54
SUT535		2.53

Name	Intron	Rpr1 TS
YJL144W		2.51
SNR9		2.51
CUT190		2.51
MAG1		2.50
SUT700		2.48
CUT734		2.47
RPS27B	+	2.46
YNL162W-A		2.46
SUT411		2.45
CUT085		2.44
SUT844		2.44
RPS8A, YBL071C-B	5´UTR intron	2.43
SUT278		2.43
CUT055		2.42
RPS24A	+	2.41
SUT404		2.41
RPL6A	+	2.40
CUT456		2.39
SUT313		2.39
YOL014W		2.39
RPL14B	+	2.38
CUT012		2.37
SUT273		2.37
CUT325		2.35
SUT482		2.34
CUT689		2.33
SUT497		2.33
CUT125		2.33
SUT056		2.32
CUT432		2.32
SUT114		2.32
SUT001		2.30
CUT238		2.29
SUT756		2.29
SUT808		2.28

Name	Intron	Rpr1 TS
SUT652		2.27
CUT830		2.27
SUT250		2.27
SMX3		2.27
CUT676		2.27
YNL050C	+	2.27
RPS11B	+	2.26
SUT288		2.26
JID1		2.25
SUT526		2.25
SUT593		2.25
RPS26A, YGL188C-A	5´UTR intron	2.24
SVS1		2.24
CUT030		2.24
SUT158		2.24
YDR461C-A		2.23
CUT112		2.23
RPL24A	5´UTR intron	2.22
SUT122		2.22
CUT837		2.22
SUT403		2.21
CUT679		2.20
SUT712		2.20
SUT401		2.19
CUT745		2.19
CUT789		2.18
SUT351		2.18
YKR075W-A		2.18
CUT911		2.18
CUT380		2.15
RPS16B	+	2.15
CUT240		2.15
YNL143C		2.14
CUT658		2.14
CUT519		2.14

Name	Intron	Rpr1 TS
SUT224		2.13
SUT347		2.13
SUT624		2.13
SUT721		2.13
YJLWtau4, YJLWdelta10		2.12
SUT428		2.12
YLR099W-A		2.12
CUT404		2.12
CUT781		2.11
SUT546		2.11
SUT696		2.11
CUT511		2.11
RPS17A	+	2.11
CUT440		2.11
YNR073C		2.11
CUT720		2.10
RPL23A	+	2.09
CDC26		2.09
RPL42A	+	2.09
SUT563		2.09
CUT616		2.08
SUT039		2.08
CUT709		2.08
SEM1		2.07
CUT545		2.07
PXA2		2.07
SRB6		2.07
RPB11		2.07
SUT415		2.07
CUT566		2.06
CUT538		2.06
CUT726		2.05
SUT846		2.05
CUT632		2.05

Name	Intron	Rpr1 TS
RPS6A	+	2.05
PEX18		2.05
CUT094		2.04
YIL046W-A		2.04
SRL3		2.04
RPL31B	+	2.04
CUT770		2.03
CUT444		2.03
BCD1		2.03
SUT413		2.03
RPS18A	+	2.03
CUT421		2.03
SNR85		2.02
CUT624		2.02
PEP12		2.02
CUT822		2.02
UMP1		2.02
CUT845		2.02
CUT138		2.02
SUT816		2.01
LOC1		2.01
SUT021		2.00
CUT659		2.00
RPL42B	+	2.00
CUT096		2.00
GLC8		2.00
CUT521		1.99
CUT531		1.99
SUT071		1.98
CUT374		1.98
YLR042C		1.98
ECM12		1.98

Name	Intron	Rpr1 TS
CYC7		1.98
YGR035C		1.98